Beyond smoothness: the art of surface texturing battling against friction

OPEN ACCESS
IOP Publishing | IMMT
International Journal of Extreme Manufacturing
Int. J. Extrem. Manuf. **7** (2025) 022014 (40pp)
https://doi.org/10.1088/2631-7990/ad9c01

Topical Review

Beyond smoothness: the art of surface texturing battling against friction

Qianhao Xiao[1,3], Xuanyao Wang[1], Yayong Wang[1], Wei Zheng[4], Jiwen Xu[4], Xichun Luo[3], Jining Sun[1,2,*] and Lei Zhang[1,2,*]

[1] School of Mechanical Engineering, Dalian University of Technology, Dalian 116024, People's Republic of China
[2] State Key Laboratory of High-performance Precision Manufacturing, Dalian University of Technology, Dalian 116024, People's Republic of China
[3] Centre for Precision Manufacturing, Department of Design, Manufacturing & Engineering Management, University of Strathclyde, Glasgow G1 1XJ, United Kingdom
[4] AVIC Shenyang Aircraft Company Limited, Shenyang 110850, People's Republic of China

E-mail: jining.sun@dlut.edu.cn and lei.zhang@dlut.edu.cn

Received 24 July 2024, revised 16 October 2024
Accepted for publication 9 December 2024
Published 30 December 2024

Abstract

Leveraging surface texturing to realize significant friction reduction at contact interfaces has emerged as a preferred technique among tribology experts, boosting tribological energy efficiency and sustainability. This review systematically demonstrates optimization strategies, advanced manufacturing methods, typical applications, and outlooks of technical challenges toward surface texturing for friction reduction. Firstly, the lubricated contact models of microtextures are introduced. Then, we provide a framework of state-of-the-art research on synergistic friction optimization strategies of microtexture structures, surface treatments, liquid lubricants, and external energy fields. A comparative analysis evaluates the strengths and weaknesses of manufacturing techniques commonly employed for microtextured surfaces. The latest research advancements in microtextures in different application scenarios are highlighted. Finally, the challenges and directions of future research on surface texturing technology are briefly addressed. This review aims to elaborate on the worldwide progress in the optimization, manufacturing, and application of microtexture-enabled friction reduction technologies to promote their practical utilizations.

Keywords: surface texturing, friction reduction, hydrodynamic lubrication, structure optimization, contact interface

* Authors to whom any correspondence should be addressed.

2631-7990/25/022014+40$33.00

Nomenclature

ρ	Local fluid density (kg·m^{-3})
V	Velocity vector
p	Local pressure (Pa)
f	External force per unit volume on a fluid
η	Dynamic viscosity (Pa·s)
h	Local film thickness (m)
u	Velocities in the x-directions (m·s^{-1})
v	Velocities in the y-directions (m·s^{-1})
Re	Reynolds number
δ	Ratio of the oil film thickness to the length of the contact area
θ	Filling ratio of lubricant in the cavitation zone
p_{cav}	Cavitation pressure (Pa)
t	Time variable (s)

1. Introduction

Friction and wear are widespread concerns across various domains of human experience, spanning man-made, natural, and biological systems. They result in reduced reliability and lifespan of crucial moving components in sliding, rolling, and rotating contact interfaces, accelerating energy consumption [1–3]. Historically, the most straightforward approach to minimize friction and wear involves smoothing contact surfaces, along with applying lubricants to diminish solid–solid contact [4]. However, recent studies have unveiled that the frictional pairs with high smoothness do not consistently reduce frictional coefficients or material wear [5]. Surprisingly, parallel rough surfaces can generate hydrodynamic pressure lubricating films, offering novel perspectives for engineering lubrication issues [6].

In 1966, Hamilton *et al* [7] noted that micrometer-scale irregularities on rotary shaft seals could provide additional load-bearing capacity, thereby reducing the coefficient of friction. These 'micrometer-scale irregularities' represent the earliest form of surface texturing. It was confirmed that micro-asperities are an effective method for lubricating mechanical face seals and parallel rotating thrust bearings some years later [8, 9]. Based on this theory, microtextured engine cylinder liners emerged as the first successful commercial application of microtexture [10]. The term 'surface texturing' refers to the process of creating patterned arrays with specific dimensions and distributions on frictional surfaces, typically deeper compared with roughness. Moreover, the lateral microtexture dimensions are at least one order of magnitude larger than the roughness features [11, 12]. Surface texturing improves tribological performance by debris storage, lubricant reservoir, and micro hydrodynamic pressure effects [13]. In starved lubrication, microtextures supply lubricant to the contact area, forming a boundary lubricating film approximately 0.005–0.010 μm thick [14]. In mixed and hydrodynamic lubrication, microtextures generate additional hydrodynamic lift, which can increase the load-bearing capacity of the contact surface and form a viscous liquid film with a thickness of 1–100 μm [15]. Moreover, the presence of microtextures reduces the overall contact area, leading to fewer asperity contacts and less adhesion/abrasion [16].

The friction reduction performance of surface texturing is greatly influenced by structural characteristics, such as shape [17, 18], density [19], depth [20, 21], aspect ratio [22], etc. Most fundamental research has concentrated on these parameters to determine if there are optimal values for achieving the best friction reduction across different lubrication regimes, and if there exists a qualitative relationship between microtexture parameters, operating conditions, and frictional performance. It is worth noting that the function of microtextures and optimal microtexture parameters are closely related to the contact type between the tribological pairs (parallel, converging, line, or point contacts) and operating conditions (load, speed [23, 24]). There is no universal selection of the microtexture parameters that could generate beneficial effects for different working conditions [25]. For certain contacts or working conditions (i.e. low-speed, high-pressure, non-conformal contacts), the propensity for microtextures to collapse makes it difficult to form a stable lubrication film, which may lead to detrimental effects. Accordingly, the design of surface texturing needs to be closely aligned with the functional requirements of specific applications [26]. Additionally, a potential strategy for improving the tribological performance of microtextured surfaces under severe conditions is to combine microtextures with modified lubricants [27, 28], surface coatings [29, 30], external energy fields [31], or surface hardening techniques [32–34] (figure 1(a)). The research focused on synergistic effects is extremely valuable for future industrial design and development, and it is likely to become a key trend in optimizing friction and wear performance.

According to the microtexture morphology of the surface, the processing methods can be divided into additive manufacturing, subtractive manufacturing, and formative manufacturing (figure 1(b)) [35]. The common microtexture manufacturing techniques mainly include laser processing [36–39], etching technology [40], ultrasonic-assisted machining [41, 42], electrical discharge machining [43, 44], 3D printing [45, 46], and traditional machining methods, such as turning, drilling and milling, etc [47]. Each technique presents its own advantages and disadvantages in terms of flexibility, accuracy, cost of microtexture fabrication, and processing speed [26]. Laser processing can rapidly create microtextures on material surfaces while precisely controlling accuracy, making it one of the most successful methods for forming controlled microtextures. At present, friction reduction technologies for surface texturing have been used in the aerospace field, transportation field, machine tool field, biomedical field, wind energy fields, and other new fields [48, 49], especially in bearings [50], gears [51], piston rings [52], tools [53], artificial joints [54], and mechanical seals [55] (figure 1(c)). Despite the considerable progress that has been made, microtextured surfaces can have adverse effects in certain circumstances. This largely depends on contact types, operational conditions, material properties, environmental factors, etc [56]. Moreover, the absence of standardized theoretical models poses challenges in designing

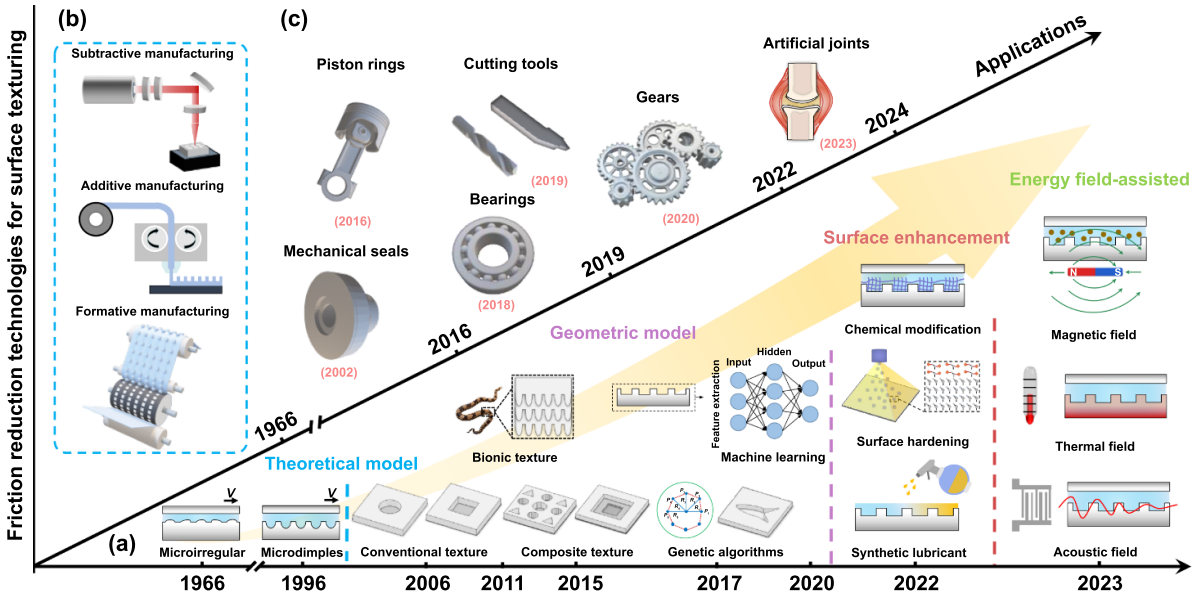

Figure 1. Development of friction reduction technologies for surface texturing. (a) Designing and optimizing friction reduction performance on microtextured surfaces involves theoretical models, geometric morphology, surface modification, and external multi-energy field-assisted. Reprinted from [58], © 2017 Elsevier Ltd All rights reserved. (b) Microtextured surface manufacturing techniques include additive manufacturing, subtractive manufacturing, and formative manufacturing. . Reprinted with permission from [59]. Copyright (2022) American Chemical Society. Reprinted from [60], © 2023 Elsevier B.V. All rights reserved. Reprinted from [61], © 2017 Elsevier Ltd and Techna Group S.r.l. All rights reserved. (c) Microtextured surfaces are primarily applied to mechanical seals, piston rings, bearings, cutting tools, gears, and artificial joints.

universally applicable microtextured surfaces. Therefore, it is essential to guide researchers to design optimal microtextures and develop efficient and green methods for scalable and large-area fabrication [57].

Various review articles from Gropper *et al* [62] (design and modeling), Gachot *et al* [63] (effects on different lubrication regimes), Marian *et al* [11] (modeling and optimization approaches), Wu *et al* [64] (manufacturing), Rosenkranz *et al* [65, 66] (application, synergistic effects with solid lubricants), Wang *et al* [67] (shape and arrangement), as well as Grützmacher *et al* [68, 69] (multi-scale microtextures, thermocapillary lubricant migration), highlight the key findings on surface texturing in various tribological contacts/systems. This review aims to provide a comprehensive overview of the synergistic effects between surface texturing technology and other friction reduction optimization strategies, the advantages and disadvantages of different manufacturing technologies, typical applications, and technical challenges. Chapter 2 provides an introduction to lubricated contact models of unit microtextures. Chapter 3 summarizes structural optimization strategies and synergistic effects with modified lubricants, surface coatings, external energy fields, or surface enhancement techniques of surface texturing. Chapter 4 and Chapter 5 review the latest research advancements in the manufacturing techniques and applications of surface texturing, respectively. Chapter 6 summarizes the challenges of surface texturing technology, including limited operational range, instability in friction reduction, and inadequate load-bearing capacity of microtextures, as well as the emerging trends in developing intelligent, environment-adaptive microtexture systems.

2. Lubricated contact model of microtextured surfaces

The hydrodynamic effect generated by surface texturing is the only one captured by theoretical models, which boosts the dynamic fluid pressure, thus increasing the overall load carrying capacity of the contact in cases of mixed and hydrodynamic lubrication. The key to developing a lubrication model for surface texturing lies in the construction of the geometric model. Due to the periodic distribution of microtextures, a single microtexture unit is often selected for analysis and is characterized by its three-dimensional geometry (surface and cross-sectional shapes) and size (base dimensions (r_p), depth ($h_{texture}$)) (figure 2(a)) [11, 14, 62]. Other critical parameters include the aspect ratio ($\lambda = h_{texture}/r_p$) and density ($\rho_{texture} = A_{texture}/A_{cell}$). Currently, two main models are commonly used to analyze the lubrication performance of surface texturing (figure 2(b)).

The first model is based on the Navier–Stokes(N–S) equations for incompressible flow [70]:

$$\rho\frac{DV}{Dt} = -\nabla p + \rho f + \mu\nabla^2 V. \tag{1}$$

Where $\rho\frac{DV}{Dt}$ represents the inertia term, describing the change in velocity of liquid microelements over time and position, and reflecting the inertia of liquid flow. ρ is the density of the lubricant, kg·m^{-3}. V is the velocity vector. $-\nabla p$ represents the scalar form of pressure gradient, where p is the pressure, Pa. ρf represents volume forces, where f is the external force per unit volume acting on the liquid. $\mu\nabla^2 V$ represents the viscous term, where η is the dynamic viscosity,

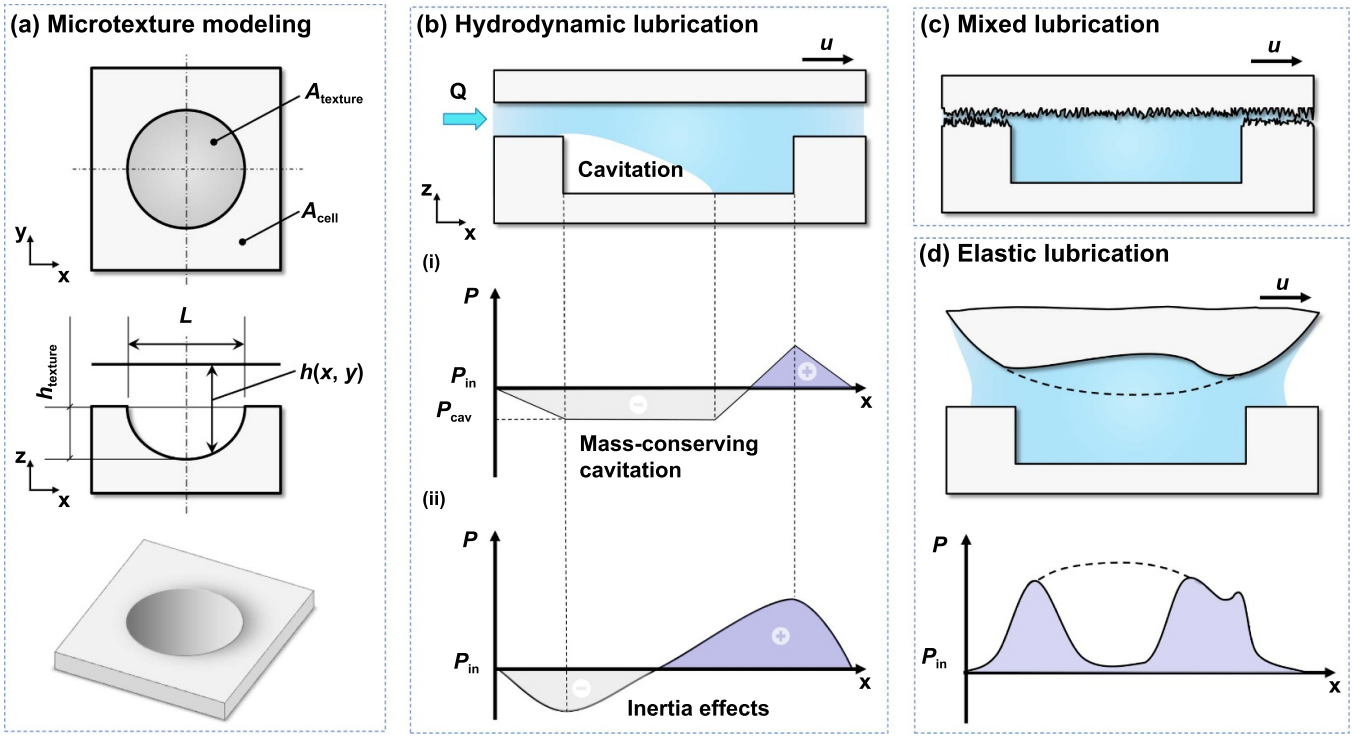

Figure 2. The lubricated contact model of microtextured surfaces. (a) Unit microtexture parameters. (b) Typical pressure distribution over a single microtexture with cavitation. (i) With mass-conserving algorithm. (ii) With inertia effects. Reproduced from [62]. CC BY 4.0. (c) Contact model of mixed lubrication for a single microtexture. Reproduced from [14]. © The Author(s). Published by IOP Publishing Ltd CC BY 4.0. (d) Contact model of elastic hydrodynamic lubrication and typical pressure distribution for a single microtexture.

Pa•s. Currently, the flow behavior of lubricants on microtextured surfaces is predominantly simulated using commercial computational fluid dynamics (CFD) software or purpose-built solvers. However, this approach still demands relatively high and time-consuming computational resources, particularly for microtextured contacts, due to the necessity of fine meshing, potential time-dependent effects, and the risk of numerical instability.

The second foundational model is the Reynolds equation based on the mass conservation method [71]:

$$\frac{\partial}{\partial x}\left(\frac{\rho h^3}{\eta}\frac{\partial p}{\partial x}\right)+\frac{\partial}{\partial y}\left(\frac{\rho h^3}{\eta}\frac{\partial p}{\partial y}\right) = 6\frac{\partial(uph)}{\partial x}+6\frac{\partial(vph)}{\partial y}+12\frac{\partial(\rho h)}{\partial t}. \quad (2)$$

Expanding the equation on the right-hand side: $u\rho(\partial h/\partial x)$, $v\rho(\partial h/\partial y)$ represent the dynamic pressure effect, $h\rho(\partial u/\partial x)$, $h\rho(\partial v/\partial y)$ represent the stretching effect, $uh(\partial\rho/\partial x)$, $vh(\partial\rho/\partial y)$ represent the variable density effect, and $\rho(\partial h/\partial t)$ represent the compression effect. Where h is the lubricant film thickness, m. u and v represent the velocities in the x-directions and y-directions of tribo-pair, $\mathrm{m{\cdot}s^{-1}}$, respectively.

In equation (2), the effect of surface texturing is incorporated through the film thickness equation $h(x, y)$. Within the microtextured region, the film thickness is influenced by the shape and dimensions of the microtexture, whereas outside the microtextured region, the film thickness is generally assumed to remain constant. The present study focuses on the fluid-lubricated region and assumes that the surface outside the microtextured region is perfectly smooth. However, if the surface roughness dimensions are comparable to the microstructure and oil film thickness, the asperities on the tribo-pair may come into contact and partial load-bearing, i.e., mixed lubrication (figure 2(c)) [72–74]. Moreover, high contact pressure induces elastic deformation of the tribo-pair, which increases the density and viscosity of the lubricating oil, thereby leading to changes in oil film thickness and stability, i.e. elastic hydrodynamic lubrication (figure 2(d)) [75–79]. That is to say, it is essential to account for the actual machined surface shape and the elastic deformation of the contacting surfaces and to incorporate these factors into the modified Reynolds equations for more accurate simulation results.

The discretization and integration methods are used to solve the governing two-dimensional Reynolds equation multiple times, which can yield performance characteristics such as load capacity, friction coefficient, and minimum film thickness [80]. Discretization methods applied to the field of surface microtextures include the finite difference method (FDM), finite volume method (FVM), finite element method (FEM), finite cell method (FCM), and spectral element method (SEM) (table 1). Also, the performance characteristics must be calculated using numerical integration methods. e.g. Newton–Cotes (NC) formulas and Gauss quadratures [80, 81].

Table 1. Discretization methods.

Approach	Characteristics	References
FDM	Discretizing the computational domain into grid points and employing approximate solutions at these points to approximate continuous functions	[82, 83]
FVM	Discretizing the computational domain into control volumes, discretizing conservation equations within these volumes, and solving for numerical solutions	[84]
FEM	Discretizing the computational domain into shape elements and generating numerical solutions by appropriately addressing continuity between elements and applying boundary conditions	[85, 86]
FCM	Discretizing the computational domain into Cartesian cells, enabling the inclusion of complex geometries without meshing, and employing high-order approximations for accurate numerical solutions.	[87]
FEM	Discretizing only the boundaries of the computational domain into elements, reducing the dimensionality of the problem, and solving for numerical solutions using boundary integral equations	[88]

The debate regarding the feasibility of using the Reynolds equation in surface texturing modeling, as opposed to the N–S equations, stems from its neglect of fluid inertia effects. However, inertia effects can often provide additional load carrying capacity only in flows with high Reynolds numbers or when the critical depth of microtexture is reached [89, 90]. Generally, when the ratio of the inertial term to the viscous term, i.e. $o(\mathrm{Re}\delta^2)$ « 1 [91], the influence of the inertial term can be neglected. In microtextured friction pairs, the Reynolds number Re generally ranges from 1 to 10^2–10^3. The depth-to-diameter ratio of the microtexture generally ranges from 10^{-2}–10^{-1}, and the ratio of the microtexture spacing to the diameter/width is typically on the order of 10°. The ratio of microtexture depth to the clearance of the friction pair surface can reach the order of 10^1, resulting in the clearance ratio δ (the ratio of the surface clearance to the length of the contact area in friction pairs) being in the range of 10^{-3}–10^{-1}. In this case, $o(\mathrm{Re}\delta^2)$ ranges from 10^{-6}–10^1, allowing the use of the Reynolds equation instead of the N–S equation [92–94].

Modeling plays a critical role in advancing the adoption of surface texturing technology, while the majority of model validations are performed through comparisons with other modeling work rather than through experimental tests. Moreover, the performance of different models mostly depends on the respective working conditions, which significantly hinders their applicability in industrial applications. Therefore, the design of microtextures must be based on the underlying kinematics, dynamics, and contact types of the tribo-pair. It is essential to develop effective optimization methods to enable the evaluation of microtexture design using robust numerical models before manufacturing, thereby avoiding time-consuming trial-and-error experiments.

3. Optimizing friction reduction performance on microtextured surfaces

The discrete (discontinuous dimples) and continuous microtextures (parallel or cross-continuous grooves) with regular geometric shapes attract great research interest, primarily investigating their effects on tribological performance from the perspectives of surface shape or bottom shape (figures 3(a) and (b)) [95]. The design of microtexture shapes mostly depends on the sliding direction of the friction pair. Under unidirectional sliding, increasing the high-pressure contact area of the microtextured surface perpendicular to the sliding direction can generate higher net thrust and reduce friction and wear. It is important to note that the comparison of tribological performance between different microtexture shapes is only meaningful at optimal geometric parameters [96]. With advancements in biomimicry, microtextures are transitioning from traditional regular geometric shapes to bio-inspired structures that enhance friction reduction and wear resistance (figure 3(c)). The complex and orderly micro–nano structure arrays found on surfaces of living organisms have significant exploratory value for frictional contact interfaces [97]. However, constrained by manufacturing techniques, biomimetic microtextures often undergo a degree of simplification. Presently, strategies to reduce friction on microtextured surfaces are predominantly centered on structures, lubricant characteristics, and energy field-assisted lubrication.

3.1. Microtexture

3.1.1. Structural optimization. In the field of friction reduction of microtextures, classification methods for microtextures vary widely, encompassing criteria such as symmetry (symmetric vs. asymmetric microtextures), composition (single vs. composite microtextures), and shape (regular vs. irregular shapes). This article categorizes microtextures based on whether their distribution has been optimized, dividing them into uniform distributions (where single structures like inverted pyramids and droplets are considered uniform) and non-uniform distributions. It describes five types of optimized non-uniform distributions: fractal structures, multi-shape composite structures, gradient structures, localized structures, and micro–nano structures (figure 4). These five configurations

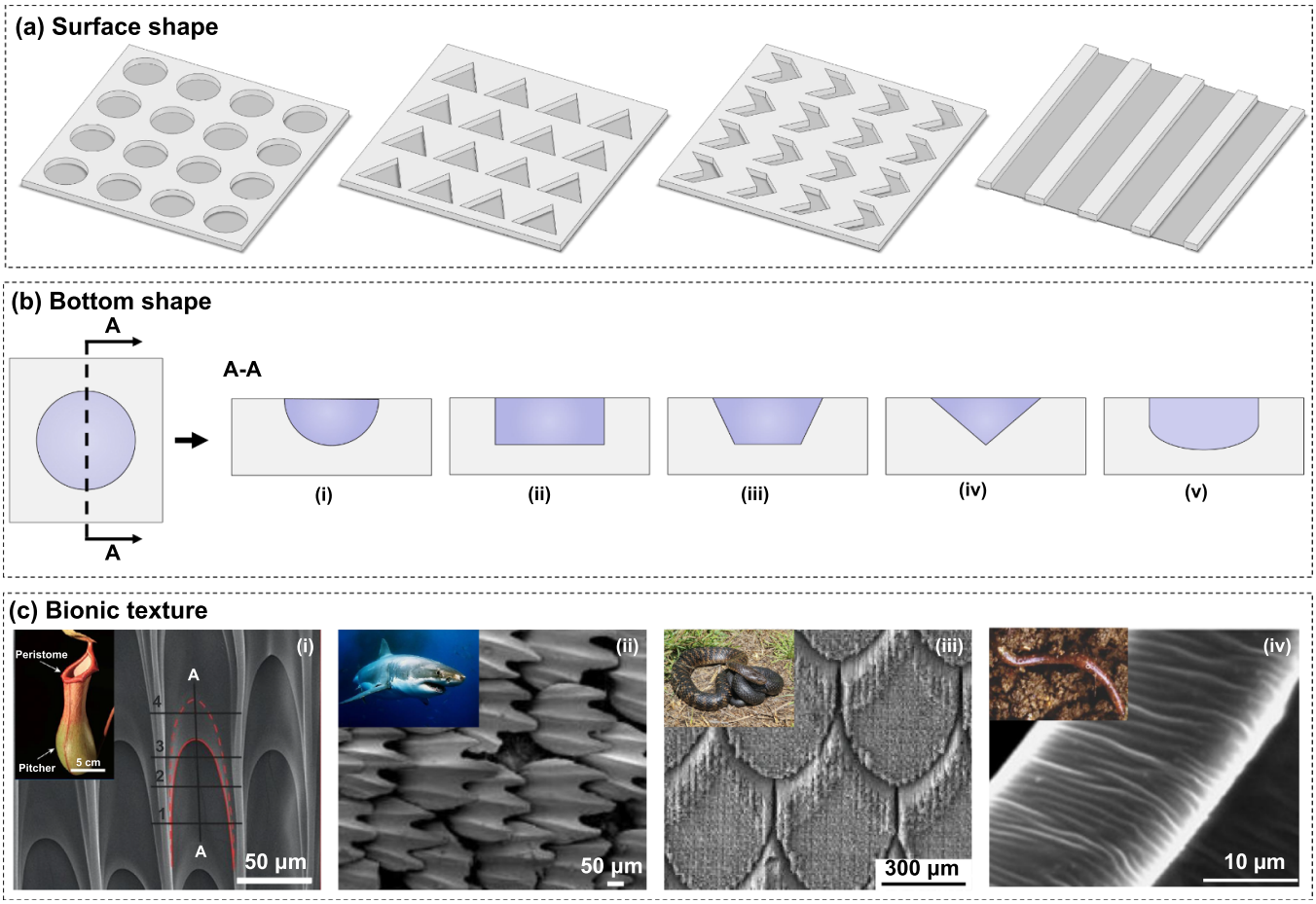

Figure 3. Microgeometry characteristics of microtextured surface. (a) Surface shapes. Circle, triangular, chevron-like, and groove. (b) Bottom shapes. (i) Spherical. (ii) Rectangular. (iii) Beveled rectangular. (iv) Triangular symmetrical. (v) Rectangle with a rounded bottom. Reproduced from [11]. CC BY 4.0. (c) Bionic microtextures, including (i) the peristome surface of nepenthes alata, (ii) shark skin, (iii) snake scale, and (iv) earthworm skin. Reproduced from [98], with permission from Springer Nature. Reprinted from [99], Copyright © 2012 Elsevier Inc. All rights reserved. Reproduced from [100]. CC BY 4.0. Reprinted with permission from [101]. Copyright (2021) American Chemical Society.

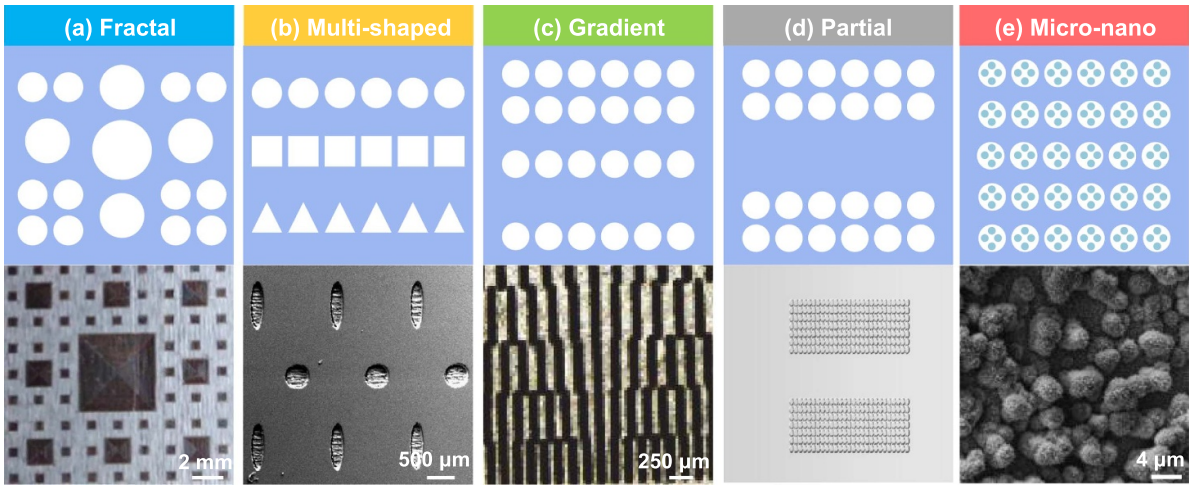

Figure 4. Composite surface texturing. (a) Fractal microtextures. Reprinted from [102], © 2016 Elsevier B.V. All rights reserved. (b) Multi-shaped microtextures. Reprinted from [103], Copyright © 2015 Elsevier Ltd All rights reserved. (c) Gradient microtextures. Reproduced from [104]. CC BY 4.0. (d) Partial microtextures. Reprinted from [105], Copyright © 2010 Elsevier Ltd All rights reserved. (e) Micro–nanotexture (white: microtexture, green: nanotexture). Reprinted from [106], © 2017 Elsevier B.V. All rights reserved.

enhance hydrodynamic effects, thereby improving the stability and uniformity of the lubrication layer by optimizing microtexture features at both micro and macro scales.

Fractal microtextures (figure 4(a)) significantly reduce the coefficient of friction and enhance wear resistance due to their self-similarity across different scales and irregular arrangements [102]. These structures improve frictional performance by influencing the critical load and exhibit superior friction reduction compared to traditional microtextures under various lubrication states. However, the friction reduction mechanism of fractal microtexture is not very clear. The micro-hydrodynamic effect and lubricating film retention effect provided by different shapes of microtextures are different. The single shape of microtexture often has favorable effects only in limited operational conditions [107]. Consequently, it is an effective method to maintain excellent friction performance by combining different shapes of microtextures to adapt to complex operational conditions. Multi-shaped microtextured surfaces formed by the combination of circular and elliptical pits (figure 4(b)) exhibit lower and more stable friction coefficients compared to non-textured surfaces. Moreover, as the dimple depth and sliding speed increase, the advantages of multi-shaped microtextures become more pronounced [108]. The gradient microtextures oriented in specific directions (figure 4(c)) can guide fluid flow to form a directional lubrication layer and better accommodate the lubricant, while also adjusting local surface pressure distribution to avoid stress concentration. Experiments have shown that gradient microtextures achieve the lowest friction coefficients and wear rates at specific angles, such as 7 degrees [109]. In applications such as thrust bearings, gradient-grooved textures significantly improve oil expulsion and reduce friction, further enhancing the lubrication state [104]. Recent studies have shown that partially microtextured surfaces have better friction reduction properties than fully microtextured surfaces. In parallel slider contact, the partial microtexture (figure 4(d)) at the entrance can increase the flow, resulting in a hydrodynamic lift and full film lubrication [105]. In the application of thrust bearings, a partially textured design can reduce friction power losses by up to 20%, demonstrating significant friction reduction advantages [110]. The surface with tunable multiscale structures plays a key role in promoting localized liquid flow [111]. The micro–nanotexture synergizes micro- and nano-structures (figure 4(e)) to optimize fluid flow and enhance hydrodynamic pressure, thereby achieving friction reduction. The lotus-leaf-like hierarchical micro–nano structure, fabricated through chemical deposition, further reduces friction due to its superhydrophobic properties. Experimental and simulation results show that the optimized distribution and geometry of the microtexture effectively lower the friction coefficient and improve surface lubrication performance [106].

While various geometric designs like fractal, multi-shape, gradient, and partially microtextured surfaces offer effective friction reduction under specific conditions, their performance limitations across diverse operating environments reveal the need for further optimization. The introduction of micro–nanotextures marks a significant breakthrough, merging the benefits of both micro and nano-scale features to enhance lubrication and friction control. Nevertheless, there are still unresolved challenges in fully understanding the underlying friction mechanisms, especially in complex and dynamic lubrication scenarios, which require further investigation.

3.1.1.1. Numerical optimization. Numerical optimization algorithms provide a new research path for the optimization of surface texturing. An optimization model for microtextures is constructed by investigating the relationship between design parameters and tribological performance characteristics, which can significantly improve load-bearing capacity and reduce frictional wear. Moreover, this approach minimizes the traditional trial-and-error process in microtexture optimization. Over the past few decades, numerous strategies for optimizing microtexture have been proposed. These works can be categorized into two primary groups: sensitivity-based optimization techniques [112] and metaheuristic optimization techniques [113].

Sensitivity-based optimization techniques, such as sequential quadratic programming (SQP) [114, 115], level set method [116], method of moving asymptotes [117–119], adjoint method [120], response surface method (RSM) [121], etc, guide the optimization process by identifying the direct relationship between variations in geometric microtexture parameters and corresponding changes in the objective function (i.e. sensitivity analysis). SQP is the most commonly used method for optimizing the shape of microtextures with a fixed depth, treating the design parameters of the microtexture as continuous optimization variables. Based on arbitrary shapes, the chevron-type shape and trapezoid-like shape microtextures exhibit the highest load-carrying capacity for parallel flat surfaces under unidirectional and bidirectional sliding, respectively (figure 5(a)) [114, 115]. However, microtexture depth, as an essential structural parameter, plays a substantial role in the hydrodynamic effects of microtexture. Generally, as the depth of the microtexture increases, the hydrodynamic lubrication effect increases and then diminishes, which results in the friction coefficient reducing first and then increasing. Level set method and adjoint method could change topology and concisely describe the optimal distribution and shape of microtextures, and confirm the linear relationship between the oil film gap and the microtexture depth, thereby maximizing the LCC (figures 5(b) and (c)) [116, 120]. The primary advantage of these methods is that they enable the optimization of the entire gap height distribution $h(x, y)$ without any predetermined geometric shapes [122]. Additionally, the optimization of structural parameters for biomimetic microtextures based on RSM has led to a 20.82% reduction in the coefficient of friction and a 65.65% decrease in wear depth, significantly enhancing the tribological performance of the material surface (figure 5(d)) [121]. Nevertheless, a major limitation of sensitivity-based optimization techniques is their strong

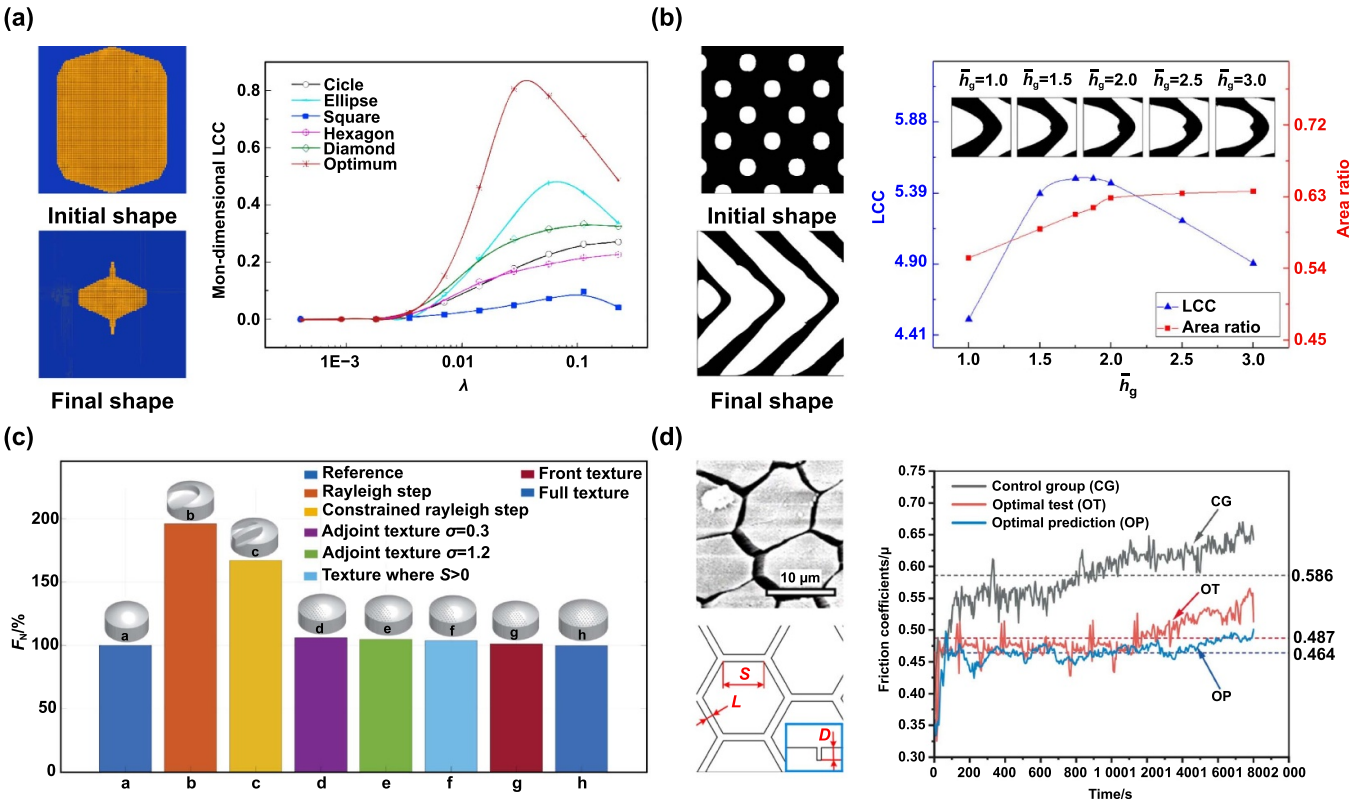

Figure 5. Sensitivity-based optimization techniques for microtextured surfaces. (a) Sequential quadratic programming method. Shape optimization of a single microtexture for reciprocating sliding. Reprinted from [115], Copyright © 2014 Elsevier Ltd All rights reserved. (b) Level set method. Shape optimization of microtexture arrays. Reprinted from [116], © 2021 Elsevier Ltd All rights reserved. (c) Adjoint method. Comparison between different optimization techniques for microtexture. Reproduced with permission from [122]. CC BY-NC-ND 4.0. (d) Response surface method. High-power micrograph (SEM) of a tree frog's pad and schematic diagram illustrating bionic microtexture analysis of surface tribological performance. Reprinted from [121], © 2021 Elsevier Ltd All rights reserved.

dependence on the initial configuration. Moreover, the numerical calculation of sensitivities requires significant computational resources.

Metaheuristic optimization techniques, such as genetic algorithms (GA) [123], particle swarm optimization [124], Monte Carlo search [125], etc, treat the design parameters of microtextures as continuous or discrete optimization variables. GA is the most commonly used method. Zhang *et al* [58, 123] effectively combined the Reynolds equation with GAs to obtain optimal microtexture shapes with low friction coefficients and high load-carrying capacity under mixed lubrication conditions. For reciprocating sliding, the optimal microtextures resemble elliptical and fusiform shapes, while for unidirectional sliding, they take on bullet or fish shapes (figure 6(a)). The study differs from [115], mainly in considering the interaction between adjacent microtextures in the *y*-direction and the detrimental effect of microtexture edges. GA serves as a global search technique, providing the global optimum to SQP for local refinement, thereby accelerating the optimization process and improving convergence rates. Wang *et al* [126] presented a hybrid approach that utilizes a GA solution as the initial configuration required by the SQP method to maximize the LCC of the oil film. The optimized profiles for various rotational speeds all exhibit chevron-shaped grooves. In certain conditions, an optimized groove texture can achieve a consistently low COF (<0.01) and also reduce temperature elevation (figure 6(b)). In general, metaheuristic optimization approaches can efficiently identify near-global-optimal surface microtextures without reliance on the initial configuration or the need for additional sensitivity analysis. However, these approaches can be associated with considerable computational time and expenses, especially given the multitude of geometric features involved. To address this, parametric methods are often employed. However, the selection of parameters is constrained by human expertise.

3.1.1.2. Intelligent optimization. Machine learning (ML) [127], such as artificial neural networks (ANN) [128, 129], transfer learning methods [130], and support vector machines [131], can predict the output of complex nonlinear friction systems without relying on human expertise, generating potential optimal microtexture patterns [132]. The training of these models typically requires a large dataset to capture representative features and patterns, thereby improving generalization capabilities [133]. The data is primarily derived from experimental datasets, simulation results, or information extracted from the literature [134]. The ANN can predict the

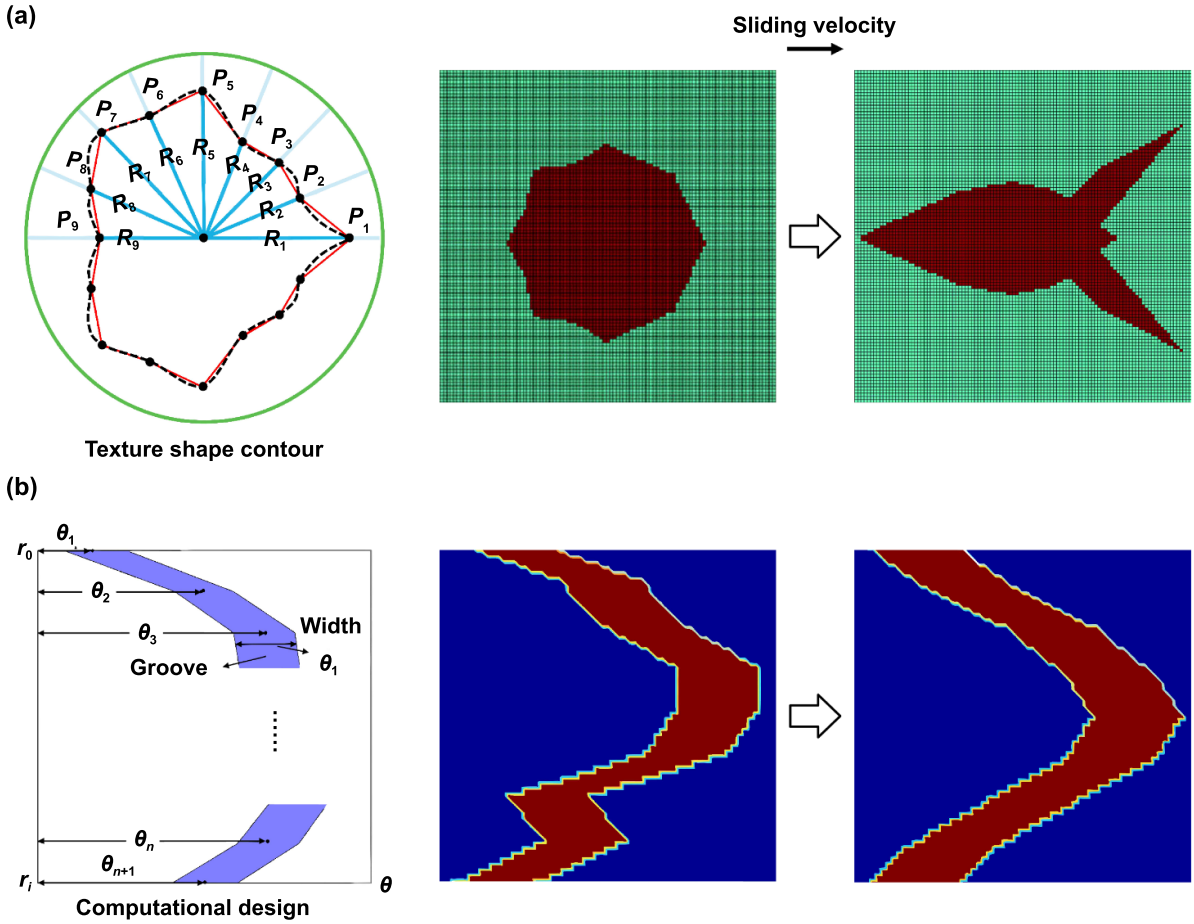

Figure 6. Genetic algorithm-based optimization techniques for microtextured surfaces. (a) Shape optimization of dimple under unidirectional. Reprinted from [58], © 2017 Elsevier Ltd All rights reserved. (b) Shape optimization of groove. Reproduced from [126]. CC BY 4.0.

relationship between microtextured geometric parameters and both frictional force and LCC with accuracies of 99.7% and 97.5%, respectively (figure 7(a)). It is also combined with GA to retrieve the optimal microtexture parameters [128, 129]. Moreover, the combination of ANN and transfer learning can examine the cross-relationships between performance parameters of surface texturing shapes from different categories. This enables the prediction and optimization of tribological performance in different microtexture profiles by training on data from one certain microtexture profile (figure 7(b)) [130]. Some machine-generated designs provide valuable insights into how surface texturing influences the tribological performance of sliding interfaces, providing microtextures with on-demand tribological properties that can be applied in various design fields. Zhu *et al* [132] proposed a machine learning-based universal generative design framework for surface texturing designing by combining specific convolutional neural networks with improved Monte Carlo search. Compared with the reported optimal microtexture, machine-generated microtextures reduce the COF by 27.3%–49.7% and increase the LCC by 126.1%–144.4%, significantly improving tribological performance (figure 7(c)). In the future, machine learning will play a pivotal role in the optimization and design of microtextures, driving the widespread application of microtexture technology across various fields.

3.1.2. Surface treatment. The combination of surface texturing and surface treatment technology can obtain better tribological properties of materials. This synergistic effect not only effectively solves or mitigates the challenges related to balancing material lubrication performance and mechanical strength, but also enhances the overall performance of the workpiece, such as fatigue resistance ability and wear-resistance performance, etc.

3.1.2.1. Advanced coating. The composite technology of surface texturing and surface coating is a potential strategy to enhance the tribological performance of the matrix. Microtextured coating surface, i.e. first coated and then microtextured so that the sliding surfaces were coated, but the microtextures were not. This design minimizes the real contact area and traps wear debris, extending the service life of the coating. Coated surface texturing, i.e. first microtextured and then coated so that the coating covers both the inner and outer surfaces of the microtextures. This design enhances the binding

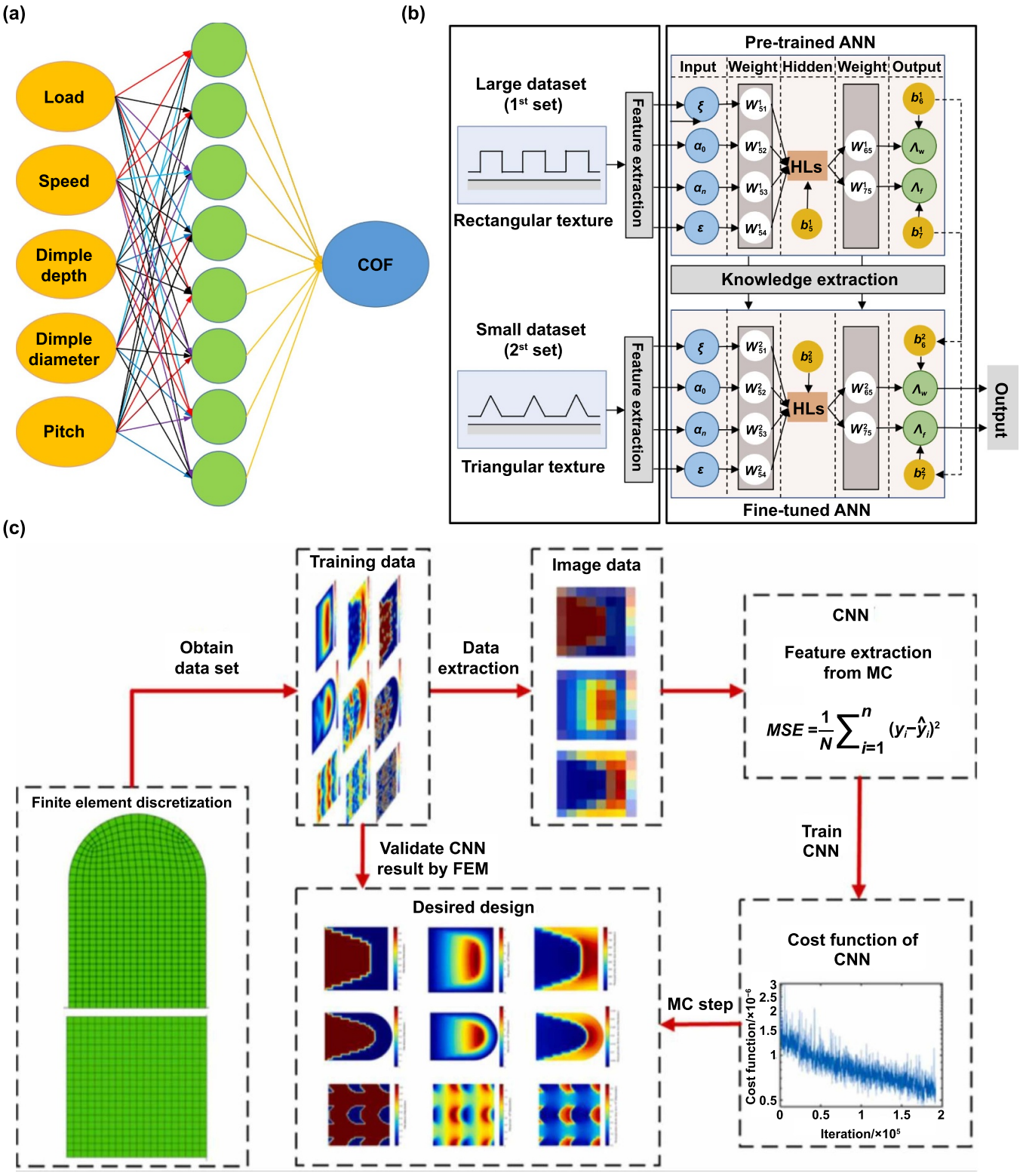

Figure 7. Machine learning-based optimization techniques for surface texturing. (a) Artificial neural network method. Reprinted from [128], © 2020 Elsevier Ltd All rights reserved. (b) Artificial neural network with transfer learning method. Reproduced from [130]. © The Author(s). Published by IOP Publishing Ltd CC BY 4.0. (c) Convolutional neural network with Monte Carlo search method. Reprinted from [132], © 2022 Elsevier Ltd All rights reserved.

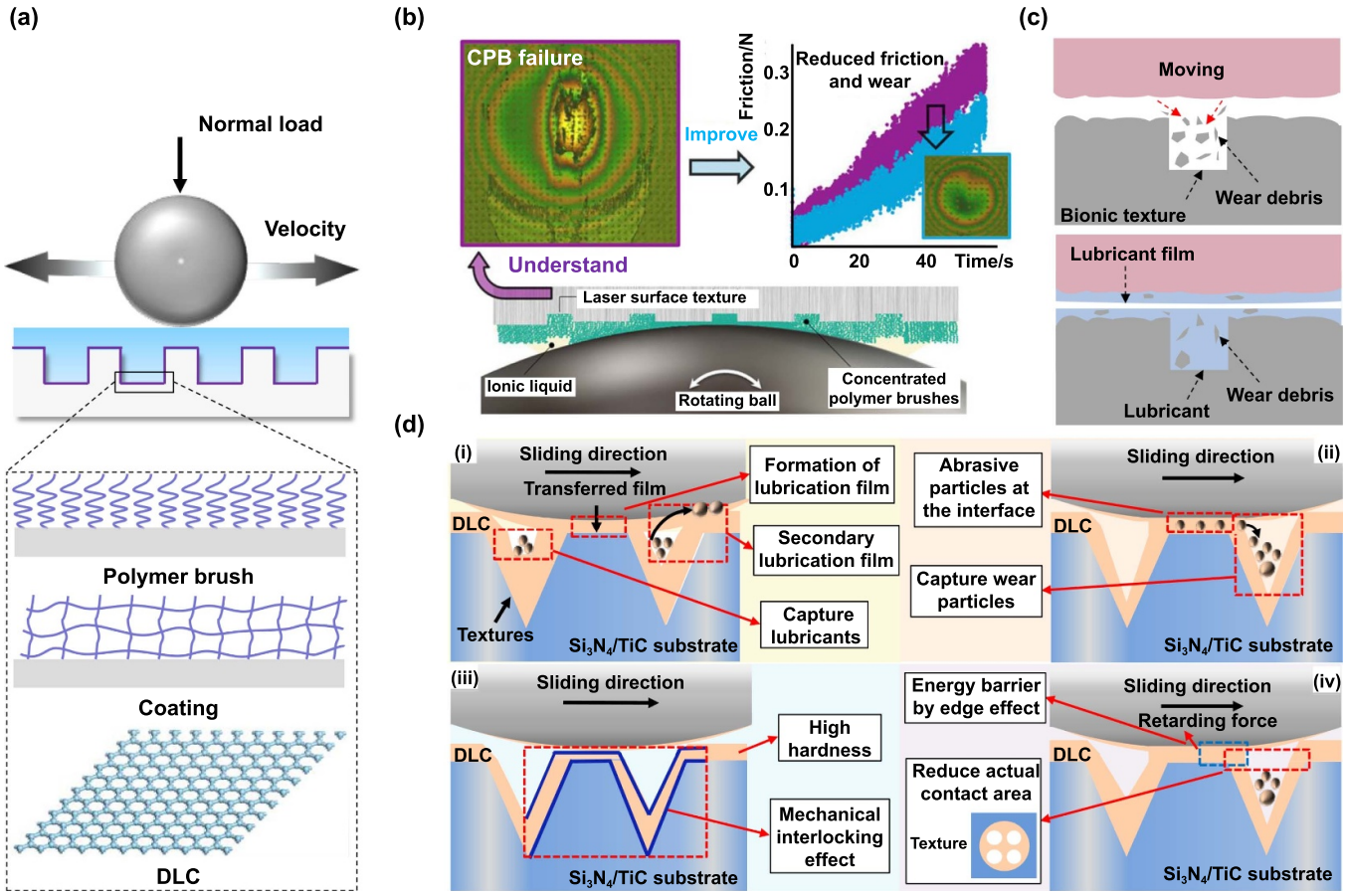

Figure 8. Synergistic effects of surface texturing and advanced coatings. (a) Schematic diagram of friction tests. (b) Polymer brush. Reproduced from [138]. CC BY 4.0. (c) Polytetrafluoroethylene (PTFE). Reprinted from [139], © 2023 Elsevier Ltd All rights reserved. (d) Diamond-like carbon (DLC) films. (i) Formation of lubrication film and secondary lubrication. (ii) Debris capture. (iii) Mechanical interlocking effect. (iv) Reduced contact area. Reprinted from [140], © 2021 Elsevier Ltd and Techna Group S.r.l. All rights reserved.

force between the coating and the matrix. The synergy is attributed to the capacity of the microtextures to store and re-supply the solid lubricant material to the contact area [95, 135]. In recent years, the synergistic reduction of friction and/or wear through the combination of surface texturing with polymer brushes [136, 137], polytetrafluoroethylene (PTFE), or diamond-like carbon (DLC) has garnered significant attention (figure 8(a)).

Polymer brushes exhibit distinctive tribological properties in different solvent environments. When two surfaces coated with polymer brushes come into contact with a good solvent, the steric hindrance effect of polymer chain segments inhibits mutual penetration of the compressed brushes. Thereby preventing contact between the frictional pairs and effectively establishing lubrication [141]. Additionally, polymer brushes can change the lubrication mode and promote the formation of a liquid lubrication film [142]. Klein [143, 144] conducted the first study on the frictional properties of polymer brushes, demonstrating that the mica surface with poly(styrene) brushes exhibits ultra-low friction when sliding against each other. Subsequently, extensive research has been conducted on the frictional properties of polymer brushes using various macroscopic friction test machines [145–148]. However, polymer brushes are easily susceptible to mechanical damage or removal, which limits their industrial applications in mechanical equipment. In a recent series of studies, the combination of CPB with laser surface texturing (LST) methods can result in an average reduction of over 99% in friction at low sliding speeds. Additionally, the microtextured surfaces can enhance the durability of the CPB layer by up to 34%, while also lowering the friction coefficient during long-term sliding tests [138] (figure 8(b)). The improvement in CPB durability stems from the lateral support mechanism of the microtexture, which effectively prevents excessive compression and wear of the flexible brush structure. Simultaneously, the geometric structure of the microtexture disperses contact stresses, reducing stress concentration at individual friction points. The flexibility of polymer brushes further releases localized high-pressure areas, providing additional relief from concentrated stresses. When the frictional interface bears a load, the polymer brushes undergo flexible deformation, penetrating into the microtextures to create localized lubrication zones. This effectively reduces the solid–solid contact area and shear forces, thereby sustaining a long-term low-friction state.

Moreover, the PTFE coating lowers deformation resistance with its low intermolecular shear strength and achieves a significantly lower COF (as low as approximately 0.05) [149].

Furthermore, PTFE can establish a durable transfer film on the counter surface at low pressures, typically in the range of a few thousand pascals. This transformation changes the original frictional contact interface to PTFE–PTFE contact, consequently reducing friction [66]. Nanoscale wear debris stored within the microtextures can enhance the formation of a transfer film. Meanwhile, the stability of the transfer film is influenced by the geometric parameters and density of microtextures, as well as the sliding direction [139, 150] (figure 8(c)). Under starved oil lubrication conditions, low aspect ratio and low areal density of microtexture promote the formation of a uniform and stable transfer film, reducing the negative edge effects of the microtexture, and consequently lowering friction and wear [151]. However, the PTFE molecular structure contains highly electronegative fluorine atoms, and the weak van der Waals forces between molecules prevent the PTFE surface from forming strong chemical attractions, making it difficult to bond with other substances. In an innovative study, Zhao *et al* [152] impregnated microtexture surfaces filled with PFPE into a dopamine solution. Polydopamine can engage in both covalent and non-covalent interactions with PTFE and substrate, enhancing the bonding strength between PTFE and the microtexture. This effectively reduces the rate of PTFE detachment, further enhancing the friction performance. The combination of PTFE with materials like MoS_2, graphene, polyimides, and more has garnered considerable attention. However, the underlying friction and wear mechanisms in these mixtures remain unclear, representing an important avenue for future research.

Combining surface texturing with DLC coating that has low elastic modulus-to-hardness ratios effectively decreases the deformation component of friction by reducing plasticity [153]. The higher contact stresses on the microtextured DLC surface resulted in additional tribochemically induced graphitization. Microtextures can serve as reservoirs for wear particles and lubricating oil. Graphitized wear particles are stored within the microtextures and gradually compacted into a dense graphitized layer during sliding. Thus, the graphitized layer combined with the liquid lubricating film produces a hybrid solid–liquid lubrication effect, resulting in further improvement in friction and wear performance [140, 154]. Furthermore, the pit-and-mountain structure between the DLC coating and the substrate creates a strong mechanical interlocking effect, improving the bonding strength of the coating and substrate then improving the wear resistance while simultaneously enhancing the friction reduction performance of the microtextured surface [155] (figure 8(d)). However, DLC coatings are highly sensitive to the presence of oxidizing agents such as oxygen and water during friction, and the major drawback is low thermal stability at higher working temperatures [156]. The mechanical and frictional properties of DLC coatings can be significantly enhanced by doping with various metals such as Cr, Si, Ti, W, etc. Amanov *et al* [157] examined the frictional properties of microtextured Si-DLC coatings within a temperature range of room temperature to 200 °C. In comparison to non-textured Si-DLC coatings, improvements were observed in both the friction coefficient and wear.

3.1.2.2. Surface hardening. Another strategy for improving the tribological performance of microtextured surfaces involves combining surface texturing with surface hardening technologies such as plasma treatment, ion implantation, and shot peening (figures 9(a)–(c)). Microgrooves treated through plasma-enhanced nitriding exhibit superior friction reduction and wear resistance, achieving a synergistic effect that exceeds the sum of its parts (figure 9(d)). Its excellent tribological performance was attributed to the high hardness of the surface nitriding layer, and the microtextures for debris storage, oil storage, and secondary lubrication [158]. Additionally, ion implantation introduces small-radius ions into the interstices of the material lattice, forming Frenkel defects that act to inhibit plastic deformation, thereby significantly enhancing surface hardness and wear resistance [159, 160]. The wear resistance of surfaces treated with nitrogen ions is significantly improved, and the introduction of nitrogen ions reduces the interaction between the surface and the mating face, further lowering the friction coefficient (figure 9(e)) [161, 162]. Shot blasting is spraying high-speed projectile flow onto the surface of parts, causing plastic deformation on the surface, and thus forming a strengthened layer. There is a high residual stress in the strengthened layer, which can offset part of the stress when the part bears the load, thus improving the fatigue strength of the part. Although this process increases surface roughness, it also creates numerous micro-pits [163, 164], which serve as effective secondary lubrication points and can reduce the friction coefficient. Resendiz *et al* [32] prepared multi-scale microtextures on aluminum alloy surfaces by shot blasting and end milling technology. The experimental results show that the friction coefficient of the microtextured surfaces after shot blasting is further reduced.

However, despite the promising results in reducing friction and enhancing wear resistance offered by these technologies, their practical application faces challenges in terms of cost-effectiveness, complexity of treatment, and durability verification. Moreover, the implementation of these technologies requires precise control over processing parameters to avoid degradation of material properties and must consider the potential increase in environmental impact.

3.2. Liquid lubricants

Conventional liquid lubricants are primarily composed of organic hydrocarbon compounds. They suffer from inadequate thermal stability, are prone to decomposition in harsh conditions, and often experience oil film rupture at friction interfaces. These factors contribute to lubrication failure and an increase in frictional resistance. Presently, enhancing lubrication performance and reducing friction and wear are effectively achieved through the inclusion of additives such as nanoparticles (NPs) and ionic liquids (ILs) in the base oil, as well as the utilization of innovative lubricants like liquid metal (LM).

3.2.1. Nanoparticle lubricants. Nanoparticles (NPs, 1–100 nm) are playing an increasingly significant role as innovative lubricant additives, contributing significantly to

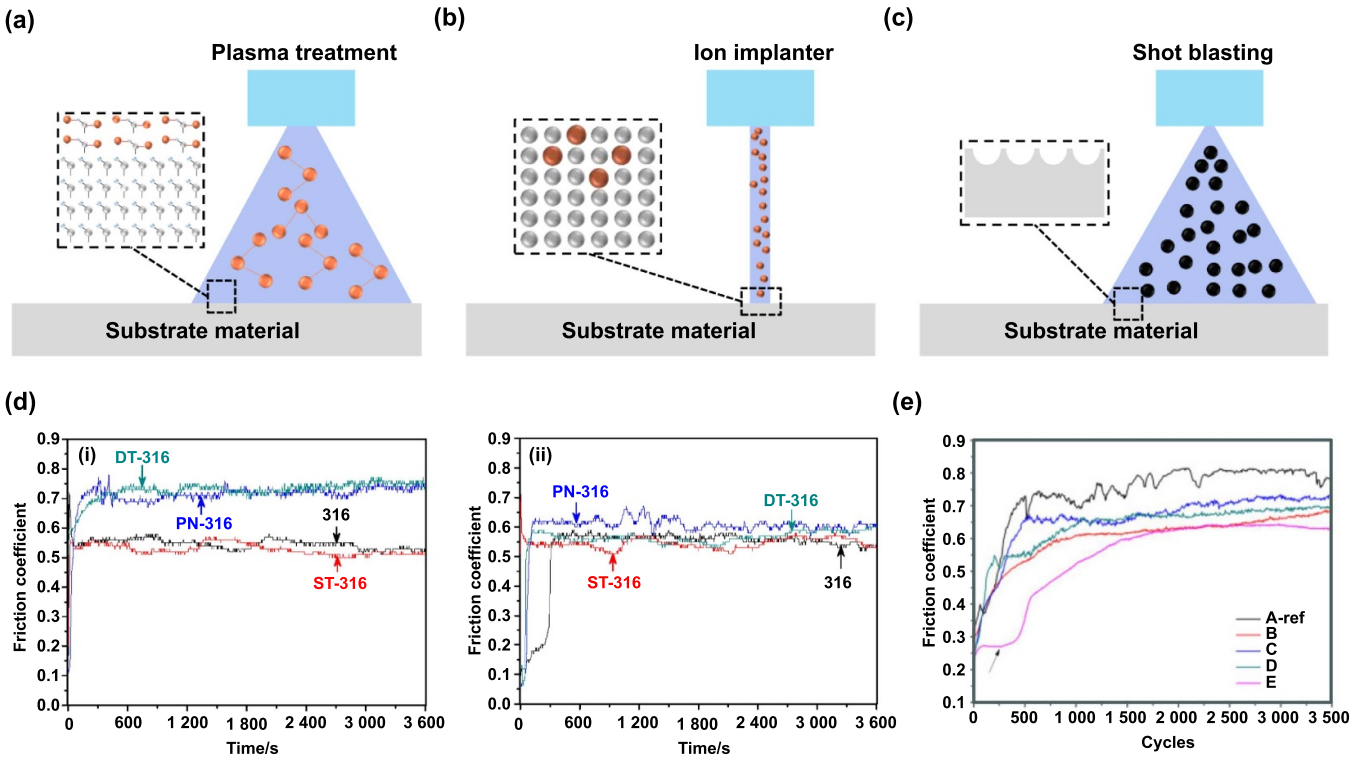

Figure 9. Surface hardening optimization methods for the microtextured surface. (a) Plasma treatment. (b) Ion implantation treatment. (c) Shot blasting treatment. (d) The COF for microtextured surfaces of different materials before and after plasma nitriding treatment. (i) GCr15. (ii) Si_3N_4. Reproduced from [158]. CC BY 4.0. (e) The COF of microtextured surfaces under various implantation energy and implantation doses. Reprinted from [162], Copyright © 2015 Elsevier B.V. All rights reserved.

the enhancement of tribological performance and emissions reduction [165]. Frequently employed nanomaterials as additives in lubricants including, metals (such as aluminum, silver, and copper) [166], oxides (such as ZrO_2, TiO_2, ZnO, CuO) [167], sulfides (such as MoS_2, WS_2, CuS) [168], and carbon nanomaterials (graphene, carbon quantum dots, carbon nanotubes) [169, 170]. Metal NPs exhibit exceptionally high surface energy, enabling them to adsorb effectively onto friction surfaces. A friction film with excellent friction reduction and wear resistance is formed through tribochemical reactions or by serving as a source of metal cations [171]. However, metal NPs tend to agglomerate, and difficult to maintain long-term dispersion stability in practical applications, which limits their applicability as lubricant additives. Surface modification is the most effective method for addressing the aforementioned issues [172]. Oxide NPs exhibit better chemical stability. However, the efficient and facile preparation of oxide NPs with homogeneous particle size and controllable morphology remains a challenge [173]. The sulfur in sulfides can promote the reaction of NPs with the friction interface, forming high-performance tribofilm that contributes to friction reduction and wear resistance [174]. However, sulfide additives may release harmful compounds, leading to environmental pollution. Carbon nanomaterials exhibit excellent oxidation resistance, chemical inertness, self-lubricating properties, and superior mechanical strength. However, the preparation of carbon nanomaterials is complex and costly, and their interfacial interactions within lubrication systems remain unclear [175, 176]. Overall, NPs exhibit friction reduction and wear resistance due to their unique structure and properties, offering promising prospects for the development of nanoscale lubricant additives.

The synergistic effects of surface texturing and NPs lubricant additives significantly enhance friction reduction and wear resistance in tribo-pair, which outperforms the simple additive effect of the two components (figure 10(a)). Firstly, microtextures serve as NPs reservoirs to enhance the hydrodynamic effect. During the friction process, the interaction and compression between the contact surfaces result in some of the lubricant and wear debris entering the microtextures. Simultaneously, part of the lubricant and NPs previously retained in the microtextures is partially transferred to the friction contact area as the friction pair moves. This not only enhances the hydrodynamic lubrication effect but also supplies secondary lubrication to oil-deficient regions near the motion extremes. Additionally, it promotes the accelerated deposition of NPs on the friction surface, forming a lubricating film layer with friction reduction and wear resistance properties. Secondly, NPs can effectively utilize the structural features of the microtextures to maximize their film-forming and surface-repairing capabilities. Due to the frictional shear forces, a portion of the NPs is deposited on the worn microtextured surface, acting as a repair agent by filling the wear scars and defect areas [177, 178]. The remaining NPs form a lubricating film on the friction surface under electrochemical or metallurgical effects, thereby reducing adhesion through the

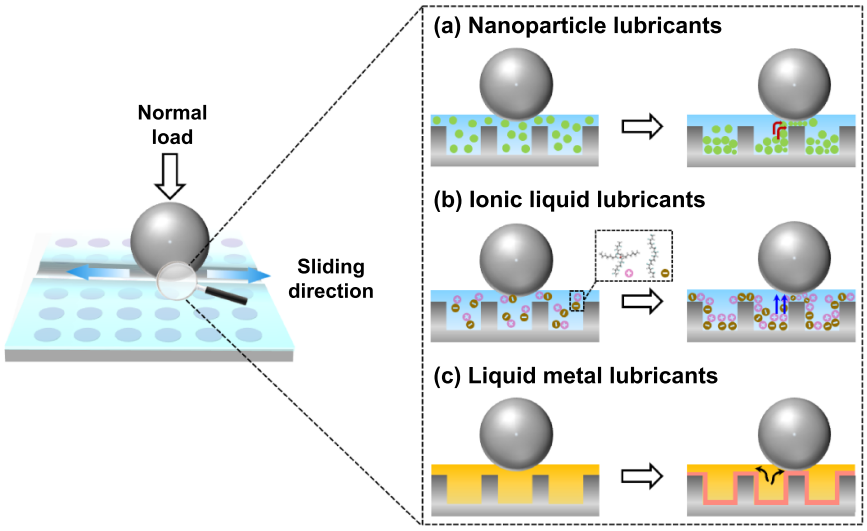

Figure 10. Synergistic principles of microtextures and lubricants. (a) Nanoparticle lubricants. (b) Ionic liquid lubricants. (c) Liquid metal lubricants.

third-body effect of the fine particles [179]. Thirdly, NPs act as rolling bearings at the friction interface. Under boundary lubrication, the NPs partially bear the load and form a protective film between the surfaces, preventing adhesion and thus improving tribological performance [180].

3.2.2. Ionic liquids lubricants. Ionic liquids refer to liquid substances composed of both anions and cations at or near room temperature [181]. Compared to traditional lubricating oils, the customizable nature of anions and cations in ILs gives rise to distinctive physical and chemical properties. These characteristics include high thermal stability, low flammability, and reduced sensitivity of rheological behavior to environmental changes [182]. Numerous studies have validated the efficacy of IL as a standalone lubricant. Nevertheless, economic constraints exist, and most IL lubricants have relatively low solubility in common lubricating oils (less than 1%). Until 2012, Qu *et al* [183] managed to enhance the solubility of IL in lubricating oils by reducing the ionic charge density. Since then, the use of IL as an oil lubricant additive has emerged as a central theme in the realm of IL lubrication [184, 185]. The synergistic effects of ILs and surface texturing are primarily reflected in two aspects (figure 10(b)). Firstly, anions in the IL are adsorbed onto the contact surfaces through electrostatic attraction, forming an effective boundary lubrication film. Meanwhile, cations interact with anions to form a chemically reactive film. The formation of these films significantly reduces friction and wear. Secondly, the high viscosity of IL enhances the hydrodynamic effect generated by the microtextures, forming a thicker lubrication film. This effectively prevents direct contact between the sliding surfaces and the substrate during the friction process, thereby contributing to friction reduction and anti-wear [186]. Currently, research on the composite systems of surface texturing and IL lubricants is relatively limited, with most studies focusing on the interactions between different IL lubricants and microtextures. Thakre *et al* [187] examined the micro-scale lubrication behavior of seven different IL lubricants on surfaces with varying roughness. They discovered that the combination of microtexture, friction pair materials, and IL lubricants has a substantial impact on the surface contact behavior of friction pairs. Samanta *et al* [188] conducted a study on the interaction between nanoscale microtextured steel surfaces and various IL lubricants. The results of friction experiments indicated that ammonium-based IL lubricants can significantly reduce the friction coefficient, while lithium-based IL lubricants offer the lowest wear rate.

3.2.3. Liquid metal lubricants. LM lubricants are a new type of liquid lubricant used in aviation and nuclear industries [189–191]. LMs can maintain remarkably low vapor pressure under high-temperature or vacuum conditions, meeting the lubrication needs of a broad temperature range and vacuum environments [192]. Furthermore, they retain the highly thermal and electrical conductivity of metals, allowing for the rapid dissipation of frictional heat, reducing adhesion within the friction pair, and showcasing outstanding extreme pressure performance [193]. As early as 1963, Hughes described the application of LMs as high-temperature conductive lubricants in bearings [194]. Subsequently, extensive research has been conducted on the lubrication performance of LM lubricants in HL, boundary lubrication, and mixed lubrication states. Under low load and high-speed friction conditions, they can provide low friction coefficients of 0.01 [195, 196]. Under boundary and mixed lubrication conditions, friction coefficients range from 0.1 to 0.6 [197, 198]. LM can be stored within the microtextured surface and subsequently migrated to the friction interface under compressive forces, forming a low-shear strength boundary layer. Simultaneously, LM generates an oxide film in aerobic and an adhesive film in anaerobic conditions. During the transition of LM to a paste, it might adhere to the contact area, thereby reducing friction and wear (figure 10(c)) [199]. LM lubricants are highly sensitive to

load and sliding speed, with higher speeds being more conducive to their lubrication capabilities [200]. Moreover, LM can replace solid lubricants and work synergistically with microtextures in vacuum environments to achieve low friction and enhanced durability. Currently, the lubrication behavior and mechanisms of LM lubricants combined with surface textures, and the tribological behavior under varying environmental conditions remains insufficiently explored.

3.3. Energy field-assisted

3.3.1. Magnetic field(MF)-assisted. MF is a colloidal system composed of dispersed single-domain magnetic NPs (10–20 nm) in a carrier liquid [201]. A homogeneous fluid can be magnetized by applying an external magnetic field. By controlling the intensity and direction of the magnetic field, the magnetic fluid can be manipulated arbitrarily [202]. This led MF to get significant applications in sealing, lubrication, and grinding engineering [203]. Magnetic fluid lubricants can be retained at frictional interfaces through the action of specially designed magnetic fields, thereby enhancing lubrication, preventing lubricant leakage, and reducing the overall amount of lubricant required [204]. The NPs in the magnetic fluid do not deteriorate but rather improve the lubricating performance [205]. Furthermore, by adjusting the applied magnetic field intensity, it is possible to change the viscosity of the magnetic lubricant, thereby controlling the load-bearing capacity of the lubricant [206]. Therefore, utilizing magnetic fluid lubricants with the assistance of a magnetic field for microtexture modulation holds great potential as a research approach for reducing friction.

Magnetic field-assisted techniques are commonly assessed using a pin-on-disk test rig [207]. This approach primarily involves depositing permanent magnetic materials within the microtexture and employing an external magnetic field to control the magnetic fluid (figure 11(a)). A frequently used experimental combination includes CoNiMnP permanent magnet material and 316 stainless steel (figure 11(b)) [208]. The magnetic-field-assisted microtextured surface facilitates the formation of effective lubrication, leading to a significant reduction in the coefficient of friction. Furthermore, the integration of magnetic nanofluids with microtextured tools is another essential application of this technology. In this scenario, conventional cutting fluids are replaced by magnetic nanofluid lubricants, which, under the influence of a magnetic field, penetrate more efficiently into the microtexture at the tool-workpiece interface (figure 11(c)), thereby ensuring continuous lubrication [209]. Compared to traditional tools and cutting fluids, the combination of microtextured tools and magnetic nanofluid lubricants reduces cutting forces by 48.6% and decreases the surface friction coefficient by 49.1% (figure 11(d)) [210]. Additionally, modifying the properties of magnetic nanofluid lubricants can lead to further improvements in anti-friction performance. For example, co-depositing conventional Fe_3O_4 nanofluid (F-0.5) with Fe_3O_4@CNTs lubricant results in a composite nanofluid (FC-0.5) [211]. Cutting experiments indicate that the cutting forces and tool wear in the microtextured tool + FC-0.5 configuration decrease under the influence of a magnetic field (figure 11(e)). At the maximum magnetic field strength (1 200 G), the cutting force for the microtextured tool + FC-0.5 is reduced by 36.9% compared to the traditional tool + F-0.5, and the surface friction coefficient is reduced by 28.15% compared to the TC + F-0.5 configuration.

However, many designs for magnetic field-assisted microtextures are still in the conceptual stage, with only a limited number successfully applied in industrial settings. Current research on composite machining technology primarily focuses on improving the cutting performance of tools through the application of magnetic fields. However, in other industrial sectors, the use of magnetic field-assisted microtexture friction reduction is uncommon. Moreover, further research is needed to explore the effects of magnetic fields on the capillary action and wettability of magnetic nanofluids at the microtextured blade interface. Additionally, the lubrication and cooling effectiveness of NPs is limited due to NP agglomeration.

3.3.2. Acoustic field-assisted. Friction and vibration are widely present in mechanical systems, and they interact and influence each other. Friction in the components of a mechanical system during operation can lead to the generation of vibrations, affecting the precision of the mechanical work. Sometimes, introducing vibrations into the mechanical system in a controlled manner (with appropriate frequency and amplitude) can significantly reduce friction during the operation of the mechanical system [212–214]. In the field of machining processes, longitudinal and transverse ultrasonic vibrations are effective means to improve processing precision and quality [215]. For instance, the most common method of using vibration to reduce friction is ultrasonic vibration cutting. It has significant applications in enhancing machining accuracy and quality, in turning [216] and cutting [217]. Ultrasonic-assisted machining can reduce cutting forces, improve surface quality, prolong tool life, and provide positive assistance in reducing friction for microtextured surfaces.

Controlled vibration could enhance the average load-bearing capacity of the microtextured surface, expel the lubricant from the dimples, increase the thickness of the lubricant film, and further improve the friction reduction effect [215]. By applying multiple vibrations in different directions to the microtexture surface (figure 12(a)), it has been found that when the amplitude of vibration velocity surpasses that of sliding velocity, a more significant anti-friction effect is observed. Additionally, the friction coefficient of the microtextured surface increases with rising vibration frequency but decreases as the amplitude of vibration velocity grows. Research on the application of microtextured tools in ultrasonic elliptical vibration cutting (UEVC) is still limited, primarily examining the replacement of conventional tools with microtextured variants (figure 12(b)). Experimental results show that,

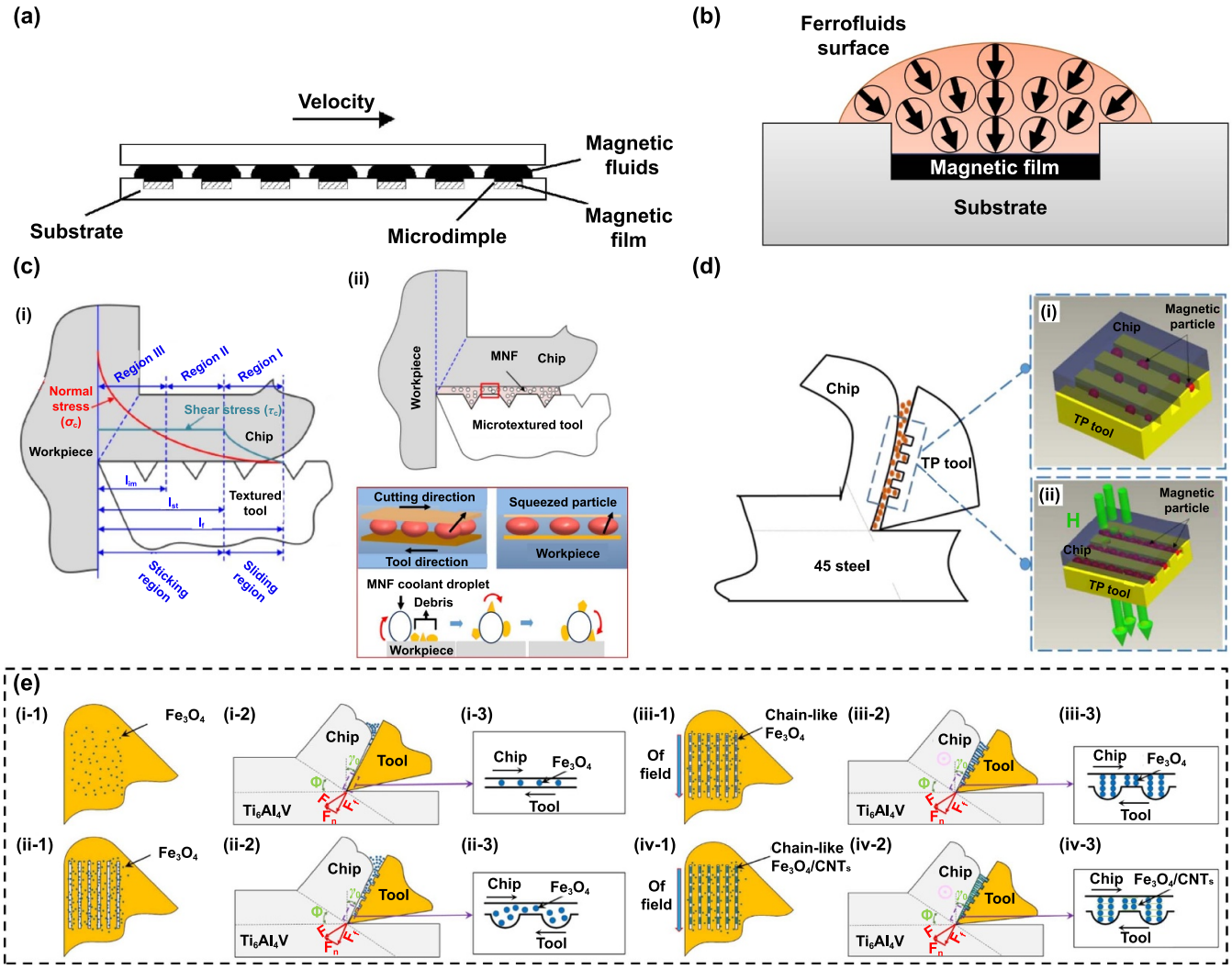

Figure 11. Magnetic field-assisted friction reduction technology for the microtextured surface. (a) Magnetically microtextured surfaces. Reprinted from [207], Copyright © 2009 Elsevier B.V. All rights reserved. (b) Schematic representation of CoNiMnP film within dimples covered with Ferrofluid (FF). (c) Schematic diagram of the 2D cutting model. (i) The correlation between sliding conditions and the location of microtextures. (ii) The infiltration of MNF to the blade interface under the influence of a magnetic field. Reprinted from [209], © 2021 Elsevier B.V. All rights reserved. (d) Schematic diagram of cutting model under the magnetic field. (i) Dispersed magnetic particles on the tool–chip interface. (ii) Gathered magnetic particles on the tool–chip interface. Reprinted from [210], © 2020 Elsevier B.V. All rights reserved. (e) Nanofluid distribution at the micro-contact zone of the tool–chip interface under varied cutting conditions. (i) TC + F-0.5 without magnetic field. (ii) TTC + F-0.5 without magnetic field. (iii) TTC + F-0.5 under magnetic field. (iv) TTC + FC-0.5 under magnetic field. Reprinted from [211], © 2022 The Society of Manufacturing Engineers. Published by Elsevier Ltd All rights reserved.

compared to conventional cutting conditions, microtextured tools exhibit superior performance in cutting force, surface morphology, chip formation, and wear characteristics, resulting in a substantial improvement in overall performance [218].

Currently, there are relatively few studies on the effects of acoustic field-assisted independent friction reduction microtextures or on the role of microtextured tools in UEVC processes. This has led to a scarcity of research samples, and the auxiliary effects of sound fields remain unclear. However, this also highlights that sound field-assisted microtexture friction reduction is a significant and promising area for future research.

3.3.3. Thermal field-assisted. In the field of mechanical engineering, elevated thermal surfaces are a commonly observed phenomenon. The working surfaces experience heating not only from external environmental factors but also generate heat due to friction. During the operation of mechanical equipment, high temperatures can decrease the viscosity of the lubricating oil and weaken the mechanical strength of the lubricating oil film. Elevated thermals also promote frictional chemical reactions on the contacting surfaces, which can be either detrimental to wear behavior (e.g. causing corrosion) or beneficial (e.g. forming a stable friction film) [219]. The removal of frictional heat by the lubricating oil, accelerates the evaporation of the lubricant, forming a vaporized oil film

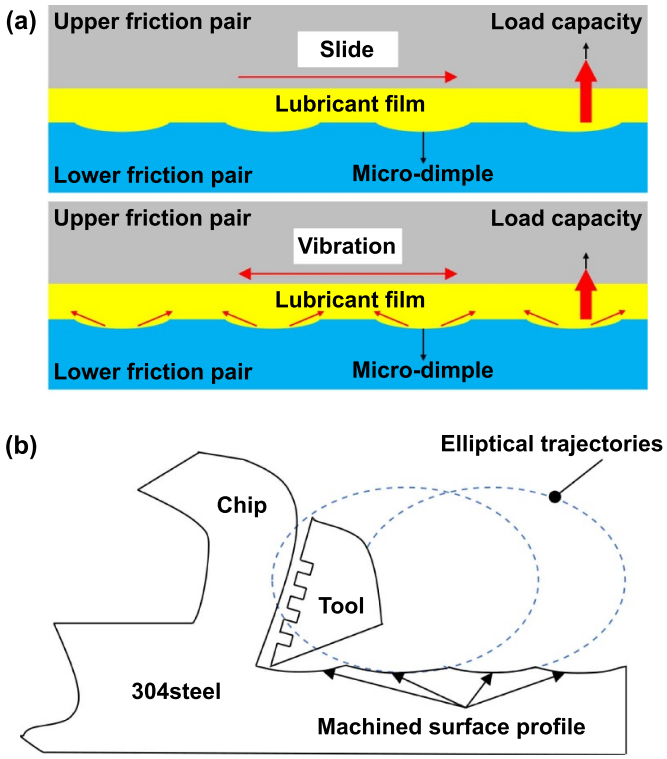

Figure 12. Ultrasonic vibration-assisted friction reduction technology for the microtextured surface. (a) Comparison of lubrication conditions during sliding motion with and without vibration. Reprinted from [215], © 2020 Elsevier Ltd All rights reserved.(b) Schematic diagram of ultrasonic elliptical vibration cutting.

[220]. Another common use of heat to reduce friction is the Leidenfrost effect [221, 222]. The Leidenfrost effect is a phenomenon in which a liquid drop impinging on a surface significantly hotter than the boiling point of the liquid immediately forms an insulating vapor layer that reduces friction. Thermal also has a certain impact on the friction reduction achieved through microtextures.

A mechanism for friction reduction in thermal field-assisted microtexture technology is temperature control, which adjusts the viscosity of the lubricating oil and influences the microtexture's friction reduction performance. Friction and wear experiments (figure 13(a)) conducted at different temperatures and loads [223] show that at normal loads of 10 N, 20 N, and 30 N, various lubricants have minimal and similar effects on the friction coefficient. However, under high-load conditions, temperature significantly affects the friction reduction performance of the microtexture, primarily due to temperature-induced changes in the lubricant's viscosity and the load-bearing capacity of the lubricant film. Additionally, the friction reduction performance of microtextures with different shapes and sizes (figure 13(b)) is also temperature-dependent [224]. Experimental results indicate that a trench structure with a 45-degree angle demonstrates the highest load-bearing capacity. Traditional temperature-field-assisted friction reduction methods typically focus on single-liquid lubricants. To overcome this limitation, Shen *et al* introduced an innovative lubrication method (figure 13(c)) [225] that combines both solid and liquid lubricants. When used alongside thermal-field-assisted microtexture friction reduction technology, this approach offers dual benefits: improving the wear resistance of the microtexture while reducing surface friction on the cylinder liner and piston ring (CLPR). Another important friction reduction mechanism in temperature-field-assisted systems is the Leidenfrost phenomenon. Hydrodynamic simulations have uncovered the coupling effect between the heat-induced gas film and the surface texturing (figure 13(d)). The vapor layer generated at high temperatures remains within the microtexture, forming a vapor vortex [226]. This vapor vortex layer separates the liquid from the solid surface, reducing friction and simultaneously generating a driving force for fluid movement.

For temperature field assistance, it is essential to precisely control the temperature of the microtexture region to achieve optimal friction reduction, as the appropriate microstructure size varies with temperature [23]. The elevated temperatures can rapidly reduce the viscosity of the lubricating oil, leading to the rupture of the oil film. Moreover, the application of the Leidenfrost phenomenon requires precise temperature regulation to maintain a stable vapor oil film. However, most existing studies primarily focus on single droplets, resulting in a limited scope of research.

4. Microtexture manufacturing techniques

Advanced surface texturing technologies are essential for ensuring the friction reduction performance of microtextures. Currently, the manufacturing methods for microtextures can

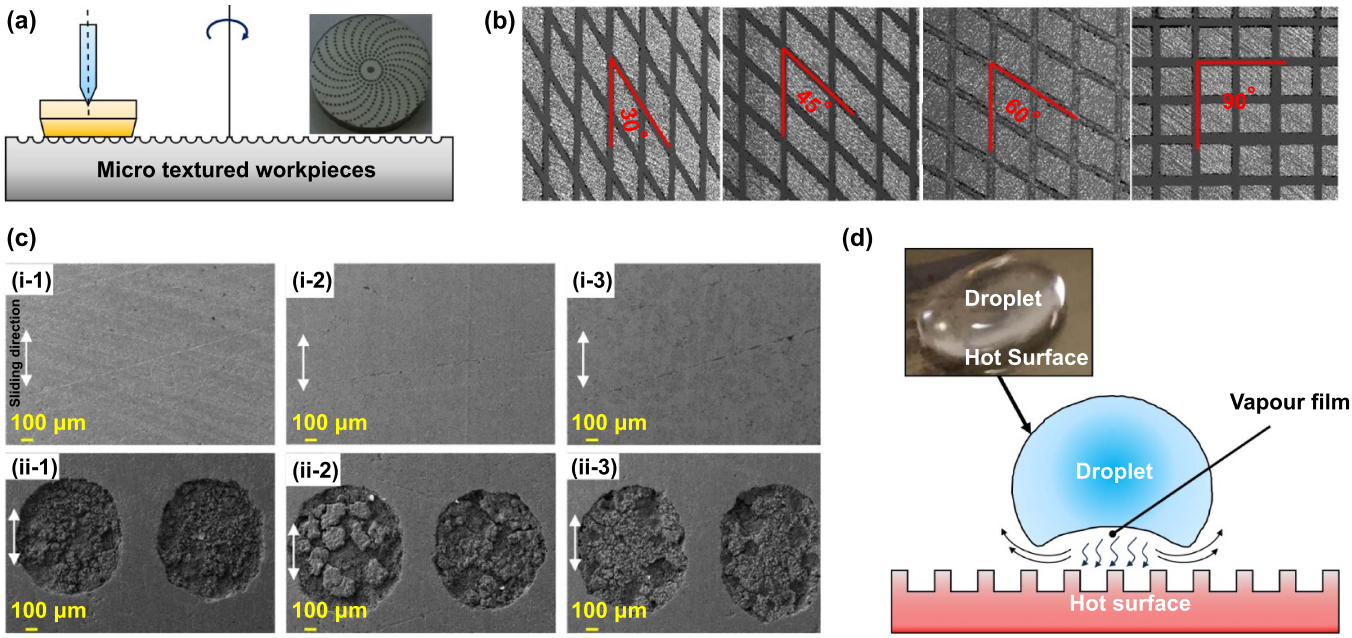

Figure 13. Thermal field-assisted friction reduction technology for the microtextured surface. (a) Microtextured discs. Reprinted from [223], © 2017 Elsevier Ltd All rights reserved. (b) Microtextures with different geometric shapes. Reproduced from [224]. CC BY 4.0. (c) A comparison between non-textured and double-sided microtextured. (i) Wear performance for non-dimpled CLPR at 150 °C, 200 °C, 250 °C. (ii) Wear performance for double-sided microtextured CLPR at 150 °C, 200 °C, 250 °C. Reprinted from [225], © 2023 Elsevier B.V. All rights reserved. (d) Leidenfrost phenomenon. [226] John Wiley & Sons. © 2021 John Wiley & Sons, Ltd.

be categorized into three main types: subtractive manufacturing, additive manufacturing, and material transfer processing. This article outlines seven commonly used in the industry: laser processing, chemical etching, abrasive waterjet machining, micro-grinding machining, diamond cutting, 3D printing, and micro-knurling (figure 14).

4.1. Laser processing

Laser processing technology harnesses high-energy-density laser beams focused on the surface of materials, inducing localized heating, melting, or vaporization, thereby achieving precise control over the microstructure and the mechanical and chemical properties of the material [232–235]. This technology is widely used in various fields, such as bearings, piston rings, gears, artificial joints, and mechanical seals. Nanosecond, picosecond, and femtosecond laser machining are commonly employed for fabricating microtextures. Nanosecond lasers are more economical and efficient compared to picosecond and femtosecond lasers, making them suitable for large-scale industrial production. However, nanosecond lasers can lead to material redeposition at the edges of microstructures, resulting in raised areas and diminished surface quality [236]. Femtosecond laser pulses are extremely short, generating almost no thermal effects, which effectively ensures surface precision [237]. Nevertheless, the high cost remains a significant drawback. At present, the thermal damage and protrusions of material surfaces caused by different laser types can be reduced by adding external media [238].

The key parameters that influence the morphology and dimensions of microtextures include laser power, scanning speed, and pulse repetition rate. Higher laser power enhances the melting or vaporization effect, forming deeper and wider microtextures. Scanning speed affects the depth of microtextures and the material removal rate. Higher scanning speed reduces energy deposition on the surface, resulting in smaller microtexture dimensions and impacting the material's wear resistance [239]. The pulse repetition rate mainly influences the material's thermal effects and melting processes. A higher repetition rate can lead to thermal accumulation, altering the formation mechanism of microtextures. By optimizing these process parameters, precise control over the size and morphology of microtextures can be achieved [240, 241].

Although this technology has significantly enhanced the performance of material surfaces, high-energy lasers may cause unintended material damage in non-target areas. Future research should focus on more precise control of laser energy distribution and interaction time to further improve processing efficiency and quality. Additionally, for cost-intensive femtosecond lasers, the primary objective is to explore more cost-effective alternatives to enable broader application in industrial production.

4.2. Chemical etching

Chemical etching technology achieves surface patterning through the directional removal of material using etching solutions, the effectiveness of which depends on the design of the masking layer and the lattice properties of the substrate material. Different sizes of microtextures can be fabricated by controlling parameters such as the proportion of solute molecules in the etchant solution, environmental temperature,

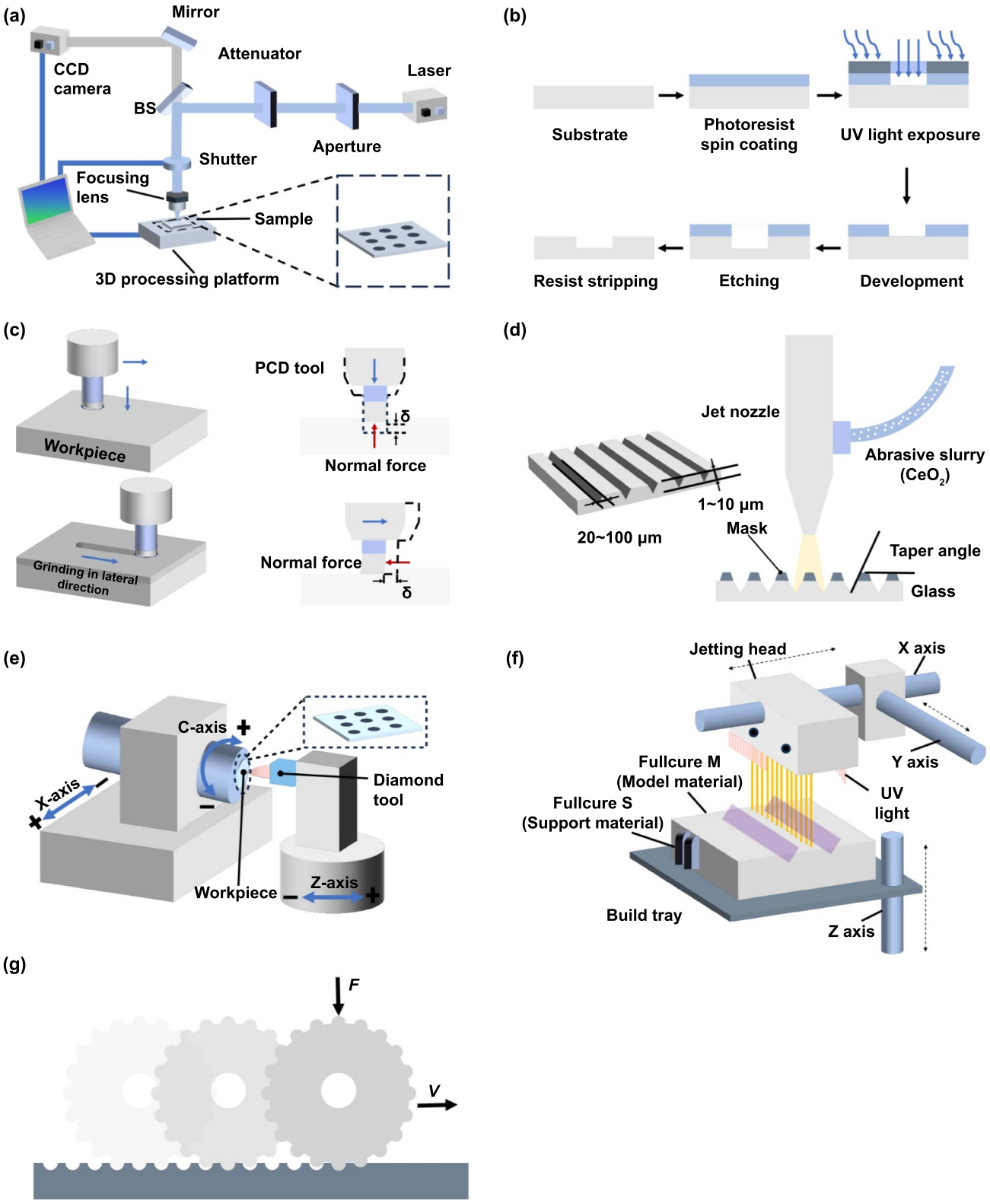

Figure 14. Microtexture manufacturing techniques. (a) Laser processing. Reproduced from [227]. CC BY 3.0. (b) Chemical etching. Reprinted from [228], Copyright © 2010 Elsevier Ltd All rights reserved. (c) Abrasive jet machining. Reprinted from [229], Copyright © 2011 CIRP. Published by Elsevier Ltd All rights reserved. (d) Micro-grinding machining. Reproduced from [230], with permission from Springer Nature. (e) Diamond cutting. Reproduced from [231]. CC BY 4.0. (f) 3D printing technology. Reproduced from [46] with permission from the Royal Society of Chemistry. (g) Micro-knurling process.

and etching time [242]. High-resolution masking layers can also be utilized to improve the dimensional accuracy of microtextures. Chemical etching is currently primarily used in laboratory research, and it is expected that its main applications will be in the field of microelectromechanical systems in the future. Research indicates that by varying photolithography parameters and etching solution solute ratios, diverse microtexture morphologies can be formed on carbon steel surfaces [243]. Additionally, chemical etching technology eliminates the need for subsequent polishing steps required in laser processing, simplifying the workflow. It also enables precise control over multi-shaped composite microtextures on steel surfaces, facilitating the production of diverse microtexture patterns [17, 244].

Chemical etching technology is effective in preserving the mechanical properties of microtextures while providing significant economic benefits and precision [245]. However, the corrosiveness of the etching solution and its relatively slow processing speed hinder its widespread application in industrial settings. To address these challenges, future research should focus on developing safer and more efficient etching techniques, as well as innovating etching solution formulations to minimize environmental impact, thereby facilitating broader industrial adoption.

4.3. Abrasive jet machining (AJM)

AJM is an advanced manufacturing technology of surface texturing that utilizes high-pressure water or gas to drive abrasive particles at high speeds against a substrate surface, enabling precise material removal and surface patterning. The effectiveness of the process is influenced by the shape, size, hardness, and velocity of the abrasive particles. Due to the particle size constraints (approximately 20–60 μm), AJM struggles to process microtextures narrower than 100 μm. Moreover, by selecting appropriate abrasive materials, such as synthetic diamonds, the efficiency and surface quality of the machining process can be significantly enhanced [246]. AJM can be integrated with other processing techniques (such as milling) to address the limitations of individual methods and enhance processing accuracy and efficiency, thereby broadening its potential applications in microtexture manufacturing [247].

Compared to laser processing, AJM avoids the generation of a heat-affected zone. Unlike chemical etching, AJM does not involve chemical reactions, thus preserving the intrinsic surface characteristics of the materials. This unique feature enables AJM to be used for the fabrication of microtextures on hard and brittle materials, e.g. alumina ceramics material for artificial joints. However, the irregularity of abrasive particles during the jetting process can lead to uneven surface quality, and the waste material generated during the processes may pose potential environmental impacts. The cost of AJM flow is considered moderate, primarily because, although it requires a certain investment in equipment, the operational and maintenance costs are relatively low.

4.4. Micro-grinding machining

Micro-grinding is a high-precision machining technique capable of producing superior surface quality. This technique involves utilizing fine abrasive particles on the surfaces of grinding tools or wheels to conduct micron-scale grinding on workpieces. It is commonly employed to fabricate high-precision surfaces, create complex surface microtextures, and precision machine hard materials [248, 249]. The key aspect of this technique lies in the precise machining of the substrate, whereby pre-defined machining paths are used to generate specific patterns and surface microtextures. Typically, micro-grooved textures are prepared using micro-grinding, with the structure dimensions controlled by adjusting the wheel thickness. At present, the smallest microtexture dimensions achievable through this technology are in the tens of microns, and the technique has been successfully extended to the fabrication of both two-dimensional and three-dimensional micro-grooves [250]. For instance, the introduction of microtextures on cutting tool surfaces has been shown to significantly reduce tool wear, thereby extending tool life considerably [251]. The cost of micro-grinding is moderate because the consumables and operational costs are relatively low.

Despite the ongoing maturation and widespread application of micro-grinding technology, several challenges persist in the fabrication of surface microtextures. Chief among these is the limitation imposed by abrasive particle size on the grinding wheel, which constrains the achievable machining precision. Additionally, the minimum wheel thickness presents a critical threshold, impeding the generation of finer-scale microtextures. Meanwhile, the geometric limitations of grinding wheels and the constraints of current manufacturing processes make it difficult to fabricate highly complex surface microtextures. Micro-grinding technology offers a promising avenue for advancements in friction reduction applications and provides potential solutions for overcoming these technical bottlenecks.

4.5. Diamond cutting

Diamond tools are essential for the high-efficiency machining of surface texturing. They also enable the fabrication of surface micro–nano structures with high machining precision and feature sizes ranging from the nano- to the submicron scale [252]. However, machining materials such as stainless steel and hardened steel remains a challenging task. High temperatures at contact points in the cutting process can cause carbon atoms to diffuse into the steel workpiece, leading to severe thermochemical tool wear and consequently reducing machining accuracy [253]. In recent years, vibration-assisted diamond cutting technology has been used to improve the machinability of difficult-to-machine materials. The cutting process is intermittent, with periodic vibration trajectories applied to the cutting tool to expel chips promptly. This approach effectively reduces chip thickness and cutting forces while significantly suppressing heat diffusion [254, 255]. Moreover, by

controlling the combination of cutting speed and vibration trajectories, a variety of sophisticated micro–nano structures can be machined on the workpiece surface [256]. It should be noted that the curvature radius of the vibration trajectory is kept smaller than the minimum curvature radius of the target structure to avoid unnecessary over-cutting [257]. The vibration generator provides periodic vibration trajectories for the cutting tool and can be classified into resonance and non-resonance modes based on its operating model [258, 259]. The resonance vibration generators work at the natural frequency of the mechanical structure, with fixed operating frequency and amplitude. Non-resonance vibration generators have adjustable frequency and amplitude, but they can only provide a single degree of freedom for the vibration trajectory of the tool. This limitation restricts the shape diversity of the machined micro–nano structures and then affects the functionality of micro–nano structures.

A major advantage of diamond cutting is its ability to achieve extremely low surface roughness and excellent surface integrity. The primary applications include preparing microtextures on the surfaces of optical devices and on the surfaces of artificial joints (Ti6Al4V). This technology maintains the microstructure of materials undamaged by avoiding significant thermal impact zones, making it particularly suitable for machining thermally sensitive or stress-sensitive materials. Although diamond cutting involves high initial investments and maintenance costs due to the need for high-precision equipment and expensive diamond tools, its unique ability to produce high-precision microtextures and enhance the long-term durability of materials brings significant economic benefits to high-end manufacturing.

4.6. 3D printing technology

3D printing technology (additive manufacturing) enhances design freedom and manufacturing flexibility by building complex parts layer-by-layer directly from digital models, offering broader possibilities for engineering design and production [260]. In the field of microtexture processing, 3D printing is widely utilized due to its superior adaptability in creating complex micro and nanostructures [261]. Adjustments in process parameters such as extrusion speed and temperature can significantly improve the surface quality and dimensional accuracy of the printed parts. For example, the printing process for the Ti6Al4V alloy can be optimized to enable the construction of curved channel structures, thereby significantly enhancing the tribological properties of the surface microtextures [262]. Furthermore, metal fusion 3D printing has been extensively applied in industrial production, particularly in the manufacture of molds for automotive parts, medical devices, and aerospace equipment, demonstrating a high degree of product customization and material diversity.

3D printing technology offers high design flexibility and complexity, but the equipment and material costs are relatively high. However, in the field of metal 3D printing, the range of metals suitable for this technology remains limited due to challenges such as columnar grain formation and periodic cracking during the melting and solidification processes. As a result, the focus primarily remains on a select few alloys, including AlSi10Mg, TiAl6V4, CoCr, and Inconel 718. Despite the challenges in material selection and microstructure control, the substantial potential of 3D printing in fabricating complex structures and its application in special materials provides an innovative research direction for the field of microtexture friction reduction.

4.7. Micro-knurling process

The micro-knurling technique employs specialized knurling tools to apply pressure on the workpiece surface, causing plastic deformation and precisely transferring the tool pattern to the substrate. This method boasts high design flexibility, excellent machining precision, rapid processing speed, and high-quality outcomes, making it suitable for forming periodic microtextures on the surfaces of cylindrical rods [263, 264]. Pettersson and Jacobson [265] employed micro-knurling technology to produce steel balls for ball bearings with surface microtextures and microtextured rollers. Characterization studies revealed that micro-knurling processing can achieve high-precision pattern and dimension transfer, resulting in the generation of high-resolution microtexture morphology. This method not only ensures the geometric shape and dimensional accuracy of textures but also offers excellent repeatability, providing a reliable technique for the design and manufacturing of complex surface structures.

Micro-knurling technology has certain limitations due to the intrinsic nature of the knurling process. It is very difficult to fabricate microtextures with overly complex shapes. Additionally, there are limitations in the choice of workpiece materials, especially when processing high-hardness materials, which require harder knurling tools, increasing the complexity and difficulty of the process. Despite these challenges, micro-knurling, with its efficient mechanical processing characteristics, continues to receive widespread attention in industrial production and remains an important method in the field of microtexture friction reduction.

Laser processing, chemical etching, abrasive waterjet machining, micro-grinding machining, diamond cutting, 3D printing, and micro-knurling each possess unique advantages and face distinct challenges. The selection of the appropriate manufacturing technologies primarily depends on the required microtexture characteristics, material compatibility, and cost-effectiveness. For more detailed information, refer to table 2.

5. Applications

5.1. Bearing

Bearings, as one of the most commonly used components in mechanical systems, have long been plagued by the issue of wear, which can result in reduced bearing performance

Table 2. Comparative analysis of manufacturing technologies for microtextures.

Manufacturing techniques	Advantages	Disadvantages	Cost efficiency	References
Laser processing	Non-physical contact Wide material compatibility	Heat affected zone Post-processing required	High	[266, 267]
Chemical etching	Large area processing	Limited precision Limited material	Low	[268]
Micro-grinding	High precision High surface quality	limited resolution Restricted processing structure	Medium	[269]
Abrasive jet machining	No thermal effect	Slow processing speed Post-processing required	Medium	[270]
Diamond cutting	Ultra-precision High surface quality	Slow processing speed	High	[271]
3D printing	Flexible design	High surface roughness Material restrictions Post-processing required	High	[272, 273]
Micro-knurling	High productivity	Limited resolution	Low	[265, 274]

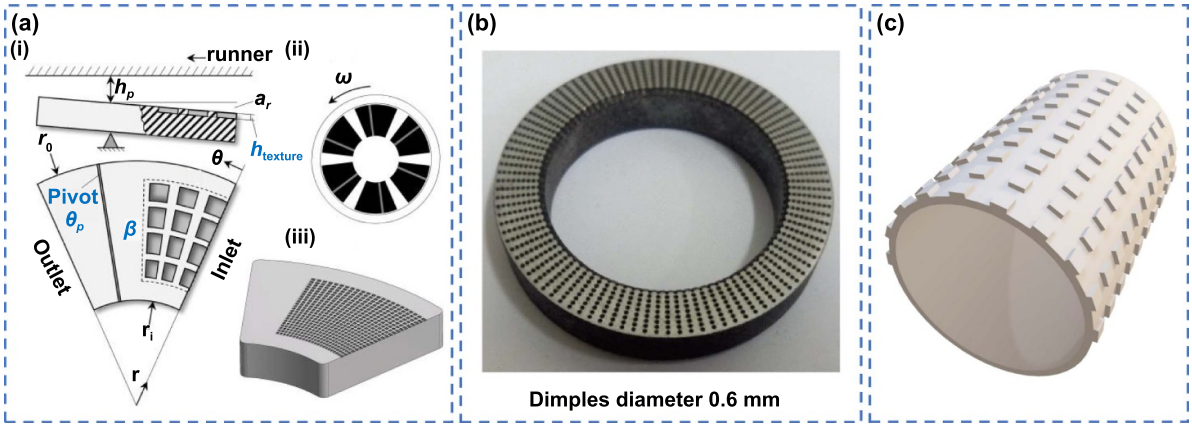

Figure 15. Bearing. (a) Tilting pad thrust bearing. (i) Pad details with the coordinate system. (ii) Tilting pad thrust bearing geometry. (iii) Exemplary microtexture pattern. Reproduced from [50]. CC BY 4.0. (b) Microtextured bearing. Reproduced from [277], with permission from Springer Nature.(c) Microtextured hydrostatic bearing.

and a shortened operational lifespan [275]. Surface microtexture technology for friction reduction, as an emerging strategy, was early applied to the surfaces of bearings to reduce frictional resistance and enhance lubrication performance. The introduction of microtextures on the bearing surface facilitates even distribution of lubricating oil, thereby minimizing direct metal-to-metal contact between the bearing and the workpiece. Consequently, this effectively reduces wear in the bearing system. The application of surface microtexture technology for friction reduction holds promise in improving the wear resistance and longevity of bearings while simultaneously decreasing energy consumption, providing robust support for the reliability and efficiency of mechanical.

In bearing applications, current research predominantly emphasizes the planar processing of microtextures in bearings, particularly thrust bearings, to improve the load-carrying capacity of the oil film. However, the specific research objectives differ across studies. For example, Henry *et al* [276] focused on observing the film/pad interface by integrating multiple thermocouples and pressure sensors. Their localized measurements of microtextured bearings showed that friction could be reduced by 30% under low loads. Other researchers have concentrated on enhancing bearing performance by optimizing microtexture parameters. Gropper *et al* [50] studied the effects of microtexture depth, circumferential extent, and radial extent on a tilting pad thrust bearing with offset line pivots (figure 15(a)), concluding that optimal microtexture parameters could increase the minimum film thickness by 12%. Similarly, Wang *et al* [277] examined how microtexture depth and coverage impact the lubrication performance of friction pairs (figure 15(b)). Aggarwal and Pandey [278] developed a novel microtexture design that combined various shapes of micro-pockets (with circular, rectangular, trapezoidal, and triangular cross-sections) and dimples (cylindrical, hemispherical, and ellipsoidal), resulting in a gasket that improved bearing capacity by 75% and reduced the friction coefficient by 42% compared to conventional fan-shaped gaskets. Atwal and Pandey [279] introduced a non-conventional microtextured fluid film thrust bearing, which

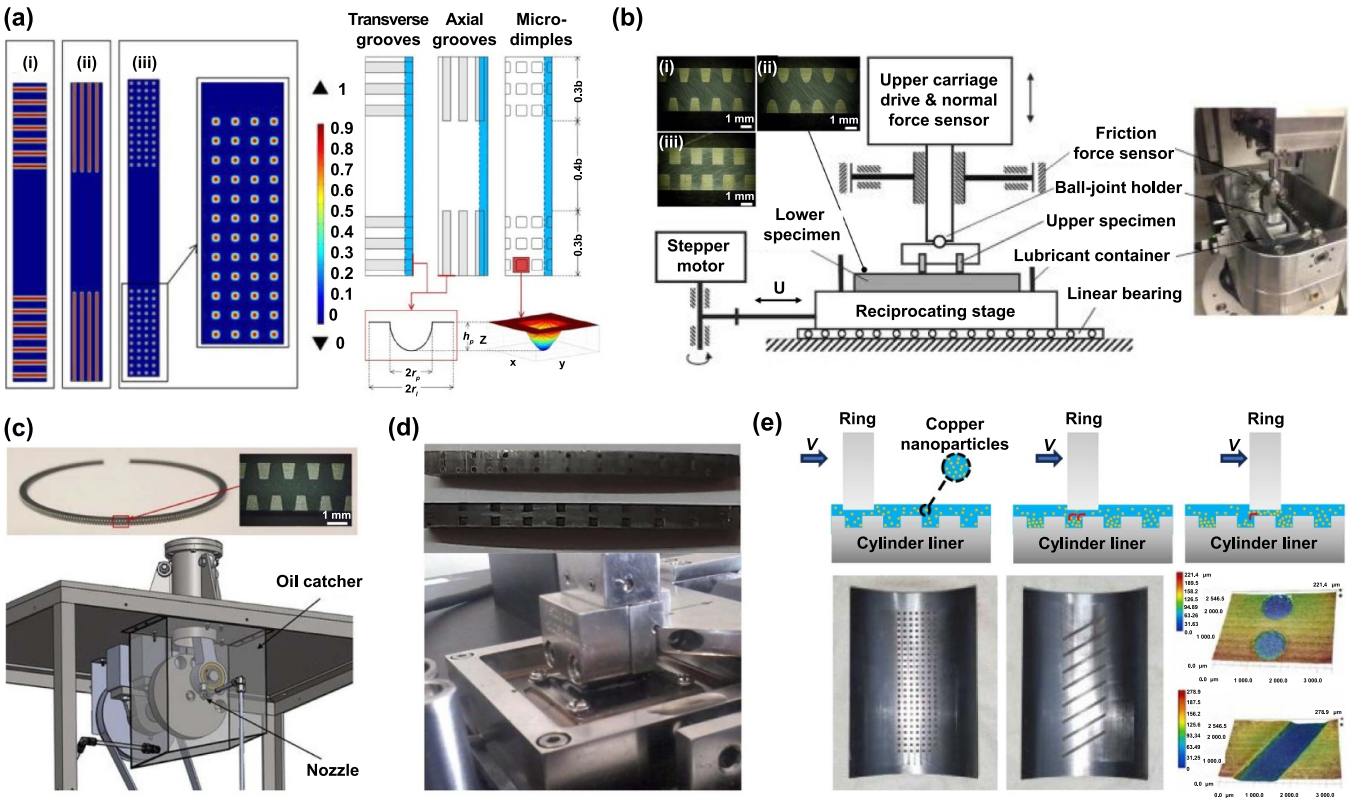

Figure 16. Piston ring-cylinder liner system. (a) Finite element analysis of microtextures pattern. (i) Transverse grooves. (ii) Axial grooves. (iii) Mircodimples. Reprinted from [281], © 2016 Elsevier Ltd All rights reserved. (b) Images of pocketed specimens and the test rig. (i) Trapezoidal pocket. (ii) Semielliptical pocket. (iii) Square pocket. Reprinted from [52], © 2016 Elsevier Ltd All rights reserved. (c) Image of pocketed compression ring and test rig. Reproduced from [282], with permission from Springer Nature. (d) Laser microtextured piston ring specimens and experimental setup with load. Reprinted from [283], © 2021 Elsevier Ltd All rights reserved. (e) Schematic of the synergistic mechanism between CNP additives and microtexture. Reprinted from [284], © 2022 Elsevier Ltd All rights reserved. Selection and peer-review under responsibility of the scientific committee of the International Conference on Materials, Processing & Characterization.

achieved a 48% increase in minimum film thickness and a 24% reduction in the coefficient of friction compared to conventional flat bearings. Although most research focuses on flat bearings, interest in cylindrical bearings, such as hydrostatic bearings, remains significant. Chen *et al* [280] designed microtextures with various distributions and arrangements on the surface of hydrostatic bearings to assess their effect on performance (figure 15(c)). The study demonstrated that distributing obtuse microtextures in regions of maximum pressure significantly enhances bearing capacity while concurrently reducing friction.

Bearings are widely studied by researchers investigating friction reduction technology of microtextured surfaces, owing to their wide range of industrial applications, making them a central focus of investigation. While microtextured bearings offer superior load-carrying capacity and operational performance compared to conventional bearings, several challenges persist. For example, optimal microtexture parameters often change with varying operating conditions, underscoring the need to improve the adaptability of these surfaces across a broader range of conditions. Furthermore, laser processing, the primary method for fabricating microtextures, is costly, which can limit its feasibility for standard industrial use. However, in high-end applications such as large-scale industrial equipment and aerospace engineering, the enhanced performance of microtextured bearings becomes a critical factor for designers. In such fields, the potential benefits may justify the higher manufacturing costs.

5.2. *Piston ring*

The CLPR is one of the most crucial friction pairs in diesel engine energy conversion. Reducing surface friction within this system is an efficient strategy to enhance piston efficiency. The implementation of a well-designed microtextured surface at the contact interface between the piston ring and cylinder liner shows considerable potential in minimizing frictional energy losses in the system.

A substantial body of research now exists on friction reduction technology of microtextured surfaces for piston rings, rendering simple, basic friction tests on microtextures largely unnecessary. The focus has shifted to optimizing the shape and size of microtextures under real-world operating conditions and varying friction environments, such as different lubrication fluids. For example, Usman and Park [281]

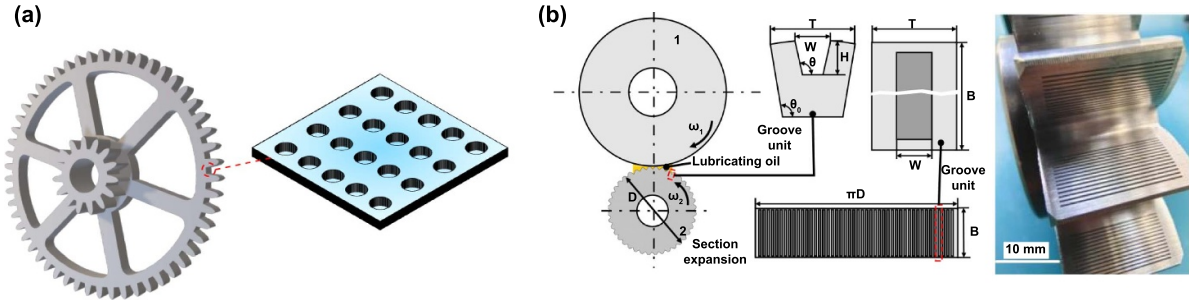

Figure 17. Gear transmission. (a) Surface topography of the specimen gear. (b) Cylindrical roller model with groove texture and groove texture unit. Reprinted from [286], © 2022 Elsevier Ltd All rights reserved.

combined a mixed lubrication model with oil flow dynamics to simulate and numerically optimize surface texturing patterns of various shapes and orientations under actual engine conditions (figure 16(a)), determining the optimal microtexture size for those conditions. Shen [52] introduced microtextures of various shapes at the inlet and outlet of the piston ring (figure 16(b)), exploring the influence of cavity area ratio (AR) and depth on piston ring friction performance, and identified the optimal geometric parameters (AR = 25%, depth = 5 μm). Shen *et al* [282] also applied this optimal microtexture to a novel friction and compression pressure testing device. Their experiments (figure 16(c)) demonstrated that the concave microtexture reduced overall friction between the cylinder liner and piston by approximately 15% across a wider range of operating speeds. To further investigate the effect of microtexture size on friction reduction performance, Patil and Shirsat [283] designed microtextures with three diameters (150 μm, 300 μm, and 500 μm) and two shapes (round and square) (figure 16(d)). They found that the size and shape of the microtexture had a synergistic effect on friction speed and piston ring load. Adopting a different approach, Yin *et al* [284] incorporated modified copper NPs (CNP) into the lubricant (figure 16(e)). Their findings indicated their results showed that the combination of surface texturing and CNP lubricant additive significantly minimized friction and wear in CLPR friction pairs.

Friction reduction technology of microtextured surfaces used in piston rings, similar to its application in bearings, has attracted considerable research interest. Numerous studies have shown that microtextures reduce the friction coefficient between the CLPRs interfaces, significantly increasing the service life of the piston ring. However, this technology faces certain limitations in CLPR applications. Many studies fail to fully consider real-world operating conditions, making it challenging to apply certain research findings directly to industrial applications. Additionally, since piston rings are primarily used in diesel engines, any damage can result in serious consequences, and their replacement can be complex. The reduced fuel consumption and extended service life provided by microtextured piston rings offer justification for their higher manufacturing costs, enhancing their viability for industrial deployment.

5.3. Gears

In response to the escalating need for mechanical systems characterized by elevated gear transmission density (a high torque-to-volume ratio), durability, and efficient operation of gear pairs, there is an imperative to augment the tribological performance at the gear-tooth interface. Such improvements are essential for preventing surface failures and minimizing vibrations. Given the pronounced variability in operating conditions, the likelihood of mixed or boundary lubrication between contacting surfaces in gear pairs increases, resulting in elevated frictional forces at the tooth contact points. Consequently, the reduction of inter-tooth friction emerges as a pivotal objective, with the application of microtextures on gear surfaces emerging as a highly effective method to achieve this goal.

Given the position and dimensions of the contact area on the tooth surface significantly affect transmission efficiency during the meshing process, it is essential to assess the real-time influence of surface topography on the gear's dynamic performance. Particular attention must be paid to the role of microtextures in minimizing drag on the tooth surface. Li *et al* [51] utilized a double-disk tester to examine the friction characteristics of laser-textured surfaces (figure 17(a)). They incorporated the time-varying friction characteristics of the tooth surface into the gear dynamics model, providing deeper insights into the relationship between surface topography and the dynamic behavior of gears. Their research demonstrated that the friction force during gear meshing is significantly influenced by the surface texturing. Furthermore, an important area of research in friction reduction technology of microtextured gear tooth surfaces involves exploring the influence of microtextures on the formation and behavior of the lubricating oil film during meshing. Zhao *et al* [285] utilized a precise three-dimensional elastohydrodynamic lubrication model to obtain deterministic solutions for predicting oil film pressure, oil film thickness, and friction coefficients for various microtextured tooth surfaces. Additionally, friction and wear tests showed that the microtexture of the tooth surface can increase local film thickness, thereby enhancing lubrication performance. By integrating CFD simulations with friction and wear experiments, Chang *et al* [286] indicate that the maximum and minimum damage ARs of gears with

groove patterns (figure 17(b)) are 84.8% and 84.9% lower, respectively, than those of gears without groove patterns. The anti-adhesion capability of gears with groove patterns is also significantly improved. Furthermore, the average friction coefficient of gears with groove patterns is notably reduced, effectively lowering dynamic pressure during transmission, as well as reducing lubrication-related friction within the gear system.

Microtextured gear tooth surfaces have demonstrated significant potential for reducing friction during transmission. However, the high contact pressure between the tooth surfaces, due to their strong load-bearing characteristics, can lead to increased contact pressure as the contact area is reduced. This can accelerate surface wear and heighten the risk of microtexture degradation. Therefore, optimizing microtexture parameters is crucial to minimize the friction coefficient while improving the wear resistance of the tooth surface. Additionally, current methods for processing microtextures on gear tooth surfaces are challenging and involve high production costs that outweigh the benefits of microtexture friction reduction technology. This imbalance has impeded the industrial production of microtextured gears in a conventional application environment. Nonetheless, the use of microtextures in high-precision gears may represent a promising application area. To enable broader adoption, it is essential to develop cost-effective surface texturing techniques that support the mass production of affordable components.

5.4. Cutting tool

Severe friction at the tool–chip interface can significantly enhance surface wear on the cutting tool and shorten its lifespan. To mitigate frictional losses effectively, a common approach involves the application of cutting fluid between the tool and the chip, as this facilitates a reduction in friction. The lubrication effect of the cutting fluid often depends on its penetrability. One of the most straightforward strategies to optimize the penetrability of the cutting fluid at the tool–chip interface is through the enhancement of the tool's microtexture.

During the turning process, significant cutting forces are often generated, impacting the tool's life. Improving the lubrication of the cutting fluid during the cutting process can be achieved by incorporating microtextures on the rake face of the cutting tool, thereby reducing cutting forces and enhancing tool life (figure 18(a)). Arulkirubakaran *et al* [287] developed microgroove textures on the rake face of tungsten carbide cutting tools. They performed turning tests on Ti6Al4V alloy and conducted numerical simulations to analyze temperature distribution, cutting forces, tool wear, and chip morphology using the Johnson–Cook model. Both experimental and simulation results showed that microtextures oriented perpendicular to the chip flow direction significantly reduced cutting forces and temperature, while also prolonging tool life. Ge *et al* [53] investigated the influence of microtexture dimensions on the lubrication efficiency of cutting fluids, using microtextured YS8 tools with varying groove widths in cutting experiments on H13 steel. Their results confirmed that microtexture enhances the permeability of cutting fluid, improves lubrication at the cutting interface, and significantly reduces both cutting forces and tool wear. Notably, 50 μm microgrooves provided optimal cutting performance in their experiments. Minimum quantity lubrication (MQL) is an economical and efficient lubrication method, widely used with conventional cutting tools. Research into MQL's application to microtextured tools is ongoing. Singh *et al* [288] employed a mixture of mustard oil and graphene as a MQL condition to investigate the wear behavior of microtextured tools during the turning of Ti6Al4V. The performance of microtextured tools was evaluated by characterizing tool wear and surface roughness. The results showed that MQL (graphene mixed in mustard oil) exhibited superior outcomes, followed by MQL (mustard oil only), and then dry conditions. The increase in the shear angle (11%–30%) and the reduction in friction coefficient (16%–39%) in the presence of graphene contributed to the enhanced cutting performance of microtextured tools. Musavi *et al* [289] studied the effect of microtexture orientation on tool wear and surface roughness under both MQL and dry conditions. Their findings further demonstrated that microtextured tools significantly improve surface quality and reduce tool wear.

In metal drilling processes, reducing sliding friction during drilling can enhance machining performance by decreasing cutting forces, improving edge stability, and enhancing surface integrity [3]. Introducing microtextures on the drill surface effectively improves friction conditions during the drilling process. The design of the microtextures facilitates the unobstructed flow of cutting fluid to the machining area, allowing it to bypass the upward movement of chips along the groove surface (figure 18(b)). Niketh and Samuel [292] designed microtextures on both sides of drill grooves and cutting edges, demonstrating that microtextured drills reduced net thrust by 10%–12% under dry conditions, 15%–20% under wet conditions, and 15%–19% with MQL. Additionally, Selvakumar *et al* [290] explored the influence of various microtexture geometries on drill performance by fabricating four distinct types of microtextured drills. A comparative analysis between these microtextured drills and non-textured counterparts revealed that the microtextured designs exhibited superior performance. This improvement can be attributed to the enhanced lubrication effect provided by the microtexture, particularly in the microdimple regions.

Broaching is extensively employed in the aerospace field because of its high efficiency and capacity for handling substantial loads. However, heavy-duty cutting creates strong extrusion and friction in the tool–chip contact area, resulting in insufficient lubrication. To address this issue, Some researchers have also constructed microtextures on the broaching tool surface to improve lubrication conditions (figure 18(c)). Therefore, Ni *et al* [293] utilized laser processing techniques to create three types of microtextures (including dimple, stripe, and mesh) on the rake face of a turning tool

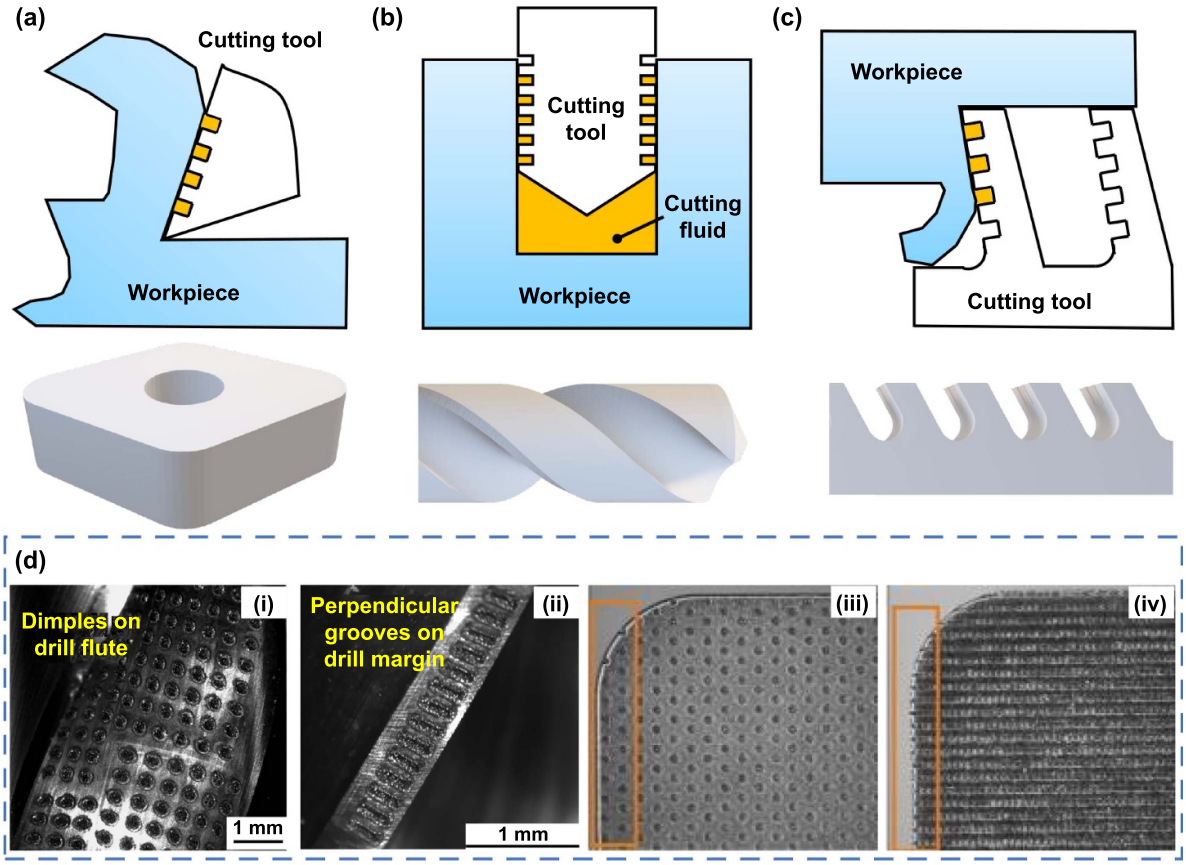

Figure 18. Cutting tool. (a) Microtextures turning tool cutting mechanism and topography. (b) Microtextures drilling tool cutting mechanism and topography. (c) Microtextures broaching tool cutting mechanism and topography. (d) SEM image of microtexture tool. (i) and (ii) Microtextured drill. Reprinted from [290], © 2023 The Society of Manufacturing Engineers. Published by Elsevier Ltd All rights reserved. (iii) and (iv) Microtextured turning tool. Reprinted from [291], Copyright © 2014 Elsevier B.V. All rights reserved.

to enhance cutting performance. Subsequently, copper was deposited onto the microtextures using reciprocating rotary friction to enhance the wettability and heat dissipation capability of the turning tool. Experimental results demonstrated that, compared to non-textured cutting teeth, the copper-covered striped textures reduced cutting forces by 14.6%, and the cutting temperature decreased from 90.13 °C to 76.9 °C.

While some studies have demonstrated the excellent performance of microtextured broaching tools, the majority of research on microtextured tools has thus far concentrated on microtextured drills and microtextured turning tools. Scholars have also fabricated various samples of these two tools (figure 18(d)). The proliferation of microtextured tools has also diversified machining methods. Compared to other industrial components, the complex geometry of tools increases the difficulty of microtexture processing and requires high-precision techniques to create microtextures with specific shapes and minimal defects. These requirements result in higher processing costs, which also limit the wider application of microtextured tools. Under severe cutting conditions, the microtextures on the tool surface may contribute to derivative cutting, leading to chip accumulation within the textures and thereby reducing their friction reduction performance. Furthermore, when machining difficult-to-process materials such as titanium alloys, effective heat dissipation becomes problematic, resulting in high temperatures at the tooltip. This elevated temperature can cause the lubricating oil film on the microtextured surface to deteriorate, further diminishing the friction reduction effectiveness of the microtextures and potentially leading to their wear and blockage.

5.5. *Artificial joints*

With the continuous advancement of medical technology, there is a significant increase in the demand for artificial joints. However, artificial joints still face many challenges, and their wear resistance is a key factor affecting the stability of implanted joints [294], it determines whether artificial joint transplantation can be successful [295]. Improving the wear resistance of artificial joints has become one of the pressing challenges in the medical field. In recent years, various materials have been employed in the fabrication of artificial joints, such as CoCrMo alloy, Ti6Al4V [296], and ceramic

[297] materials with good mechanical properties. These materials exhibit superior biocompatibility and mechanical properties compared to others, including corrosion resistance, wear resistance, and low friction coefficients [298]. Experimental results demonstrate that incorporating microtextures can further enhance lubrication performance and reduce joint wear [299].

In comparison to metal-on-polyethylene and ceramic-on-polyethylene materials, ceramic-on-ceramic (CoC) composites demonstrate superior mechanical properties and are progressively being considered as a preferred base material for artificial joint application. Roy *et al* [300] created circular microtextures (figure 19(a)) on ceramic substrates to study the frictional behavior of CoC hip prostheses through friction testing. The results indicated that both the diameter and density of the joint socket significantly influenced the frictional properties of the joint. Microtextures with diameters of ϕ400 μm and density of 15% demonstrated a significant enhancement in frictional performance, with a reduction in friction by approximately 22% and a decrease in wear by about 53%. In contrast to the ceramic materials utilized by Roy and his colleagues, Ti6Al4V is extensively utilized in biomedical implants due to its outstanding properties, including corrosion resistance, high strength, and excellent chemical stability. Pratap and Patra [301] created circular microtextures with different sectional shapes (micro flat-end textured surface, micro ball-end textured surface, micro-drill textured surface) on the surface of Ti-6Al-4 V. Among various microdimple surfaces, the semi-spherical-ended microdimple surface proved to be more suitable for hip joint prosthetics due to its superior surface wettability and lower COF. Building on this research, Pratap *et al* [302] subsequently developed three additional microtexture (figure 19(b)) designs (parallel (PD), staggered (SD), and microgrid (MG)) to examine the impact of different microtexture geometries on the COF and surface wear. The research results indicate that the MG with intermediate spacing and the highest depth exhibits the lowest COF. The decrease in COF was verified as a result of the combined effects of wettability and microhardness. In addition to the study of basic microtexture geometries on Ti6Al4V, Cui *et al* [303] simulated the graded texture of articular cartilage and its unique lubrication mechanism (figure 19(c)). They prepared a biomimetic bilayer coating on laser microtextured Ti6Al4V alloy using LST, thermal oxidation, and ultraviolet radiation techniques. The coating consisted of a TiO_2 layer and a hydrogel layer (addition of zwitterionic polymer). When lubricated in deionized water, the Ti6Al4V hydrogel-bearing interface exhibits a lower COF (0.06) and improved wear resistance, with the lowest measured COF (0.039) observed in phosphate-buffered saline solution. CoCrMo alloy, another widely studied material for artificial joint substrates, has attracted significant research interest. Han *et al* [304] overcame the limitations associated with simple concave microtextures in Co–Cr–Mo materials by utilizing LST to create various patterned microtextures on the alloy's surface (figure 19(d)). The patterns included groove arrays, hexagonal arrays, and concentric arrays. Friction experiments demonstrated that the concentric circle structure exhibited the most advantageous tribological properties. Under a 10 N loading condition, the COF and weight loss of PEEK spheres with a 20% density in the concentric circular microtexture sample (C-20) decreased by 49.22% and 52.3%, respectively, compared to non-textured samples. Liu *et al* [54] explored the friction-reducing performance of CoCrMo alloy artificial joints with specially designed microtextures (figure 19(e)). The experimental results indicate a significant improvement in the frictional performance of CoCrMo artificial knee joints with microtextures. Among them, the lamellar-textured structure (STT-3) exhibits the best frictional performance, with the lowest COF.

Artificial joints incorporating microtextures exhibit enhanced performance. However, their fabrication continues to face several challenges. Mainstream laser processing technologies can produce burrs at the edges of microtextures. Additionally, the laser processing method may lead to a transition in surface wettability from hydrophilic to hydrophobic over time, which negatively impacts the friction reduction performance of the microtextures. In contrast, micromachining technology is limited by the size and shape of the tool, restricting its capacity to create highly complex or minuscule microtextures. Moreover, the friction reduction efficacy of artificial joints is influenced by various factors, such as the rolling direction of the workpiece and the performance of the lubricant. Therefore, it is crucial to customize the microtexture of artificial joints and select suitable lubricants according to specific operational requirements. Unlike other applications of microtextures, the manufacturing cost of microtextures on artificial joints is no longer a primary concern due to their high market value and long service life. The focus has instead shifted towards optimizing their functional performance, which enhances the potential for widespread application of microtextured artificial joints.

5.6. Mechanical seals

Mechanical seals are dynamic sealing devices comprising a pair of mating rings (rotor and stator), widely used in pumps and compressors [305]. The sealing function primarily relies on the liquid film generated between the mating rings through high-speed rotation. However, the sharp increase in friction and leakage under extreme conditions (high load, high temperature, and high speed) can easily result in seal failure. Using microtextures on mechanical seals can enhance load-carrying capacity, fluid film stiffness, anti-seizer ability, and wetting behavior. Additionally, microtextures can also reduce wear, friction, leakage, and interface temperature [306]. In this section, the use of microtexture in liquid-lubricated seals is going to be discussed.

The application of microtexture technology in mechanical seals has been the subject of extensive research over an extended period. Early studies primarily focused on the frictional characteristics of microtextured mechanical seals. Yu *et al* [55] demonstrated that the porous surface of a microtextured

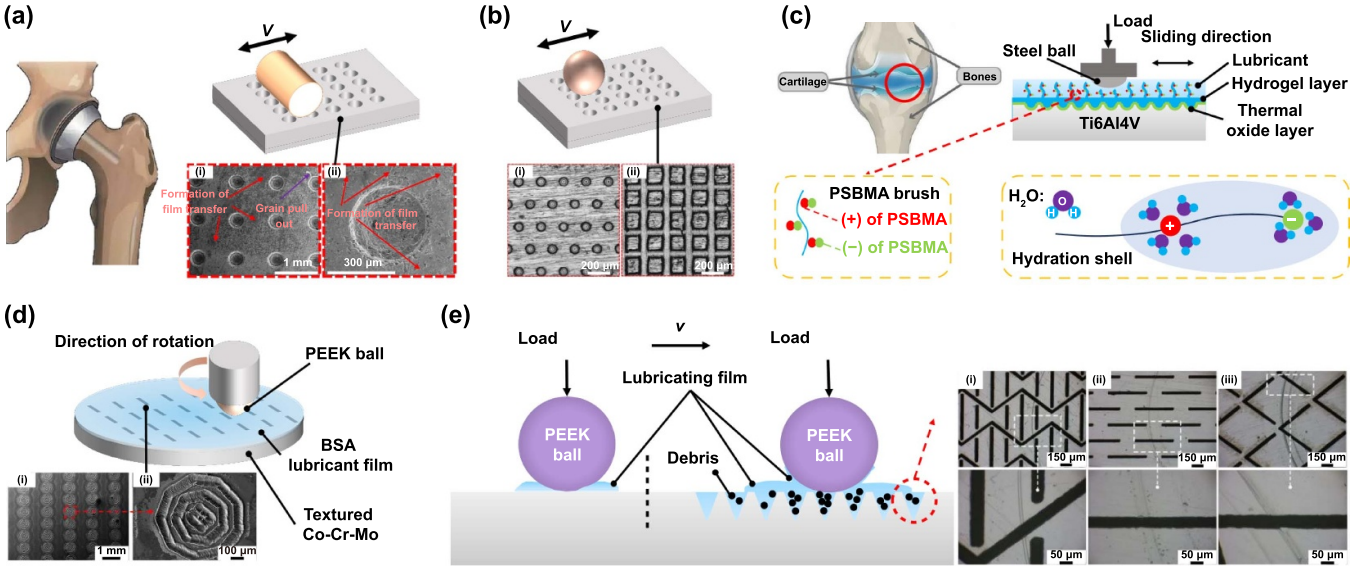

Figure 19. Artificial joints. (a) Hip joint friction mechanism and SEM images of the dimpled surface after tribology testing. (i) Image of wear on the dimpled surface. (ii) Image of wear near the dimple after tribology test. Reprinted from [300], Copyright © 2014 Elsevier Ltd and Techna Group S.r.l. All rights reserved. (b) Hip joint friction mechanism and optical microscopic image of wear pattern of different microtextured artificial hip joints. (i) Image of SD. (ii) Image of MG. Reprinted from [302], © 2020 Elsevier Ltd All rights reserved. (c) Schematic diagram of lubrication mechanisms of the unique lubrication mechanisms of articular cartilage. Reprinted from [303], © 2022 Elsevier Ltd and Techna Group S.r.l. All rights reserved. (d) Images and surface profiles of laser microtextured surface. (i) The overall image of concentric circles microtextures. (ii) The local image of concentric circles microtextures. Reprinted from [304], © 2020 Elsevier Ltd All rights reserved. (e) Schematic diagram of the microtexture effect on friction behaviors between CoCrMo artificial knee joint. (i) Image of shark-skin microtextures. (ii) Image of stripy microtextures. (iii) Image of scaly microtextures. Reprinted from [54], © 2022 Elsevier Ltd All rights reserved.

mechanical seal (figure 20(a)) resulted in a lower temperature rise, reduced frictional torque, and a decreased COF. Additionally, the incorporation of microtextures significantly enhanced the hydrodynamic pressure effect, thereby improving tribological performance between sealing surfaces and extending the seal's operational lifespan. As research on the frictional properties of microtextured mechanical seals progressed, there has been a growing interest in utilizing numerical simulations to predict frictional behavior and conducting theoretical investigations into sealing efficiency. Siripuram and Stephens [307] employed numerical simulations to analyze the influence of fluid films generated by microtextures of varying shapes on seal surface lubrication (figure 20(b)). Their results indicated that the COF of the sealing surface is affected by sectional dimensions, with both sectional shape and size impacting the leakage rate. Furthermore, they identified the optimal microtexture shape and size parameters to minimize leakage. In contrast to Siripuram's approach, Brunetière and Tournerie [308] focused on verifying the hydrodynamic lift enhancement mechanism introduced by microtextures (figure 20(c)). Using the Reynolds equation in conjunction with a mass-conservative cavitation algorithm and a realistic rough contact model, they found that microtextured seal surfaces generate higher loads, improving the tribological performance between sealing surfaces. Adjemout *et al* [309] considered the effects of manufacturing defects in microtextures when developing a hydrodynamic lubrication model (figure 20(d)). Their numerical simulations revealed a critical threshold for surface defects, beyond which imperfections counteracted the beneficial effects of microtextures. They concluded that cavity shape control is essential for achieving effective friction reduction in microtextured surfaces. Unlike other applications of microtextures, the design of microtextured surfaces for mechanical seals necessitates careful consideration of both frictional performance and leakage rate. Siripuram and Stephens [307] demonstrated that microtexture significantly influences leakage rate. Shi *et al* [310] further investigated the combined effects of microgrooves and microcavities on the COF and leakage rate (figure 20(e)). They identified optimal microtexture parameters, concluding that an inner groove radius at an angle of $\alpha = 45°$ through the rotor ring reduces both COF and leakage rate.

The application of microtextures in mechanical seals is primarily intended to reduce friction and wear between metal components, as excessive friction can lead to seal failure. However, excessively large microtextures can also cause seal leakage. Therefore, it is essential to determine the optimal size for microtextures used in mechanical seals to achieve a balance between friction reduction and the risk of leakage. The integration of microtextures into mechanical seals often results in rising manufacturing costs, which severely limits industrial applications. Nevertheless, for large-scale industrial equipment with demanding sealing requirements, microtexture friction reduction technology remains a viable and advantageous option. Moreover, existing theoretical models that incorporate

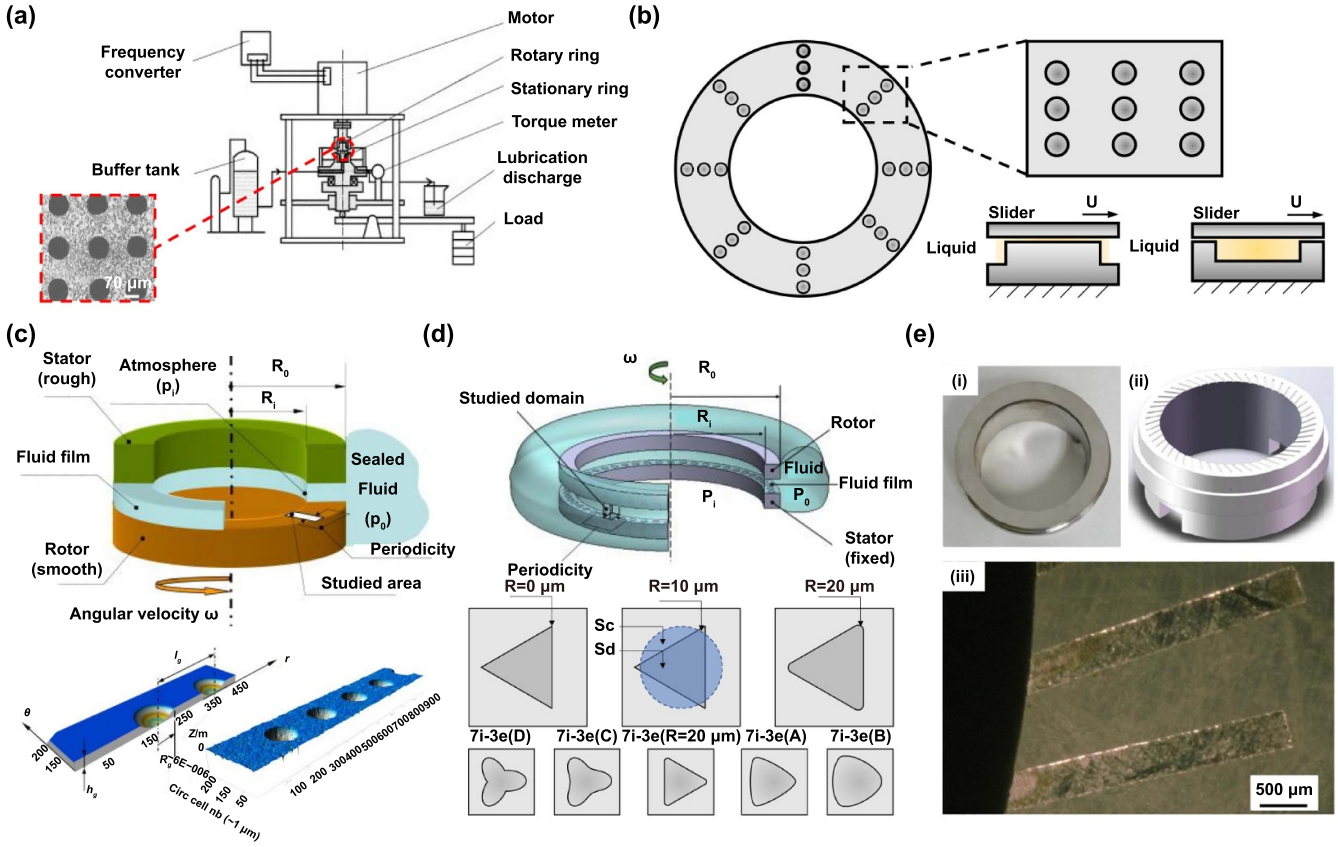

Figure 20. Mechanical seals. (a) Images of pocketed specimens and the test rig. Reprinted from [55], Copyright © 2002 Elsevier Science B.V. All rights reserved. (b) Schematic diagram of microtexture on the sealing ring and sliding mechanism. (c) Sealing ring leakage mechanism and microtexture schematic diagram. Reprinted from [308], Copyright © 2012 Elsevier Ltd All rights reserved. (d) Geometric scheme of the model and configurations used to study the effects of boundary deformations. Reprinted from [309], © 2017 Elsevier Ltd All rights reserved. (e) The physical picture of the microtexture sealing ring. (i) Rotor specimen. (ii) Rotor model. (iii) Image and profile of surface texturing patterns. Reproduced from [310], with permission from Springer Nature.

microtexture friction reduction technology are often overly idealized and frequently overlook the effects of machining processes. As a result, some proposed microtexture designs remain theoretical and have yet to be fully implemented in practical applications.

6. Concluding remarks

6.1. Concluding remarks

Friction reduction technologies of surface texturing have been demonstrated as an effective measure for reducing friction and wear at contact interfaces. This review comprehensively summarizes the latest advancements in the optimization, manufacturing, and applications of microtextures. The primary research focuses can be summarized as follows:

(1) The Reynolds equation is the most favored theoretical model in numerical computations for lubrication on microtextured surfaces. Integrating numerical optimization methods with intelligent optimization algorithms effectively avoids the time-consuming process of trial and error in experiments. It is noteworthy that the validity of the Reynolds equation should be assessed based on the application environment and operating conditions before utilization.

(2) The optimization of microtexture shapes is gradually shifting from predefined geometries to intelligent self-generated patterns, enabling the achievement of optimal microtexture morphologies without relying on human expertise. Generally, the optimal microtexture shape features a larger convergence area and a smaller dispersion area. The distribution of microtextures in the contact zone shifts from fully microtextured to partially microtextured. The optimized microtextured surface reduces the coefficient of friction by more than 20%. However, achieving this performance may require careful consideration of cost-effectiveness in practical applications.

(3) The synergistic interaction between microtextured surfaces and advanced coatings regulates interfacial micromechanical properties, promoting lubrication film formation and enhancing coating durability. This combination further improves the friction-reducing performance of the microtextures. Ion implantation, plasma processing, and shot blasting effectively enhance the wear resistance

and structural load-bearing capacity of microtextures, and the frictional performance is moderately improved. Additionally, the integration of microtexture with novel liquid lubricants is an effective strategy for optimizing tribological performance. This synergistic effect is not only manifested in the storage and secondary lubrication role of microtexture but also in the formation of lubricant films, micro-bearing action, and self-repairing effects on the microtextured surface.

(4) Under an applied magnetic field, magnetic nanofluids are retained within the microtexture, enhancing lubrication at the friction interface. However, the theoretical understanding of magnetic field-assisted technology remains limited, particularly in terms of the infiltration behavior of magnetic nanofluids in microtextured surfaces, which requires further investigation. Ultrasonic vibrations can enhance the average load-bearing capacity of microtextured surfaces by expelling trapped lubricants and increasing lubricating film thickness. Despite this, rare theoretical research and experimental data, have hindered progress in this area, highlighting an urgent need for further development. Within a specific temperature range, increasing the temperature in the microtextured zone can reduce lubricant viscosity, which in turn lowers shear stress within the lubrication film, thereby reducing friction. Precise temperature control in the microtextured region is crucial for maintaining optimal friction reduction performance.

(5) We have extensively discussed various microtexture surface technologies, including laser processing, chemical etching, abrasive jet machining, micro-grinding machining, diamond cutting, 3D printing, and micro-knurling. Each technology has its unique advantages and faces specific challenges. When selecting the appropriate microtexture method, multiple factors must be considered, including the desired microtexture characteristics, material compatibility, and cost-effectiveness of the process. Additionally, we have evaluated the potential of each technology to meet specific industrial needs based on the material properties and operational environments of different industries, ensuring the most suitable technological approach is chosen.

(6) Microtextured surfaces have shown considerable success in reducing friction and wear across various applications. However, due to the high cost of manufacturing technologies and the distinct requirements of different operational environments, large-scale industrial production of certain microtextured applications remains challenging. The effect of surface microtextures on tribological properties is heavily influenced by contact conditions and lubrication states. To minimize friction, different types of microtextures must be applied to specific regions of a component, based on factors such as speed, normal load, temperature, and lubricant supply conditions.

6.2. Challenges and perspectives

Despite the vast research progress made for microtextured surface-mediated friction reduction technology over the past few decades, many challenges remain that need to be addressed, such as limited operational range, instability in friction reduction, and inadequate load-bearing capacity (figure 21(c)). To transition microtexture from laboratory exploration to practical application, further investigation into the following research directions is necessary.

(1) Limited operational range. In specific operational conditions, fixed-shape microtexture exhibits favorable tribological performance. However, in friction motion, both the load and velocity are often subject to continuous variations. For instance, load and velocity can experience rapid fluctuations when traversing bumps or negotiating turns in automotive suspension systems, as well as during the start-up and acceleration processes of turbine engines. The microtexture is limited by its structure, so it is difficult to adapt to the changing operating conditions, once beyond the applicable range of operating conditions, adverse effects may be introduced. ML techniques can be employed to establish a mapping relationship between the geometric characteristics of microtextures and the applicable operating condition range (figure 21(a)). Thereby enabling the automated generation of microtexture shapes with broad applicability.

(2) Instability in friction reduction. The microtextured surfaces experience wear during prolonged friction processes, resulting in changes to structural parameters (such as depth and width). This subsequently increases fluctuations in the friction coefficient, negatively impacting the stable operation of mechanical systems. The integration of smart materials (such as shape memory alloys) with real-time monitoring and feedback control technologies enables the dynamic adjustment of microtexture morphology during the wear process. This approach maintains optimal structural parameters and effectively stabilizes friction-reduction performance.

(3) Inadequate load-bearing capacity. Components of large-scale machinery, such as aircraft and heavy ships, are subjected to exceptionally high loads. However, under high-speed, high-load, or extreme operating conditions, it becomes difficult to form and maintain a stable oil film on the microtextured surface over extended periods. Additionally, suboptimal microstructure design may lead to oil film rupture and reduced load-bearing capacity. The intelligent response system, assisted by energy fields (figure 21(b)), can adjust liquid flow behavior at the lubrication interface, thereby increasing oil film thickness and improving load-bearing capacity. This system enables adaptive friction reduction of microtextures under complex and variable conditions.

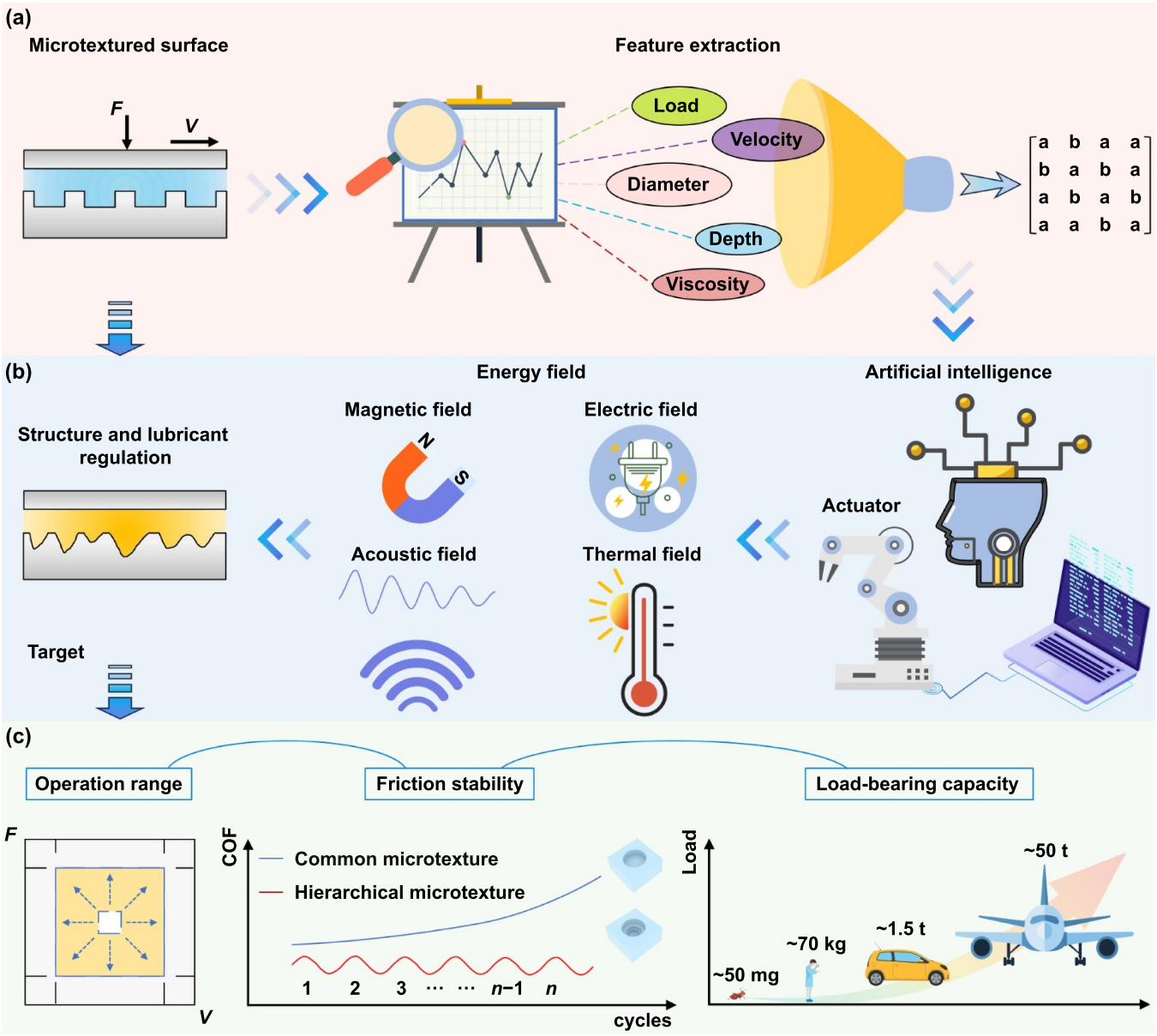

Figure 21. Advanced design strategies for microtextured surfaces based on the joint effort of artificial intelligence and external multi-energy fields, addressing the most challenges in operation range, friction stability, and load-bearing capacity. (a) Extraction of microtexture features and operating condition parameters. (b) Artificial intelligence optimizes feature parameters to drive external energy field modulation of microtexture structure and lubricant properties. (c) The range of operating conditions, friction stability, and load-bearing capacity of the microtextured surface.

Acknowledgments

The authors gratefully acknowledge the National Natural Science Foundation of China (Award No. 07120016), the startup funding support by the Dalian University of Technology (DUT) (Award Nos. 82232022, 82232043, and DUT22LAB404) and AVIC Shenyang Aircraft Company (Award No. 12020641 and 12020642).

ORCID iDs

Qianhao Xiao https://orcid.org/0009-0005-4029-3447
Xichun Luo https://orcid.org/0000-0002-5024-7058
Jining Sun https://orcid.org/0000-0003-4457-6047

References

[1] Holmberg K and Erdemir A 2017 Influence of tribology on global energy consumption, costs and emissions *Friction* **5** 263–84
[2] Li M J *et al* 2022 Super-wetting interfaces as a multiphase composite prototype for ultra-low friction *Green Chem.* **24** 7492–9
[3] Liang X L, Liu Z Q, Wang B, Wang C J and Cheung C F 2023 Friction behaviors in the metal cutting process: state of the art and future perspectives *Int. J. Extrem. Manuf.* **5** 012002

[4] He B, Chen W and Jane Wang Q 2008 Surface texture effect on friction of a microtextured poly(dimethylsiloxane) (PDMS) *Tribol. Lett.* **31** 187–97

[5] Shinkarenko A, Kligerman Y and Etsion I 2009 The effect of surface texturing in soft elasto-hydrodynamic lubrication *Tribol. Int.* **42** 284–92

[6] Zhou L, Kato K, Umehara N and Miyake Y 2000 Friction and wear properties of hard coating materials on textured hard disk sliders *Wear* **243** 133–9

[7] Hamilton D B, Walowit J A and Allen C M 1966 A theory of lubrication by microirregularities *J. Basic Eng.* **88** 177–85

[8] Anno J N, Walowit J A and Allen C M 1968 Microasperity lubrication *J. Lubr. Technol.* **90** 351–5

[9] Anno J N, Walowit J A and Allen C M 1969 Load support and leakage from microasperity-lubricated face seals *J. Lubr. Technol.* **91** 726–31

[10] Willis E 1986 Surface finish in relation to cylinder liners *Wear* **109** 351–66

[11] Marian M, Almqvist A, Rosenkranz A and Fillon M 2022 Numerical micro-texture optimization for lubricated contacts—a critical discussion *Friction* **10** 1772–809

[12] Ma R, Zhang X D, Sutherland D, Bochenkov V and Deng S K 2024 Nanofabrication of nanostructure lattices: from high-quality large patterns to precise hybrid units *Int. J. Extrem. Manuf.* **6** 062004

[13] Lian Z X, Zhou J H, Ren W F, Chen F Z, Xu J K, Tian Y L and Yu H D 2024 Recent progress in bio-inspired macrostructure array materials with special wettability—from surface engineering to functional applications *Int. J. Extrem. Manuf.* **6** 012008

[14] Lu P and Wood R J K 2020 Tribological performance of surface texturing in mechanical applications—a review *Surf. Topogr.: Metrol. Prop.* **8** 043001

[15] Wang H H, Lin N M, Yuan S, Liu Z Q, Yu Y, Zeng Q F, Li D Y, Fan J F and Wu Y C 2023 Numerical simulation on hydrodynamic lubrication performance of bionic multi-scale composite textures inspired by surface patterns of *subcrenata* and *clam* shells *Tribol. Int.* **181** 108335

[16] Lu P, Wood R J K, Gee M G, Wang L and Pfleging W 2018 A novel surface texture shape for directional friction control *Tribol. Lett.* **66** 51

[17] Xu Y F, Zheng Q, Abuflaha R, Olson D, Furlong O, You T, Zhang Q Q, Hu X G and Tysoe W T 2019 Influence of dimple shape on tribofilm formation and tribological properties of textured surfaces under full and starved lubrication *Tribol. Int.* **136** 267–75

[18] Romano J M, Garcia-Giron A, Penchev P and Dimov S 2018 Triangular laser-induced submicron textures for functionalising stainless steel surfaces *Appl. Surf. Sci.* **440** 162–9

[19] Liu W L, Ni H J, Chen H L and Wang P 2019 Numerical simulation and experimental investigation on tribological performance of micro-dimples textured surface under hydrodynamic lubrication *Int. J. Mech. Sci.* **163** 105095

[20] Wakuda M, Yamauchi Y, Kanzaki S and Yasuda Y 2003 Effect of surface texturing on friction reduction between ceramic and steel materials under lubricated sliding contact *Wear* **254** 356–63

[21] Choi Y and Lee J 2015 A study on the effects of surface dimple geometry on fretting fatigue performance *Int. J. Precis. Eng. Manuf.* **16** 707–13

[22] Schneider J, Braun D and Greiner C 2017 Laser textured surfaces for mixed lubrication: influence of aspect ratio, textured area and dimple arrangement *Lubricants* **5** 32

[23] Braun D, Greiner C, Schneider J and Gumbsch P 2014 Efficiency of laser surface texturing in the reduction of friction under mixed lubrication *Tribol. Int.* **77** 142–7

[24] Hua X J, Puoza J C, Zhang P Y, Xie X and Yin B F 2017 Experimental analysis of grease friction properties on sliding textured surfaces *Lubricants* **5** 42

[25] Pettersson U and Jacobson S 2003 Influence of surface texture on boundary lubricated sliding contacts *Tribol. Int.* **36** 857–64

[26] Arslan A, Masjuki H H, Kalam M A, Varman M, Mufti R A, Mosarof M H, Khuong L S and Quazi M M 2016 Surface texture manufacturing techniques and tribological effect of surface texturing on cutting tool performance: a review *Crit. Rev. Solid State Mater. Sci.* **41** 447–81

[27] Vo T D, Deng G Y, Tieu A K, Su L H, Wu X T, Nguyen C, Wexler D and Yang J 2023 Excellent tribological performance at elevated temperatures and associated mechanisms of novel AlCoCrFeNi-MoS_2 solid self-lubricating composite *Tribol. Int.* **189** 109011

[28] Souza de Carvalho M J, Rudolf Seidl P, Pereira Belchior C R and Ricardo Sodré J 2010 Lubricant viscosity and viscosity improver additive effects on diesel fuel economy *Tribol. Int.* **43** 2298–302

[29] Aurelian F, Patrick M and Mohamed H 2011 Wall slip effects in (elasto) hydrodynamic journal bearings *Tribol. Int.* **44** 868–77

[30] Chen M, Briscoe W H, Armes S P and Klein J 2009 Lubrication at physiological pressures by polyzwitterionic brushes *Science* **323** 1698–701

[31] Li R, Zhang X R, Zeng C, Yang P A, Shou M J, Zhu D, Cao Z F, Xie H Q and Lee C H 2023 Magneto-controlled friction behaviors of magnetorheological elastomers with cosine-shaped surface structure *Tribol. Int.* **186** 108658

[32] Resendiz J, Egberts P and Park S S 2018 Tribological behavior of multi-scaled patterned surfaces machined through inclined end milling and micro shot blasting *Tribol. Lett.* **66** 132

[33] Kang J J, Wang M Z, Yue W, Fu Z Q, Zhu L N, She D S and Wang C B 2019 Tribological behavior of titanium alloy treated by nitriding and surface texturing composite technology *Materials* **12** 301

[34] Li Y L, Li M X, Utaka Y, Yang C J and Wang M 2020 Effect of copper surface modification applied by combined modification of metal vapor vacuum arc ion implantation and laser texturing on anti-frosting property *Energy Build* **223** 110132

[35] Costa H L and Hutchings I M 2015 Some innovative surface texturing techniques for tribological purposes *Proc. Inst. Mech. Eng. J* **229** 429–48

[36] Mao B, Siddaiah A, Liao Y L and Menezes P L 2020 Laser surface texturing and related techniques for enhancing tribological performance of engineering materials: a review *J. Manuf. Process.* **53** 153–73

[37] Shi Z, Duan X F, Chen Z H, Liu B, Fu H, Ji J H and Zhang Y H 2024 Precision fabrication of micro-textures array for surface functionalization using picosecond pulse laser *Opt. Laser Technol.* **177** 111200

[38] Kawabata S, Bai S, Obata K, Miyaji G and Sugioka K 2023 Two-dimensional laser-induced periodic surface structures formed on crystalline silicon by GHz burst mode femtosecond laser pulses *Int. J. Extrem. Manuf.* **5** 015004

[39] Zwahr C, Serey N, Nitschke L, Bischoff C, Rädel U, Meyer A, Zhu P H and Pfleging W 2023 Targeting new ways for large-scale, high-speed surface functionalization using direct laser interference patterning in a roll-to-roll process *Int. J. Extrem. Manuf.* **5** 035006

[40] Li H Y, Xu W H, Li L Q, Xia H B, Chen X, Chen B, Song X G and Tan C W 2022 Enhancing the wettability for 4043 aluminum alloy on 301L stainless steel via chemical-etched surface texturing *J. Mater. Process. Technol.* **305** 117577

[41] Liu X F, Wu D B, Zhang J H, Hu X Y and Cui P 2019 Analysis of surface texturing in radial ultrasonic vibration-assisted turning *J. Mater. Process. Technol.* **267** 186–95

[42] Zhu L D, Ni C B, Yang Z C and Liu C F 2019 Investigations of micro-textured surface generation mechanism and tribological properties in ultrasonic vibration-assisted milling of Ti-6Al-4V *Precis. Eng.* **57** 229–43

[43] Mao B, Siddaiah A, Menezes P L and Liao Y L 2018 Surface texturing by indirect laser shock surface patterning for manipulated friction coefficient *J. Mater. Process. Technol.* **257** 227–33

[44] Meng Y, Deng J X, Lu Y, Wang S J, Wu J X and Sun W 2021 Fabrication of AlTiN coatings deposited on the ultrasonic rolling textured substrates for improving coatings adhesion strength *Appl. Surf. Sci.* **550** 149394

[45] Lu W L, Zhai W Z, Wang J, Liu X J, Zhou L P, Ibrahim A M M, Li X C, Lin D and Wang Y M 2021 Additive manufacturing of isotropic-grained, high-strength and high-ductility copper alloys *Addit. Manuf.* **38** 101751

[46] Studart A R 2016 Additive manufacturing of biologically-inspired materials *Chem. Soc. Rev.* **45** 359–76

[47] Ranjan P and Hiremath S S 2019 Role of textured tool in improving machining performance: a review *J. Manuf. Process.* **43** 47–73

[48] Spear J C, Ewers B W and Batteas J D 2015 2D-nanomaterials for controlling friction and wear at interfaces *Nano Today* **10** 301–14

[49] Akhtar S S 2021 A critical review on self-lubricating ceramic-composite cutting tools *Ceram. Int.* **47** 20745–67

[50] Gropper D, Harvey T J and Wang L 2018 Numerical analysis and optimization of surface textures for a tilting pad thrust bearing *Tribol. Int.* **124** 134–44

[51] Li Z, Wang J M, Zhang H, Chen J and Liu K 2020 Influence of surface topography on the friction and dynamic characteristics of spur gears *Proc. Inst. Mech. Eng. J* **234** 1892–907

[52] Shen C and Khonsari M M 2016 The effect of laser machined pockets on the lubrication of piston ring prototypes *Tribol. Int.* **101** 273–83

[53] Ge D L, Deng J X, Duan R, Liu Y Y, Li X M and Yue H Z 2019 Effect of micro-textures on cutting fluid lubrication of cemented carbide tools *Int. J. Adv. Manuf. Technol.* **103** 3887–99

[54] Liu Y Y, Zhu Q, Wang C Y and Li J Q 2023 Tribological behavior of CoCrMo artificial knee joint with symmetrically biomimetic textured surfaces on PEEK *Opt. Laser Technol.* **157** 108774

[55] Yu X Q, He S and Cai R L 2002 Frictional characteristics of mechanical seals with a laser-textured seal face *J. Mater. Process. Technol.* **129** 463–6

[56] Aymard A, Delplanque E, Dalmas D and Scheibert J 2024 Designing metainterfaces with specified friction laws *Science* **383** 200–4

[57] Dongming G 2024 High-performance manufacturing *Int. J. Extrem. Manuf.* **6** 060201

[58] Zhang H, Hua M, Dong G Z, Zhang D Y, Chen W J and Dong G N 2017 Optimization of texture shape based on genetic algorithm under unidirectional sliding *Tribol. Int.* **115** 222–32

[59] Götz J, Alvarez Rueda A, Ruttloff S, Kuna L, Belegratis M, Palfinger U, Nees D, Hartmann P and Stadlober B 2022 Finite element simulations of filling and demolding in roll-to-roll UV nanoimprinting of micro- and nanopatterns *ACS Appl. Nano Mater.* **5** 3434–49

[60] Han Y L, Sun J N, Xu J W, Zhang Y, Xiao Q H, Jing H, Chen B X, Kong X W, Cabezudo N and Zhang L 2024 Direct 3D printing functional surfaces stacked with microstructured filaments *Addit. Manuf.* **79** 103900

[61] Liu Y Y, Liu L L, Deng J X, Meng R, Zou X Q and Wu F F 2017 Fabrication of micro-scale textured grooves on green ZrO_2 ceramics by pulsed laser ablation *Ceram. Int.* **43** 6519–31

[62] Gropper D, Wang L and Harvey T J 2016 Hydrodynamic lubrication of textured surfaces: a review of modeling techniques and key findings *Tribol. Int.* **94** 509–29

[63] Gachot C, Rosenkranz A, Hsu S M and Costa H L 2017 A critical assessment of surface texturing for friction and wear improvement *Wear* **372–373** 21–41

[64] Wu Z, Bao H, Xing Y Q and Liu L 2021 Tribological characteristics and advanced processing methods of textured surfaces: a review *Int. J. Adv. Manuf. Technol.* **114** 1241–77

[65] Rosenkranz A, Grützmacher P G, Gachot C and Costa H L 2019 Surface texturing in machine elements− a critical discussion for rolling and sliding contacts *Adv. Eng. Mater.* **21** 1900194

[66] Rosenkranz A, Costa H L, Baykara M Z and Martini A 2021 Synergetic effects of surface texturing and solid lubricants to tailor friction and wear – a review *Tribol. Int.* **155** 106792

[67] Wang X M, Li C H, Zhang Y B, Said Z, Debnath S, Sharma S, Yang M and Gao T 2022 Influence of texture shape and arrangement on nanofluid minimum quantity lubrication turning *Int. J. Adv. Manuf. Technol.* **119** 631–46

[68] Grützmacher P G, Jalikop S V, Gachot C and Rosenkranz A 2021 Thermocapillary lubricant migration on textured surfaces-a review of theoretical and experimental insights *Surf. Topogr.: Metrol. Prop.* **9** 013001

[69] Grützmacher P G, Profito F J and Rosenkranz A 2019 Multi-scale surface texturing in tribology-current knowledge and future perspectives *Lubricants* **7** 95

[70] Chorin A J 1968 Numerical solution of the Navier-Stokes equations *Math. Comput.* **22** 745–62

[71] Reynolds O 1886 IV. On the theory of lubrication and its application to Mr. Beauchamp tower's experiments, including an experimental determination of the viscosity of olive oil *Phil. Trans.* **177** 157–234

[72] Wang Q J, Zhu D, Zhou R S and Hashimoto F 2008 Investigating the effect of surface finish on mixed EHL in rolling and rolling-sliding contacts *Tribol. Trans.* **51** 748–61

[73] Epstein D, Keer L M, Wang Q J, Cheng H S and Zhu D 2003 Effect of surface topography on contact fatigue in mixed lubrication *Tribol. Trans.* **46** 506–13

[74] Patir N and Cheng H S 1978 An average flow model for determining effects of three-dimensional roughness on partial hydrodynamic lubrication *J. Lubr. Technol.* **100** 12–17

[75] Spikes H A 2006 Sixty years of EHL *Lubr. Sci.* **18** 265–91

[76] Shinkarenko A, Kligerman Y and Etsion I 2009 The effect of elastomer surface texturing in soft elasto-hydrodynamic lubrication *Tribol. Lett.* **36** 95–103

[77] Li J F, Zhou F and Wang X L 2011 Modify the friction between steel ball and PDMS disk under water lubrication by surface texturing *Meccanica* **46** 499–507

[78] Marian M, Tremmel S and Wartzack S 2018 Microtextured surfaces in higher loaded rolling-sliding EHL line-contacts *Tribol. Int.* **127** 420–32

[79] Hamrock B J and Dowson D 1977 Isothermal elastohydrodynamic lubrication of point contacts: Part IV—starvation results *J. Lubr. Technol.* **99** 15–23

[80] Woloszynski T, Podsiadlo P and Stachowiak G W 2015 Evaluation of discretization and integration methods for the analysis of finite hydrodynamic bearings with surface texturing *Proc. Inst. Mech. Eng. J* **229** 465–77

[81] Pagani L, Townsend A, Zeng W H, Lou S, Blunt L, Jiang X Q and Scott P J 2019 Towards a new definition of

areal surface texture parameters on freeform surface: re-entrant features and functional parameters *Measurement* **141** 442–59
[82] Vijayaraghavan D and Keith T G 1990 An efficient, robust, and time accurate numerical scheme applied to a cavitation algorithm *J. Tribol.* **112** 44–51
[83] Payvar P and Salant R F 1992 A computational method for cavitation in a wavy mechanical seal *J. Tribol.* **114** 199–204
[84] Ausas R, Ragot P, Leiva J, Jai M, Bayada G and Buscaglia G C 2007 The impact of the cavitation model in the analysis of microtextured lubricated journal bearings *J. Tribol.* **129** 868–75
[85] Kumar A and Booker J F 1991 A finite element cavitation algorithm: application/validation *J. Tribol.* **113** 255–60
[86] Hajjam M and Bonneau D 2007 A transient finite element cavitation algorithm with application to radial lip seals *Tribol. Int.* **40** 1258–69
[87] Pei S Y, Ma S L, Xu H, Wang F C and Zhang Y L 2011 A multiscale method of modeling surface texture in hydrodynamic regime *Tribol. Int.* **44** 1810–8
[88] Woloszynski T, Podsiadlo P and Stachowiak G W 2013 Evaluation of discretisation and integration methods for the analysis of hydrodynamic bearings with and without surface texturing *Tribol. Lett.* **51** 25–47
[89] Cupillard S, Glavatskih S and Cervantes M J 2009 3D thermohydrodynamic analysis of a textured slider *Tribol. Int.* **42** 1487–95
[90] Cupillard S, Glavatskih S and Cervantes M J 2010 Inertia effects in textured hydrodynamic contacts *Proc. Inst. Mech. Eng. J* **224** 751–6
[91] Feldman Y, Kligerman Y, Etsion I and Haber S 2006 The validity of the Reynolds equation in modeling hydrostatic effects in gas lubricated textured parallel surfaces *J. Tribol.* **128** 345–50
[92] Ma C B and Zhu H 2011 An optimum design model for textured surface with elliptical-shape dimples under hydrodynamic lubrication *Tribol. Int.* **44** 987–95
[93] Dobrica M B and Fillon M 2009 About the validity of Reynolds equation and inertia effects in textured sliders of infinite width *Proc. Inst. Mech. Eng.J* **223** 69–78
[94] Almqvist T and Larsson R 2004 Some remarks on the validity of Reynolds equation in the modeling of lubricant film flows on the surface roughness scale *J. Tribol.* **126** 703–10
[95] Huang Q P, Shi X L, Xue Y W, Zhang K P and Wu C H 2023 Recent progress on surface texturing and solid lubricants in tribology: designs, properties, and mechanisms *Mater. Today Commun.* **35** 105854
[96] Etsion I 2013 Modeling of surface texturing in hydrodynamic lubrication *Friction* **1** 195–209
[97] Zhang B S, Jiang Y C, Ren T C, Chen B J, Zhang R Y and Mao Y C 2024 Recent advances in nature inspired triboelectric nanogenerators for self-powered systems *Int. J. Extrem. Manuf.* **6** 062003
[98] Chen H W, Zhang P F, Zhang L W, Liu H L, Jiang Y, Zhang D Y, Han Z W and Jiang L 2016 Continuous directional water transport on the peristome surface of *Nepenthes alata Nature* **532** 85–89
[99] Liu Y H and Li G J 2012 A new method for producing "Lotus Effect" on a biomimetic shark skin *J. Colloid Interface Sci.* **388** 235–42
[100] Zhao Y Z, Su Y L, Hou X Y and Hong M H 2021 Directional sliding of water: biomimetic snake scale surfaces *Opto-Electron. Adv.* **4** 210008
[101] Xu L Y, Yang L L, Yang S, Xu Z, Lin G J, Shi J J, Zhang R Y, Yu J Y, Ge D T and Guo Y 2021 Earthworm-inspired ultradurable superhydrophobic fabrics from adaptive wrinkled skin *ACS Appl. Mater. Interfaces* **13** 6758–66
[102] Wang H T, Li Y and Zhu H 2016 Experimental study on the tribological performance of fractal-like textured surface under mixed lubrication conditions *Surf. Coat. Technol.* **307** 220–6
[103] Segu D Z and Hwang P 2015 Friction control by multi-shape textured surface under pin-on-disc test *Tribol. Int.* **91** 111–7
[104] Wu C, Yang K, Ni J, Lu S G, Yao L D and Li X L 2023 Investigations for vibration and friction torque behaviors of thrust ball bearing with self-driven textured guiding surface *Friction* **11** 894–910
[105] Tala-Ighil N, Fillon M and Maspeyrot P 2011 Effect of textured area on the performances of a hydrodynamic journal bearing *Tribol. Int.* **44** 211–9
[106] Lu Y 2017 Fabrication of a lotus leaf-like hierarchical structure to induce an air lubricant for drag reduction *Surf. Coat. Technol.* **331** 48–56
[107] Wang X L, Adachi K, Otsuka K and Kato K 2006 Optimization of the surface texture for silicon carbide sliding in water *Appl. Surf. Sci.* **253** 1282–6
[108] Segu D Z, Choi S G, Choi J H and Kim S S 2013 The effect of multi-scale laser textured surface on lubrication regime *Appl. Surf. Sci.* **270** 58–63
[109] Yang H, Yang X F, Cong J C, Sun J, Shao S B, Hou Q M and Zhang Y F 2023 Wear behavior of microgroove texture of cemented carbide tool prepared by laser surface texture *Microfluid. Nanofluid.* **27** 44
[110] Sharma S C and Yadav S K 2016 A comparative study of full and partial textured hybrid orifice compensated circular thrust pad bearing system *Tribol. Int.* **95** 170–80
[111] Sun J, Qin X Z, Song Y X, Xu Z Y, Zhang C, Wang W, Wang Z K, Wang B and Wang Z K 2023 Selective liquid directional steering enabled by dual-scale reentrant ratchets *Int. J. Extrem. Manuf.* **5** 025504
[112] Buscaglia G C, Ausas R F and Jai M 2006 Optimization tools in the analysis of micro-textured lubricated devices *Inverse Probl. Sci. Eng.* **14** 365–78
[113] Simpson T W, Poplinski J D, Koch P N and Allen J K 2001 Metamodels for computer-based engineering design: survey and recommendations *Eng. Comput.* **17** 129–50
[114] Shen C and Khonsari M M 2016 Texture shape optimization for seal-like parallel surfaces: theory and experiment *Tribol. Trans.* **59** 698–706
[115] Shen C and Khonsari M M 2015 Numerical optimization of texture shape for parallel surfaces under unidirectional and bidirectional sliding *Tribol. Int.* **82** 1–11
[116] Tu Z R, Meng X K, Ma Y and Peng X D 2021 Shape optimization of hydrodynamic textured surfaces for enhancing load-carrying capacity based on level set method *Tribol. Int.* **162** 107136
[117] Kalliorinne K, Pérez-Ràfols F, Fabricius J and Almqvist A 2020 Application of topological optimisation methodology to infinitely wide slider bearings operating under compressible flow *Proc. Inst. Mech. Eng. J* **234** 1035–50
[118] Kalliorinne K and Almqvist A 2021 Application of topological optimisation methodology to finitely wide slider bearings operating under incompressible flow *Proc. Inst. Mech. Eng. J* **235** 698–710
[119] Zhang G J, Li J, Tian Z X, Huang Y and Chen R C 2016 Film shape optimization for two-dimensional rough slider bearings *Tribol. Trans.* **59** 17–27
[120] van Ostayen R A J 2010 Film height optimization of dynamically loaded hydrodynamic slider bearings *Tribol. Int.* **43** 1786–93
[121] Huang Q P, Shi X L, Xue Y W, Zhang K P and Wu C H 2021 Optimization of bionic textured parameter to improve the tribological performance of AISI 4140 self-lubricating composite through response surface methodology *Tribol. Int.* **161** 107104

[122] Codrignani A, Savio D, Pastewka L, Frohnapfel B and Van Ostayen R 2020 Optimization of surface textures in hydrodynamic lubrication through the adjoint method *Tribol. Int.* **148** 106352
[123] Zhang H, Dong G N, Hua M and Chin K S 2017 Improvement of tribological behaviors by optimizing concave texture shape under reciprocating sliding motion *J. Tribol.* **139** 011701
[124] Zhang X Y, Liu C P and Zhao B 2021 An optimization research on groove textures of a journal bearing using particle swarm optimization algorithm *Mech. Ind.* **22** 1
[125] Zhang W X and Zhu B 2023 Optimization design for slip/no-slip configuration of hydrophobic sliding bearings using Monte Carlo search *Tribol. Int.* **178** 108034
[126] Wang W, He Y Y, Zhao J, Mao J Y, Hu Y T and Luo J B 2020 Optimization of groove texture profile to improve hydrodynamic lubrication performance: theory and experiments *Friction* **8** 83–94
[127] Marian M and Tremmel S 2021 Current trends and applications of machine learning in tribology—a review *Lubricants* **9** 86
[128] Bhaumik S, Chowdhury D, Batham A, Sehgal U, Ghosh C, Bhattacharya B and Datta S 2020 Analysing the frictional properties of micro dimpled surface created by milling machine under lubricated condition *Tribol. Int.* **146** 106260
[129] Mo F, Shen C, Zhou J and Khonsari M M 2017 Statistical analysis of the influence of imperfect texture shape and dimensional uncertainty on surface texture performance *IEEE Access* **5** 27023–35
[130] Mousavirad S J, Rahmani R and Dolatabadi N 2023 A transfer learning based artificial neural network in geometrical design of textured surfaces for tribological applications *Surf. Topogr.: Metrol. Prop.* **11** 025001
[131] Rosenkranz A, Marian M, Profito F J, Aragon N and Shah R 2021 The use of artificial intelligence in tribology—a perspective *Lubricants* **9** 2
[132] Zhu B, Zhang W X, Zhang W S and Li H X 2023 Generative design of texture for sliding surface based on machine learning *Tribol. Int.* **179** 108139
[133] Hao Y P, Zhu L D, Qin S Q, Pei X Y, Yan T M, Qin Q Y, Lu H and Yan B L 2024 On-machine inspection and compensation for thin-walled parts with sculptured surface considering cutting vibration and probe posture *Int. J. Extrem. Manuf.* **6** 065602
[134] Johns-Rahnejat P M, Rahmani R and Rahnejat H 2023 Current and future trends in tribological research *Lubricants* **11** 391
[135] Rosenkranz A and Marian M 2022 Combining surface textures and MXene coatings—towards enhanced wear-resistance and durability *Surf. Topogr.: Metrol. Prop.* **10** 033001
[136] Watanabe S, Kodama E, Tadokoro C, Sakakibara K, Nakano K, Sasaki S and Tsujii Y 2021 Durability improvement of concentrated polymer brushes by multiscale texturing *Tribol. Lett.* **69** 99
[137] Miyazaki M, Nakano K, Tadokoro C, Vlădescu S C, Reddyhoff T, Sasaki S and Tsujii Y 2021 Enhancing durability of concentrated polymer brushes using microgrooved substrates *Wear* **482–483** 203984
[138] Vlădescu S C, Tadokoro C, Miyazaki M, Reddyhoff T, Nagamine T, Nakano K, Sasaki S and Tsujii Y 2022 Exploiting the synergy between concentrated polymer brushes and laser surface texturing to achieve durable superlubricity *ACS Appl. Mater. Interfaces* **14** 15818–29
[139] Wu C, Wu Y W, Zhao H J, Li S S, Ni J and Li X L 2023 Influence of hardness of nanoparticle additive in PTFE solid lubricant on tribological properties of GCr15 steel with bionic texture *Tribol. Int.* **189** 108915
[140] Xing Y Q, Wang X S, Du Z H, Zhu Z W, Wu Z and Liu L 2022 Synergistic effect of surface textures and DLC coatings for enhancing friction and wear performances of Si_3N_4/TiC ceramic *Ceram. Int.* **48** 514–24
[141] Cui W Y, Chen H Z, Zhao J X, Ma Q S, Xu Q and Ma T B 2023 Progresses on cryo-tribology: lubrication mechanisms, detection methods and applications *Int. J. Extrem. Manuf.* **5** 022004
[142] Kobayashi M, Tanaka H, Minn M, Sugimura J and Takahara A 2014 Interferometry study of aqueous lubrication on the surface of polyelectrolyte brush *ACS Appl. Mater. Interfaces* **6** 20365–71
[143] Klein J 1994 Shear of polymer brushes *Colloids Surf.* A **86** 63–76
[144] Klein J, Kumacheva E, Mahalu D, Perahia D and Fetters L J 1994 Reduction of frictional forces between solid surfaces bearing polymer brushes *Nature* **370** 634–
[145] Bielecki R M, Benetti E M, Kumar D and Spencer N D 2012 Lubrication with oil-compatible polymer brushes *Tribol. Lett.* **45** 477–87
[146] Bielecki R M, Crobu M and Spencer N D 2013 Polymer-brush lubrication in oil: sliding beyond the stribeck curve *Tribol. Lett.* **49** 263–72
[147] Heeb R, Bielecki R M, Lee S and Spencer N D 2009 Room-temperature, aqueous-phase fabrication of poly(methacrylic acid) brushes by UV-LED-induced, controlled radical polymerization with high selectivity for surface-bound species *Macromolecules* **42** 9124–32
[148] Rong M M, Liu H, Scaraggi M, Bai Y Y, Bao L Y, Ma S H, Ma Z F, Cai M R, Dini D and Zhou F 2020 High lubricity meets load capacity: cartilage mimicking bilayer structure by brushing up stiff hydrogels from subsurface *Adv. Funct. Mater.* **30** 2004062
[149] Nunez E E, Gheisari R and Polycarpou A A 2019 Tribology review of blended bulk polymers and their coatings for high-load bearing applications *Tribol. Int.* **129** 92–111
[150] Ye J X, Zhang Y F, Zhang K S, Wang W, Liu X J and Liu K 2020 Hybrid wear-reducing micro-pits counterface texture against polymeric solid lubricants *Tribol. Lett.* **68** 33
[151] Xiong D S, Qin Y K, Li J L, Wan Y and Tyagi R 2015 Tribological properties of PTFE/laser surface textured stainless steel under starved oil lubrication *Tribol. Int.* **82** 305–10
[152] Zhao S, Yu A B, Zou P, Wang G L, Li K F, Wang J W, Qi S C and Ye J W 2023 Tribological properties of dopamine-modified dimple textured surfaces filled with PTFE *Proc. Inst. Mech. Eng. J* **237** 655–66
[153] Suh N P, Mosleh M and Howard P S 1994 Control of friction *Wear* **175** 151–8
[154] He D Q, He C, Li W S, Shang L L, Wang L P and Zhang G G 2020 Tribological behaviors of *in-situ* textured DLC films under dry and lubricated conditions *Appl. Surf. Sci.* **525** 146581
[155] Jin L, Li Y T, Liu C B, Fan X Q and Zhu M H 2023 Friction mechanism of DLC/MAO wear-resistant coatings with porous surface texture constructed *in-situ* by micro-arc oxidation *Surf. Coat. Technol.* **473** 130010
[156] Chiu M C, Hsieh W P, Ho W Y, Wang D Y and Shieu F S 2005 Thermal stability of Cr-doped diamond-like carbon films synthesized by cathodic arc evaporation *Thin Solid Films* **476** 258–63
[157] Amanov A, Watabe T, Tsuboi R and Sasaki S 2013 Improvement in the tribological characteristics of Si-DLC coating by laser surface texturing under oil-lubricated point contacts at various temperatures *Surf. Coat. Technol.* **232** 549–60

[158] Lin N M, Liu Q, Zou J J, Guo J W, Li D L, Yuan S, Ma Y, Wang Z X, Wang Z H and Tang B 2016 Surface texturing-plasma nitriding duplex treatment for improving tribological performance of AISI 316 stainless steel *Materials* **9** 875
[159] Fan P F, Goel S, Luo X C and Upadhyaya H M 2022 Atomic-scale friction studies on single-crystal gallium arsenide using atomic force microscope and molecular dynamics simulation *Nanomanuf. Metrol.* **5** 39–49
[160] Sun J N, Zhang L, Zhang Y, Han Y L and Zhang L 2023 Effect of refresh time on XeF_2 gas-assisted FIB milling of GaAs *Nanomanuf. Metrol.* **6** 29
[161] Cao L, Chen Y, Cui J, Li W, Lin Z D and Zhang P 2020 Corrosion wear performance of pure titanium laser texturing surface by nitrogen ion implantation *Metals* **10** 990
[162] Liu D R, Zhang Q, Qin Z B, Luo Q, Wu Z and Liu L 2016 Tribological performance of surfaces enhanced by texturing and nitrogen implantation *Appl. Surf. Sci.* **363** 161–7
[163] Bagherifard S, Slawik S, Fernández-Pariente I, Pauly C, Mücklich F and Guagliano M 2016 Nanoscale surface modification of AISI 316L stainless steel by severe shot peening *Mater. Des.* **102** 68–77
[164] Torres H, Slawik S, Gachot C, Prakash B and Rodríguez Ripoll M 2018 Microstructural design of self-lubricating laser claddings for use in high temperature sliding applications *Surf. Coat. Technol.* **337** 24–34
[165] Wu H, Jia F H, Li Z, Lin F, Huo M S, Huang S Q, Sayyar S, Jiao S H, Huang H and Jiang Z Y 2020 Novel water-based nanolubricant with superior tribological performance in hot steel rolling *Int. J. Extrem. Manuf.* **2** 025002
[166] Peng R L, Guo J D, Han S X, Zeng Q F, Cao W and Du H 2020 Tribological performance of freeze-drying nano-copper particle as additive of paroline oil *Mater. Res. Express* **7** 025028
[167] Birleanu C, Pustan M, Cioaza M, Molea A, Popa F and Contiu G 2022 Effect of TiO_2 nanoparticles on the tribological properties of lubricating oil: an experimental investigation *Sci. Rep.* **12** 5201
[168] Wang X Z, Li C C, Gong K L and Wu X H 2023 Surface-modified MoS_2 nanoparticles as tribological additives in a glycerol solution *ACS Appl. Nano Mater.* **6** 6662–9
[169] Zhang Y P, Guo X H, Li Z H, Wang C D, Liu T S and Zhang K D 2022 Study on the tribological properties of Fe_3O_4@CNTs nanofluids acting on the textured ceramics *Appl. Phys.* A **128** 161
[170] Zheng D, Cai Z B, Shen M X, Li Z Y and Zhu M H 2016 Investigation of the tribology behaviour of the graphene nanosheets as oil additives on textured alloy cast iron surface *Appl. Surf. Sci.* **387** 66–75
[171] Kumara C, Luo H M, Leonard D N, Meyer H M and Qu J 2017 Organic-modified silver nanoparticles as lubricant additives *ACS Appl. Mater. Interfaces* **9** 37227–37
[172] Qu M N, Yao Y L, He J M, Ma X R, Feng J, Liu S S, Hou L G and Liu X R 2017 Tribological study of polytetrafluoroethylene lubricant additives filled with Cu microparticles or SiO_2 nanoparticles *Tribol. Int.* **110** 57–65
[173] Zhao Z S, Zhang Y S, Wang S F, Guo K, Tang J, Wu Z G, Zhang G G, Zhu Y X, Yan P X and Zhang W Y 2019 Tribological properties of oleylamine-modified nickel nanoparticles as lubricating oil additive *Mater. Res. Express* **6** 105037
[174] Han K, Zhang Y J, Song N N, Yu L G, Zhang P Y, Zhang Z J, Qian L and Zhang S M 2022 The current situation and future direction of nanoparticles lubricant additives in China *Lubricants* **10** 312
[175] Tang W W, Zhang Z and Li Y F 2021 Applications of carbon quantum dots in lubricant additives: a review *J. Mater. Sci.* **56** 12061–92
[176] Kumar S, Nehra M, Kedia D, Dilbaghi N, Tankeshwar K and Kim K H 2019 Nanodiamonds: emerging face of future nanotechnology *Carbon* **143** 678–99
[177] Zhao J, Gao T, Li Y R, He Y Y and Shi Y J 2021 Two-dimensional (2D) graphene nanosheets as advanced lubricant additives: a critical review and prospect *Mater. Today Commun.* **29** 102755
[178] Lu Q, Zhang T Y, Wang Y X, Liu S J, Ye Q and Zhou F 2023 Boron-nitrogen codoped carbon nanosheets as oil-based lubricant additives for antioxidation, antiwear, and friction reduction *ACS Sustain. Chem. Eng.* **11** 11867–77
[179] Yu H L, Xu Y, Shi P J, Xu B S, Wang X L, Liu Q and Wang H M 2008 Characterization and nano-mechanical properties of tribofilms using Cu nanoparticles as additives *Surf. Coat. Technol.* **203** 28–34
[180] Segu D Z, Chae Y, Lee S J and Kim C L 2023 Synergistic influences of laser surface texturing and ZrO_2-MoDTC hybrid nanofluids for enhanced tribological performance *Tribol. Int.* **183** 108377
[181] Cai M R, Yu Q L, Liu W M and Zhou F 2020 Ionic liquid lubricants: when chemistry meets tribology *Chem. Soc. Rev.* **49** 7753–818
[182] Zhou Y and Qu J 2017 Ionic liquids as lubricant additives: a review *ACS Appl. Mater. Interfaces* **9** 3209–22
[183] Qu J *et al* 2012 Antiwear performance and mechanism of an oil-miscible ionic liquid as a lubricant additive *ACS Appl. Mater. Interfaces* **4** 997–1002
[184] Singh J, Chatha S S and Bhatia R 2022 Behaviour and applications of ionic liquids as lubricants in tribology: a review *Mater. Today: Proc.* **56** 2659–65
[185] Reeves C J, Kasar A K and Menezes P L 2021 Tribological performance of environmental friendly ionic liquids for high-temperature applications *J. Clean. Prod.* **279** 123666
[186] Shi G Q, Yu X D, Meng H, Zhao F H, Wang J F, Jiao J H and Jiang H 2023 Effect of surface modification on friction characteristics of sliding bearings: a review *Tribol. Int.* **177** 107937
[187] Thakre G D, Sharma S C, Harsha S P and Tyagi M R 2016 A theoretical study of ionic liquid lubricated μ-EHL line contacts considering surface texture *Tribol. Int.* **94** 39–51
[188] Samanta A, Huang W, Lee K, He X, Kumara C, Qu J and Ding H 2023 Role of surface wetting on tribological behavior for laser nanotextured steel using ionic liquid lubricants *J. Manuf. Process.* **95** 302–11
[189] Zhang J, Yao Y Y, Sheng L and Liu J 2015 Self-fueled biomimetic liquid metal mollusk *Adv. Mater.* **27** 2648–55
[190] Li H Y, Yang Y and Liu J 2012 Printable tiny thermocouple by liquid metal gallium and its matching metal *Appl. Phys. Lett.* **101** 073511
[191] Guo J, Cheng J, Wang S, Yu Y, Zhu S Y, Yang J and Liu W M 2018 A protective $FeGa_3$ film on the steel surface prepared by *in-situ* hot-reaction with liquid metal *Mater. Lett.* **228** 17–20
[192] Guo J, Cheng J, Tan H, Zhu S Y, Qiao Z H, Yang J and Liu W M 2018 Ga-based liquid metal: lubrication and corrosion behaviors at a wide temperature range *Materialia* **4** 10–19
[193] Li H J, Tian P Y, Lu H Y, Jia W P, Du H D, Zhang X J, Li Q Y and Tian Y 2017 State-of-the-art of extreme pressure lubrication realized with the high thermal diffusivity of liquid metal *ACS Appl. Mater. Interfaces* **9** 5638–44
[194] Hughes W F 1963 Magnetohydrodynamic lubrication and application to liquid metals *Ind. Lubr. Tribol.* **15** 125–33
[195] Kezik V Y, Kalinichenko A S and Kalinitchenko V A 2003 The application of gallium as a liquid metal lubricant *Int. J. Mater. Res.* **94** 81–90

[196] Gerkema J 1985 Gallium-based liquid-metal full-film lubricated journal bearings *ASLE Trans.* **28** 47–53

[197] Li Y, Zhang S W, Ding Q, Feng D P, Qin B F and Hu L T 2018 Liquid metal as novel lubricant in a wide temperature range from −10 to 800 °C *Mater. Lett.* **215** 140–3

[198] Guo J, Si Y X, Liu Q, Cao X J, Cheng J, Yang J and Liu W M 2023 The lubrication regimes and transition laws of gallium liquid-metal *Tribol. Int.* **188** 108838

[199] Nsilani Kouediatouka A, Ma Q, Liu Q, Mawignon F J, Rafique F and Dong G N 2022 Design methodology and application of surface texture: a review *Coatings* **12** 1015

[200] Li X, Li Y H, Tong Z, Ma Q, Ni Y Q and Dong G N 2019 Enhanced lubrication effect of gallium-based liquid metal with laser textured surface *Tribol. Int.* **129** 407–15

[201] Fannin P C, Marin C N, Malaescu I and Stefu N 2007 An investigation of the microscopic and macroscopic properties of magnetic fluids *Physica* B **388** 87–92

[202] Chandra P, Sinha P and Kumar D 1992 Ferrofluid lubrication of a journal bearing considering cavitation *Tribol. Trans.* **35** 163–9

[203] Umehara N and Komanduri R 1996 Magnetic fluid grinding of HIP-Si_3N_4 rollers *Wear* **192** 85–93

[204] Prajapati B L 1995 Magnetic-fluid-based porous squeeze films *J. Magn. Magn. Mater.* **149** 97–100

[205] Huang W, Wang X L, Ma G L and Shen C 2009 Study on the synthesis and tribological property of Fe_3O_4 based magnetic fluids *Tribol. Lett.* **33** 187–92

[206] Uhlmann E, Spur G, Bayat N and Patzwald R 2002 Application of magnetic fluids in tribotechnical systems *J. Magn. Magn. Mater.* **252** 336–40

[207] Shen C, Huang W, Ma G L and Wang X L 2009 A novel surface texture for magnetic fluid lubrication *Surf. Coat. Technol.* **204** 433–9

[208] Liao S J, Huang W and Wang X L 2012 Micro-magnetic field arrayed surface for ferrofluids lubrication *J. Tribol.* **134** 021701

[209] Guo X H, Huang Q, Wang C D, Liu T S, Zhang Y P, He H D and Zhang K D 2022 Effect of magnetic field on cutting performance of micro-textured tools under Fe_3O_4 nanofluid lubrication condition *J. Mater. Process. Technol.* **299** 117382

[210] Zhang L, Guo X H, Zhang K D, Wu Y Q and Huang Q 2020 Enhancing cutting performance of uncoated cemented carbide tools by joint-use of magnetic nanofluids and micro-texture under magnetic field *J. Mater. Process. Technol.* **284** 116764

[211] Zhang K D, Li Z H, Wang S S, Wang P, Zhang Y P and Guo X H 2023 Study on the cooling and lubrication mechanism of magnetic field-assisted Fe_3O_4@CNTs nanofluid in micro-textured tool cutting *J. Manuf. Process.* **85** 556–68

[212] Gutowski P and Leus M 2012 The effect of longitudinal tangential vibrations on friction and driving forces in sliding motion *Tribol. Int.* **55** 108–18

[213] Wallaschek J 1998 Contact mechanics of piezoelectric ultrasonic motors *Smart Mater. Struct.* **7** 369–81

[214] Wang P, Ni H J, Wang R H, Li Z N and Wang Y 2016 Experimental investigation of the effect of in-plane vibrations on friction for different materials *Tribol. Int.* **99** 237–47

[215] Liu W L, Ni H J, Wang P and Chen H L 2020 Investigation on the tribological performance of micro-dimples textured surface combined with longitudinal or transverse vibration under hydrodynamic lubrication *Int. J. Mech. Sci.* **174** 105474

[216] Mitrofanov A V, Ahmed N, Babitsky V I and Silberschmidt V V 2005 Effect of lubrication and cutting parameters on ultrasonically assisted turning of Inconel 718 *J. Mater. Process. Technol.* **162–163** 649–54

[217] Sun Z T, Shuang F and Ma W 2018 Investigations of vibration cutting mechanisms of Ti6Al4V alloy *Int. J. Mech. Sci.* **148** 510–30

[218] Usman M M, Zou P, Yang Z Y, Lin T Y and Muhammad I 2022 Evaluation of micro-textured tool performance in ultrasonic elliptical vibration-assisted turning of 304 stainless steel *Int. J. Adv. Manuf. Technol.* **121** 4403–18

[219] Mistry K K, Morina A and Neville A 2011 A tribochemical evaluation of a WC–DLC coating in EP lubrication conditions *Wear* **271** 1739–44

[220] Wang X L, Kato K, Adachi K and Aizawa K 2001 The effect of laser texturing of SiC surface on the critical load for the transition of water lubrication mode from hydrodynamic to mixed *Tribol. Int.* **34** 703–11

[221] Agapov R L, Boreyko J B, Briggs D P, Srijanto B R, Retterer S T, Collier C P and Lavrik N V 2014 Asymmetric wettability of nanostructures directs leidenfrost droplets *ACS Nano* **8** 860–7

[222] Li B H, Jiang L, Li X W, Wang Z P and Yi P 2024 Self-propelled Leidenfrost droplets on femtosecond-laser-induced surface with periodic hydrophobicity gradient *Int. J. Extrem. Manuf.* **6** 025502

[223] Wos S, Koszela W, Pawlus P, Drabik J and Rogos E 2018 Effects of surface texturing and kind of lubricant on the coefficient of friction at ambient and elevated temperatures *Tribol. Int.* **117** 174–9

[224] Gao H C and Chen X Y 2020 Effect of surface texturing on hydrodynamic lubrication at various temperatures *AIP Adv.* **10** 055301

[225] Shen Y, Li Q, Liu Z X, Ye B, Fan J J and Xu J J 2023 Influence of different loads and temperatures on solid lubricant-filled micro-dimples existing on both cylinder liner and piston ring *Wear* **526–527** 204926

[226] Chen C, Lu Y and Xue C 2021 Drag reduction mechanism of vapour-assisted liquid membrane lubrication on texture surface with elevated temperature *Lubr. Sci.* **33** 358–68

[227] Yong J L, Chen F, Li M J, Yang Q, Fang Y, Huo J L and Hou X 2017 Remarkably simple achievement of superhydrophobicity, superhydrophilicity, underwater superoleophobicity, underwater superoleophilicity, underwater superaerophobicity, and underwater superaerophilicity on femtosecond laser ablated PDMS surfaces *J. Mater. Chem.* A **5** 25249–57

[228] Suh M S, Chae Y H, Kim S S, Hinoki T and Kohyama A 2010 Effect of geometrical parameters in micro-grooved crosshatch pattern under lubricated sliding friction *Tribol. Int.* **43** 1508–17

[229] Matsumura T, Muramatsu T and Fueki S 2011 Abrasive water jet machining of glass with stagnation effect *CIRP Ann.* **60** 355–8

[230] Maeng S, Lee P A, Kim B H and Min S 2020 An analytical model for grinding force prediction in ultra-precision machining of WC with PCD micro grinding tool *Int. J. Precis. Eng. Manuf. Green Technol.* **7** 1031–45

[231] Mukaida M and Yan J W 2017 Fabrication of hexagonal microlens arrays on single-crystal silicon using the tool-servo driven segment turning method *Micromachines* **8** 323

[232] Shu T, Liu F, Chen S, Liu X T, Zhang C and Cheng G J 2022 Origins of ultrafast pulse laser-induced nano straight lines with potential applications in detecting subsurface defects in silicon carbide wafers *Nanomanuf. Metrol.* **5** 167–78

[233] Wang J S, Fang F Z, An H J, Wu S, Qi H M, Cai Y X and Guo G Y 2023 Laser machining fundamentals: micro, nano, atomic and close-to-atomic scales *Int. J. Extrem. Manuf.* **5** 012005

[234] Li X R, Zhang B Y, Jakobi T, Yu Z L, Ren L Q and Zhang Z H 2024 Laser-based bionic manufacturing *Int. J. Extrem. Manuf.* **6** 042003

[235] Zhang J G, Zheng Z D, Huang K, Lin C T, Huang W Q, Chen X, Xiao J F and Xu J F 2024 Field-assisted machining of difficult-to-machine materials *Int. J. Extrem. Manuf.* **6** 032002
[236] Yuan Y J, Yu K K, Zhang C, Chen Q and Yang W X 2023 Generation of textured surfaces by vibration-assisted ball-end milling *Nanomanuf. Metrol.* **6** 19
[237] Mao W Q, Li H N, Tang B, Zhang C, Liu L, Wang P, Dong H X and Zhang L 2023 Laser patterning of large-scale perovskite single-crystal-based arrays for single-mode laser displays *Int. J. Extrem. Manuf.* **5** 045001
[238] Tangwarodomnukun V 2016 Cavity formation and surface modeling of laser milling process under a thin-flowing water layer *Appl. Surf. Sci.* **386** 51–64
[239] Bharatish A, Harish V, Bathe R N, Senthilselvan J and Soundarapandian S 2018 Effect of scanning speed and tin content on the tribological behavior of femtosecond laser textured tin-bronze alloy *Opt. Laser Technol.* **108** 17–25
[240] Salguero J, Del Sol I, Vazquez-Martinez J M, Schertzer M J and Iglesias P 2019 Effect of laser parameters on the tribological behavior of Ti6Al4V titanium microtextures under lubricated conditions *Wear* **426–427** 1272–9
[241] Allahyari E *et al* 2020 Femtosecond laser surface irradiation of silicon in air: pulse repetition rate influence on crater features and surface texture *Opt. Laser Technol.* **126** 106073
[242] Chen Y *et al* 2021 Achieving a sub-10 nm nanopore array in silicon by metal-assisted chemical etching and machine learning *Int. J. Extrem. Manuf.* **3** 035104
[243] Xu Y F, Yu J Y, Geng J, Abuflaha R, Olson D, Hu X G and Tysoe W T 2018 Characterization of the tribological behavior of the textured steel surfaces fabricated by photolithographic etching *Tribol. Lett.* **66** 55
[244] Basir A, Liza S, Fukuda K and Tahir N A M 2023 Tribological behaviour of multi-shape photochemical textured surfaces *Surf. Topogr.: Metrol. Prop.* **11** 025009
[245] Xie M Z, Zhan Z H, Li Y F, Zhao J K, Zhang C, Wang Z L and Wang Z K 2024 Functional microfluidics: theory, microfabrication, and applications *Int. J. Extrem. Manuf.* **6** 032005
[246] Shi L P, Fang Y, Dai Q W, Huang W and Wang X L 2018 Surface texturing on SiC by multiphase jet machining with microdiamond abrasives *Mater. Manuf. Process.* **33** 1415–21
[247] Nakano M, Korenaga A, Korenaga A, Miyake K, Murakami T, Ando Y, Usami H and Sasaki S 2007 Applying micro-texture to cast iron surfaces to reduce the friction coefficient under lubricated conditions *Tribol. Lett.* **28** 131–7
[248] Sedlaček M, Vilhena L M S, Podgornik B and Vižintin J 2011 Surface topography modelling for reduced friction *Strojniski Vestn.-J. Mech. Eng.* **57** 674–80
[249] Shichao X, Minghe L, Caixia C X and Shujun S J 2014 Study on micro-surface texture and tribology characters of ground surface in point grinding process *Int. J. Surf. Sci. Eng.* **8** 225
[250] Stępień P 2011 Deterministic and stochastic components of regular surface texture generated by a special grinding process *Wear* **271** 514–8
[251] Xie J, Luo M J, He J L, Liu X R and Tan T W 2012 Micro-grinding of micro-groove array on tool rake surface for dry cutting of titanium alloy *Int. J. Precis. Eng. Manuf.* **13** 1845–52
[252] Liu H Z, Yan Y D, Cui J W, Geng Y Q, Sun T, Luo X C and Zong W J 2024 Recent advances in design and preparation of micro diamond cutting tools *Int. J. Extrem. Manuf.* **6** 062008
[253] Yan J W, Oowada T, Zhou T F and Kuriyagawa T 2009 Precision machining of microstructures on electroless-plated NiP surface for molding glass components *J. Mater. Process. Technol.* **209** 4802–8
[254] Zou L, Huang Y, Zhou M and Duan L 2017 Investigation on diamond tool wear in ultrasonic vibration-assisted turning die steels *Mater. Manuf. Process.* **32** 1505–11
[255] Yin X M, Li X, Liu Y H, Geng D X and Zhang D Y 2023 Surface integrity and fatigue life of Inconel 718 by ultrasonic peening milling *J. Mater. Res. Technol.* **22** 1392–409
[256] Li Z W, Zhang J F, Zheng Z P, Feng P F, Yu D W and Wang J J 2024 Elliptical vibration chiseling: a novel process for texturing ultra-high-aspect-ratio microstructures on the metallic surface *Int. J. Extrem. Manuf.* **6** 025102
[257] Zhang J J, Zhang J G, Rosenkranz A, Zhao X L and Song Y L 2018 Surface textures fabricated by laser surface texturing and diamond cutting–influence of texture depth on friction and wear *Adv. Eng. Mater.* **20** 1700995
[258] Du H H, Jiang M N, Wang Z K, Zhu Z W and To S 2023 Generating micro/nanostructures on magnesium alloy surface using ultraprecision diamond surface texturing process *J. Magnesium Alloys* **11** 1472–83
[259] Wang J J, Liao W H and Guo P 2020 Modulated ultrasonic elliptical vibration cutting for ductile-regime texturing of brittle materials with 2-D combined resonant and non-resonant vibrations *Int. J. Mech. Sci.* **170** 105347
[260] Zhai W Z, Zhao Y J, Zhou R H, Lu W L, Zhai W C, Liu X J, Zhou L P and Chang S P 2022 Additively manufactured (Fe, Ni)Al-reinforced nickel aluminum bronze with nearly-isotropic mechanical properties in build and transverse directions *Mater. Charact.* **184** 111706
[261] Chivate A and Zhou C 2024 Additive manufacturing of micropatterned functional surfaces: a review *Int. J. Extrem. Manuf.* **6** 042004
[262] Yang K, Ma H R, Wang L F, Cao Z Z and Zhang C L 2021 Analysis of self-regulating tribological functions of the MgAl microchannels prepared in the Ti alloys *Tribol. Int.* **154** 106717
[263] Vrbka M, Šamánek O, Šperka P, Návrat T, Křupka I and Hartl M 2010 Effect of surface texturing on rolling contact fatigue within mixed lubricated non-conformal rolling/sliding contacts *Tribol. Int.* **43** 1457–65
[264] Szurdak A, Rosenkranz A, Gachot C, Hirt G and Mücklich F 2014 Manufacturing and tribological investigation of hot micro-coined lubrication pockets *Key Eng. Mater.* **611–612** 417–24
[265] Pettersson U and Jacobson S 2006 Tribological texturing of steel surfaces with a novel diamond embossing tool technique *Tribol. Int.* **39** 695–700
[266] Sahu A K, Malhotra J and Jha S 2022 Laser-based hybrid micromachining processes: a review *Opt. Laser Technol.* **146** 107554
[267] Yang J H, Sun S J, Brandt M and Yan W Y 2010 Experimental investigation and 3D finite element prediction of the heat affected zone during laser assisted machining of Ti6Al4V alloy *J. Mater. Process. Technol.* **210** 2215–22
[268] Masuzawa T 2000 State of the art of micromachining *CIRP Ann.* **49** 473–88
[269] Ren Y H, Li C F, Li W, Li M J and Liu H 2019 Study on micro-grinding quality in micro-grinding tool for single crystal silicon *J. Manuf. Process.* **42** 246–56
[270] Melentiev R and Fang F Z 2018 Recent advances and challenges of abrasive jet machining *CIRP J. Manuf. Sci. Technol.* **22** 1–20
[271] Zhang S J, To S and Zhang G Q 2017 Diamond tool wear in ultra-precision machining *Int. J. Adv. Manuf. Technol.* **88** 613–41

[272] Zhao Y, Mei H, Chang P, Yang Y B, Huang W F, Liu Y, Cheng L F and Zhang L T 2021 3D-printed topological MoS_2/$MoSe_2$ heterostructures for macroscale superlubricity *ACS Appl. Mater. Interfaces* **13** 34984–95
[273] Zhang D Y, Qiu D, Gibson M A, Zheng Y F, Fraser H L, StJohn D H and Easton M A 2019 Additive manufacturing of ultrafine-grained high-strength titanium alloys *Nature* **576** 91–95
[274] Divin-Mariotti S, Amieux P, Pascale-Hamri A, Auger V, Kermouche G, Valiorgue F and Valette S 2019 Effects of micro-knurling and femtosecond laser micro texturing on aluminum long-term surface wettability *Appl. Surf. Sci.* **479** 344–50
[275] Zhang G H, Huang M, Chen G L, Li J S, Liu Y, He J G, Zheng Y Q, Tang S W and Cui H L 2024 Design and optimization of fluid lubricated bearings operated with extreme working performances—a comprehensive review *Int. J. Extrem. Manuf.* **6** 022010
[276] Henry Y, Bouyer J and Fillon M 2015 An experimental analysis of the hydrodynamic contribution of textured thrust bearings during steady-state operation: a comparison with the untextured parallel surface configuration *Proc. Inst. Mech. Eng. J* **229** 362–75
[277] Wang L L, Guo S H, Wei Y L, Yuan G T and Geng H 2019 Optimization research on the lubrication characteristics for friction pairs surface of journal bearings with micro texture *Meccanica* **54** 1135–48
[278] Aggarwal S and Pandey R K 2018 Performance investigation of micro-pocketed textured pad thrust bearing *Ind. Lubr. Tribol.* **70** 1388–95
[279] Atwal J C and Pandey R K 2021 Film thickness and friction investigations in a fluid film thrust bearing employing a new conceived micro-texture on pads *J. Tribol.* **143** 061801
[280] Chen D J, Sun Y Q, Zhao Y, Sun K and Fan J W 2023 Influence of the distribution position and arrangement of micro-textured on the performance of the hydrostatic bearing *Ind. Lubr. Tribol.* **75** 721–8
[281] Usman A and Park C W 2016 Optimizing the tribological performance of textured piston ring–liner contact for reduced frictional losses in SI engine: warm operating conditions *Tribol. Int.* **99** 224–36
[282] Shen C and Khonsari M M 2016 Tribological and sealing performance of laser pocketed piston rings in a diesel engine *Tribol. Lett.* **64** 26
[283] Patil A S and Shirsat U M 2021 Effect of laser textured dimples on tribological behavior of piston ring and cylinder liner contact at varying load *Mater. Today: Proc.* **44** 1005–20
[284] Yin H B, Zhang X C, Guo Z W, Xu Y C, Rao X and Yuan C Q 2023 Synergetic effects of surface textures with modified copper nanoparticles lubricant additives on the tribological properties of cylinder liner-piston ring *Tribol. Int.* **178** 108085
[285] Zhao J, Li Z M Q, Zhang H and Zhu R P 2021 Effect of micro-textures on lubrication characteristics of spur gears under 3D line-contact EHL model *Ind. Lubr. Tribol.* **73** 1132–45
[286] Chang X F, Renqing D J, Liao L X, Zhu P Y, Lin B J, Huang Y B and Luo S M 2023 Study on hydrodynamic lubrication and friction reduction performance of spur gear with groove texture *Tribol. Int.* **177** 107978
[287] Arulkirubakaran D, Senthilkumar V and Kumawat V 2016 Effect of micro-textured tools on machining of Ti–6Al–4V alloy: an experimental and numerical approach *Int. J. Refract. Hard Met.* **54** 165–77
[288] Singh R, Dureja J S, Dogra M, Gupta M K, Mia M and Song Q H 2020 Wear behavior of textured tools under graphene-assisted minimum quantity lubrication system in machining Ti-6Al-4V alloy *Tribol. Int.* **145** 106183
[289] Musavi S H, Sepehrikia M, Davoodi B and Niknam S A 2022 Performance analysis of developed micro-textured cutting tool in machining aluminum alloy 7075-T6: assessment of tool wear and surface roughness *Int. J. Adv. Manuf. Technol.* **119** 3343–62
[290] Selvakumar S J, Muralidharan S M and Raj D S 2023 Performance analysis of drills with structured surfaces when drilling CFRP/AA7075 stack under MQL condition *J. Manuf. Process.* **89** 194–219
[291] Kümmel J, Braun D, Gibmeier J, Schneider J, Greiner C, Schulze V and Wanner A 2015 Study on micro texturing of uncoated cemented carbide cutting tools for wear improvement and built-up edge stabilisation *J. Mater. Process. Technol.* **215** 62–70
[292] Niketh S and Samuel G L 2018 Drilling performance of micro textured tools under dry, wet and MQL condition *J. Manuf. Process.* **32** 254–68
[293] Ni J, Feng K, Zhuang K, Sang Z Q, Meng Z and Rahman M M 2022 Combined lubrication of surface texturing and copper covering for broaching tool *Int. J. Adv. Manuf.* **119** 3617–29
[294] Shah R, Gashi B, Hoque S, Marian M and Rosenkranz A 2021 Enhancing mechanical and biomedical properties of protheses—surface and material design *Surf. Interfaces* **27** 101498
[295] Marian M, Shah R, Gashi B, Zhang S, Bhavnani K, Wartzack S and Rosenkranz A 2021 Exploring the lubrication mechanisms of synovial fluids for joint longevity—a perspective *Colloids Surf.* B **206** 111926
[296] Nagentrau M, Tobi A L M, Jamian S, Otsuka Y and Hussin R 2021 Delamination-fretting wear failure evaluation at HAp-Ti-6Al–4V interface of uncemented artificial hip implant *J. Mech. Behav. Biomed. Mater.* **122** 104657
[297] Oonishi H, Ueno M, Kim S C, Oonishi H, Iwamoto M and Kyomoto M 2009 Ceramic versus cobalt-chrome femoral components; wear of polyethylene insert in total knee prosthesis *J. Arthroplasty* **24** 374–82
[298] Jahn S, Seror J and Klein J 2016 Lubrication of articular cartilage *Annu. Rev. Biomed. Eng.* **18** 235–58
[299] Gao L M, Yang P R, Dymond I, Fisher J and Jin Z M 2010 Effect of surface texturing on the elastohydrodynamic lubrication analysis of metal-on-metal hip implants *Tribol. Int.* **43** 1851–60
[300] Roy T, Choudhury D, Ghosh S, Mamat A B and Pingguan-Murphy B 2015 Improved friction and wear performance of micro dimpled ceramic-on-ceramic interface for hip joint arthroplasty *Ceram. Int.* **41** 681–90
[301] Pratap T and Patra K 2018 Mechanical micro-texturing of Ti-6Al-4V surfaces for improved wettability and bio-tribological performances *Surf. Coat. Technol.* **349** 71–81
[302] Pratap T and Patra K 2020 Tribological performances of symmetrically micro-textured Ti-6Al-4V alloy for hip joint *Int. J. Mech. Sci.* **182** 105736
[303] Cui L L, Li H, Gong C Y, Huang J W and Xiong D S 2022 A biomimetic bilayer coating on laser-textured Ti6Al4V alloy with excellent surface wettability and biotribological properties for artificial joints *Ceram. Int.* **48** 26264–73
[304] Han Y J, Liu F, Zhang K D, Huang Q, Guo X H and Wang C D 2021 A study on tribological properties of textured Co-Cr-Mo alloy for artificial hip joints *Int. J. Refract. Hard Met.* **95** 105463
[305] Meng X K, Bai S X and Peng X D 2014 Lubrication film flow control by oriented dimples for liquid lubricated mechanical seals *Tribol. Int.* **77** 132–41
[306] Ahmed A, Masjuki H H, Varman M, Kalam M A, Habibullah M and Al Mahmud K A H 2016 An overview

of geometrical parameters of surface texturing for piston/cylinder assembly and mechanical seals *Meccanica* **51** 9–23

[307] Siripuram R B and Stephens L S 2004 Effect of deterministic asperity geometry on hydrodynamic lubrication *J. Tribol.* **126** 527–34

[308] Brunetière N and Tournerie B 2012 Numerical analysis of a surface-textured mechanical seal operating in mixed lubrication regime *Tribol. Int.* **49** 80–89

[309] Adjemout M, Andrieux A, Bouyer J, Brunetière N, Marcos G and Czerwiec T 2017 Influence of the real dimple shape on the performance of a textured mechanical seal *Tribol. Int.* **115** 409–16

[310] Shi L P, Wei W, Wang T, Zhang Y C, Zhu W and Wang X L 2020 Experimental investigation of the effect of typical surface texture patterns on mechanical seal performance *J. Braz. Soc. Mech. Sci. Eng.* **42** 227